EFFECTS OF CHLORIDE ION ON MECHANICAL PROPERTIES AND DURABILITY OF SEA SAND CONCRETE CONTAINING SUPPLEMENTARY CEMENTITIOUS MATERIALS UNDER ACCELERATED CARBONATION

(セメント質混和材を含む海砂使用コンクリートの

促進炭酸化時における力学特性及び耐久性に及ぼす塩化物イオンの影響)

March 2021

DANG QUOC VIET

ABSTRACT

Concrete, which is a composite material consisting of cement, water, coarse aggregate, and fine aggregate, is the material most used for infrastructure and construction. The greater the usage of concrete, the higher is the use of aggregate. The considerable use of aggregate for concrete production has led to shortages of this resource, especially of natural fine aggregate, such as river sand (RS). The mining of RS can, however, lead to significant environmental impacts, including erosion of riverbanks, the shift of river courses, and the introduction of salinity into rivers; therefore, many researchers have studied other potential materials, such as non-desalted sea sand (NSS), for application as a fine aggregate to replace RS in the construction industry. The use of NSS in concrete manufacture can resolve supply issues in areas where RS has become a scarce resource. The transportation of material will not only be convenient but also take advantage of local material, resulting in the reduction of construction cost. Replacement of RS by NSS could play a key role in reducing the former's overexploitation. However, the high chloride ion content in NSS can cause a potential risk of corrosion and is the primary reason for its limited use in reinforced-concrete manufacture. Washing with fresh water is the most suitable method to reduce the amount of salts in NSS, but causes a serious impact in areas in which freshwater is a scarce resource, especially coastal areas.

Supplementary cementitious materials (SCMs) such as fly ash (FA) and ground granulated blast furnace slag (BFS), have been widely used in concrete production as a partial replacement of ordinary Portland cement (OPC). One of the primary reasons for the use of SCMs in concrete production is to reduce the environmental impacts by utilizing industrial by-products and reducing cement usage. The addition of SCMs has improved the long-term mechanical properties and durability of concrete under the sealed condition. However, there are limited data concerning the influence of chloride ion in NSS on the properties of fresh and hardened

concretes incorporating SCMs. In addition, concrete containing SCMs is extremely sensitive to carbonation. This is a process in which atmospheric carbon dioxide penetrates the cementitious materials and reacts with calcium-bearing phases of concrete and changes the microstructure of concrete. Moreover, carbonation results in the formation of microcracks. As a consequence, the carbonation process affects the mechanical properties and durability of concrete. As aforementioned, carbonation causes some disadvantages; however, most researchers evaluated the feasibility of NSS for concrete production without considering the effects of carbonation. Therefore, to fill this knowledge gap, the influence of chloride ion on the mechanical properties and durability performance of hardened concrete containing SCMs considering an accelerated carbonation was investigated in this study. Additionally, the influence of chloride ion on the fresh concrete properties was studied.

The study aims to investigate the effect of chloride ion as well as SCMs on the variation of fresh properties of concrete with time. Additionally, the effect of chloride ion and carbonation on the machenical properties and durability of concrete containing SCMs is studied. To fulfill the objectives of the investigation, NSS and desalted sea sand (DSS) concretes were prepared with a constant water-to-cementitious materials ratio of 0.50. FA and BFS were used to partially replace ordinary Portland cement with the ratios of 15% and 45% by mass, respectively. Non-desalted sea sand used as fine aggregate in this study was exploited from the Karatsu harbor in Saga prefecture, Japan. Meanwhile, DSS was obtained by removing salts from the NSS. The chloride ion content in NSS and DSS was 0.1968% and 0.0054% by mass of dry sand, respectively. Japanese standard specifies that the fine aggregate can be accepted for concrete production when chloride ion content is less than 0.04% by mass of dry sand or less than 0.3 kg/m^3 in the concrete; therefore, concrete specimens with OPC and DSS were considered as the reference concrete in this study. After mixing, the fresh concrete was divided into two parts: one part was used to measure the properties of the fresh concrete with time; the

other was cast into cylindrical plastic molds, of 100-mm diameter and 200-mm height, in two layers and compacted to reduce air voids. The surfaces of the specimens were smoothed and hermetically sealed with aluminum adhesive tape to prevent excessive water evaporation and carbonation. Then, all the concrete specimens were placed at 20 ± 2 °C for 28 days. After hermetically curing for 28 days, the cylindrical specimens were divided into two groups and cured under sealed and carbonation conditions until 182 days. The sealed specimens were continuously placed at 20 ± 2 °C, whereas those under the carbonation condition were completely demolded and placed in an accelerated carbonation chamber with 5% concentration of CO_2, 60% relative humidity, and 20 °C temperature. The mechanical tests were carried out to determine the compressive strength, and modulus of elasticity of specimens, to evaluate the effects of chloride ion, carbonation on mechanical properties of NSS concrete. In addition, the permeability, sorptivity, and carbonation depth tests were also conducted to assess the durability performance of NSS concrete containing supplementary cementitious materials. The chemical and microstructural tests such as thermogravimetry, scanning electron microscope, ion chromatography, and mercury intrusion microscopy (MIP) were also conducted to explain the results effectively. The various results observed in this study are given in the following paragraphs.

The results showed that the chloride ion in NSS had no influence on the slump loss and air content reduction of concrete for 60 min after mixing. Replacement of OPC by FA and BFS increased the initial slump of fresh concrete, even when NSS was used. Chloride ion in NSS not only accelerated cement hydration but also enhanced pozzolanic reactivity of FA and hydraulicity of BFS at early ages (i.e., 3 and 7 days), resulting in a significant increase in the compressive strength and elastic modulus of concrete. FA and BFS replacement reduced the early mechanical properties of concrete even in the presence of chloride ion. However, when FA and BFS contained together with the presence of chloride ion in NSS, their mechanical

properties were significantly improved after 182 days in comparison with the reference concrete under sealed condition.

Carbonation reduced the modulus of elasticity of FA and BFS concretes due to carbonation shrinkage. The use of NSS could restrict the reduction of modulus of elasticity of FA and BFS concretes under carbonation condition. The presence of chloride ion could maintain the compressive strength of FA and BFS concretes under carbonation condition compared with that of the reference concrete at 182 days. The FA and BFS replacements caused an increase in the carbonation coefficient of concrete. However, the presence of chloride ion in NSS could contribute to the improvement of carbonation resistance of concrete. Under the sealed condition, FA and BFS seemed to have a beneficial effect on the reduction of sorptivity of concrete due to the pozzolanic reaction of FA and hydraulicity of BFS. Sorptivity reduced more when FA or BFS concretes were produced using NSS. However, the carbonation shrinkage led to a significant increase in sorptivity of FA and BFS concretes in comparison with that of OPC-DSS concrete due to the formation of cracks. This could facilitate the penetration of water containing some aggressive ions (e.g. sulfate ions) which will affect the durability of FA or BFS concrete than OPC concrete. However, the presence of chloride ion in NSS could restrict the formation of cracks, resulting in the extensive durability of concrete. The chloride binding of concrete containing FA or BFS under sealed condition could be improved. However, it was remarkably decreased by carbonation. In conclusion, it should be emphasized that the NSS concretes showed better mechanical properties and durability performance than DSS concretes under both sealed and carbonation conditions regardless of SCMs replacement. The results found in this study contribute to the useful knowledge and discussion for verifying the applicability of NSS for concrete production while considering the effect of carbonation.

ACKNOWLEDGEMENT

First, I would like to express my deepest gratitude to my supervisor, Professor KENJI KAWAI, for his invaluable guidance and encouragement during the entire course of study, not only in research work, but also in the life. This dissertation could not be completed without his suggestions, comments, contributions and hard work.

I would also like to thank Professor KENICHIRO NAKARAI, Professor TOSHIROU HATA, and Professor TAKAAKI OOKUBO as my co-supervisors for their helpful advice and constant motivation throughout my research to obtain a high level of success.

I am indebted to Assistant Professor YUKO OGAWA for her kindness support, precious comments and contributions through all experiments. Her great support helped me to complete this thesis.

I greatly appreciate Assistant Professor RIYA CATHERINE GEORGE for her kind help to check the dissertation.

My gratitude also extends to Vietnamese Government and MienTrung University of Civil Engineering for supporting finance during my study at Hiroshima University.

I am very thankful to all members of Structure Materials and Concrete Structures laboratory of Hiroshima University for their cooperation and great help to conduct the experiments.

Finally, I would like to express my gratitude to my parents, my beloved family and friends for their encouragement and support for my study in Japan.

Dang Quoc Viet

Hiroshima University

March 2021

TABLE OF CONTENTS

LIST OF FIGURES

LIST OF TABLES

CHAPTER 1. INTRODUCTION

1.1. Background

Nowadays, concrete which is a composite material consisting of cement, coarse aggregate, fine aggregate, and water has become an important material in the construction industries due to its more significant characteristics than other materials such as high strength, easy mold in any forms, maintenance, flexible workability and good fire resistance. The great advantage of concrete will be excellent mechanical and physical properties if it is properly designed and manufactured. It has been predicted that the demand for concrete will reach approximately 18 billion tons per year by 2050 [1]. The river sand is the most widely used fine aggregate in concrete production. The rapidly increasing demand for concrete production requires a large amount of fine aggregate which in general is natural sand exploited from quarries or alluvial rivers. However, these resources of natural sand are in the process of critical depletion and their extraction also has harmful consequences for the environment, including increasing in river beds, lowering water level, and intruding salinity into rivers [2]. Under the circumstance, the application of alternative materials for replacing RS is vitally important for concrete production in an environmentally friendly manner. As one possible solution, the non-desalted sea sand (NSS) becomes a potential candidate because of its abundance in coastal areas in order to avoid the high consumption of RS.

Non-desalted sea sand or dredged marine sand is the natural sand that is found in the sea or dredged from the seabed. It can be used as a fine aggregate in concrete production after appropriate desalting treatments. The washing by freshwater is offered the most suitable method in order to reduce the salts of NSS. However, the use of freshwater for washing NSS causes a serious impact on those areas in which freshwater is a scarce resource, especially in coastal areas. Additionally, according to the report of the World Meteorological Organization, more

than half of the world population would not be able to get enough drinking water by 2025. Freshwater will be very difficult to obtain in some regions in the world [3]. Therefore, the utilization of sea sand without desalting (i.e., NSS) in concrete production is not only in saving freshwater but also reduces the cost of construction in coastal areas by taking advantage of local materials. Nevertheless, the most important ion in NSS is chloride which affects the mechanical properties and durability of concrete, leading to the applicability of NSS for concrete production.

Chloride ion in NSS is the primary reason for its limitation in reinforced-concrete structure. The investigation of NSS for concrete production has been reported by several researchers [4–11]. One important issue has been debating that the undesirable ion in NSS, e.g., chloride ion, may lead to a detrimental effect on the mechanical properties of NSS concrete. Rachid Zentar [4] and Vincent Dubois [5] have proposed that the marine dredged sand was a potential material in road construction for the base and sub-base of pavement. Other researchers concluded that NSS can be successfully used as a fine aggregate for plain concrete production when crushed limestone sand is partially substituted by NSS at 15% to 50% [6–8]. On the contrary, some researchers conducted experiments on NSS as fine aggregate for concrete production and concluded that the compressive strength of NSS concrete at 28 days was lower than that of RS concrete [9–11]. Tulashie et al. [11] even recommended that NSS should not be used as a construction material because of its adverse effects on the compressive strength of concrete.

Supplementary cementitious materials (SCMs) such as fly ash, ground granulated blast furnace slag, metakaolin, silica fume were widely used in concrete as a partial replacement of ordinary Portland cement (OPC) [12–15]. One of the primary reasons for the use of SCMs in concrete production is to reduce the environmental impact by utilizing the industrial by-products and declining the cement usage. Supplementary cementitious materials, which are essential components in concrete mixtures, are used as partial replacements for clinker in cement or cement in concrete. The addition of SCMs improves the long-term mechanical

properties and durability of concrete under sealed condition [16–20]. However, concrete containing SCMs is very sensitive to carbonation which is a process of atmospheric carbon dioxide penetrating into cementitious materials [21–24]. The carbonation can not only decompose the solid Friedel's salt [25–27] but also react with the calcium bearing phase of concrete, resulting in the change in the microstructure of concrete [24,28–33]. Moreover, the carbonation resulted in the formation of microcracks [24,31,33–35]. As a consequence, the carbonation process affects the mechanical properties and durability of concrete.

Xiao et al. [36] recently reviewed existing studies on the effect of NSS and/or seawater as raw materials on the properties of concrete; however, there are limited data concerning the influence of chloride ion in NSS on the properties of fresh and hardened concretes incorporating SCMs, especially considering carbonation. The review [36] concluded that further study on the contribution of SCMs to the mechanical properties and durability of concrete is necessary for a better understanding of their effects on the properties of NSS concrete.

Based on the aforementioned background, this study is conducted to explore the applicability of NSS for the production of concrete under considering carbonation effect.

1.2. Objectives

This study aims to evaluate the effect of chloride ion in NSS on the properties of fresh and hardened concrete incorporating SCMs under carbonation condition. To achieve the aim, the fresh properties as well as mechanical and durability performance of hardened concrete using NSS is evaluated by considering the effects of carbonation and chloride ion in NSS as well as SCMs.

The main objectives of this study are:

- To study the effect of chloride ion in NSS as well as SCMs on the variation of fresh properties of concrete with time.

- To study of the effect of chloride ion and carbonation on the mechanical properties and durability of NSS concrete incorporating SCMs.

1.3. Methodology

Non-desalted sea sand (NSS) was used as fine aggregate in concrete production. The SCMs including fly ash (FA) and ground granulate blast furnace slag (BFS) were used to partially replace OPC with a dosage of 15% and 45% by mass, respectively. On the other hand, desalted sea sand (DSS) was also used for making the reference concrete. After sealing for 28 days, half of the specimens were continued to be sealed and placed on a controlled room at 20 ^{o}C, whereas the remained specimens were exposed to accelerated carbonation at 20 ^{o}C, 5% CO_2, and 60% relative humidity until 182 days.

The fresh properties (slump, air content), mechanical properties (compressive strength and modulus of elasticity), and durability performance of concrete, namely water permeability, sorptivity, carbonation depth, were evaluated. The thermogravimetric and differential thermal analysis, mercury intrusion porosimetry, scanning electronic microscope, and fluorescent dye were used to assess the hydration process, pore structure, microstructure, and cracking on the surface in order to explain the effects of chloride ion in NSS, SCMs, and carbonation on the obtained results.

1.4. Dissertation outline

The structure of the dissertation outline is shown in Fig. 1.1. which includes seven chapters as follows:

Chapter 1 describes the background of this study. Also, the objectives and methodology of this study are listed.

Chapter 2 presents a brief literature review on the investigation of sea-sand concrete. Some factors relative to the strength and durability of sea-sand concrete are viewed. The contribution to the mechanical properties and durability of concrete of mineral admixtures such as FA and BFS is also expressed.

Chapter 3 illustrates the experimental program of this study, including the materials and mixture proportions, the mixing and casting progress, and the curing conditions. All measurements were performed to study the effects of chloride ion in NSS, carbonation, and SCMs on the mechanical properties and durability of NSS concrete.

Chapter 4 Verifies the applicability of NSS for concrete production by investigating the effect of chloride ion in SS on the properties of fresh and hardened concrete containing supplementary cementitious materials.

Chapter 5 evaluates the mechanical properties of NSS concrete containing supplementary cementitious materials in terms of compressive strength and elasticity modulus by considering accelerated carbonation.

Chapter 6 discusses the effect of chloride ion in NSS on the durability of concrete containing supplementary cementitious materials under carbonation influence by testing the carbonation resistance, permeability, sorptivity, and chloride binding.

Chapter 7 expresses the conclusions of this study. The recommendations for future works are also proposed.

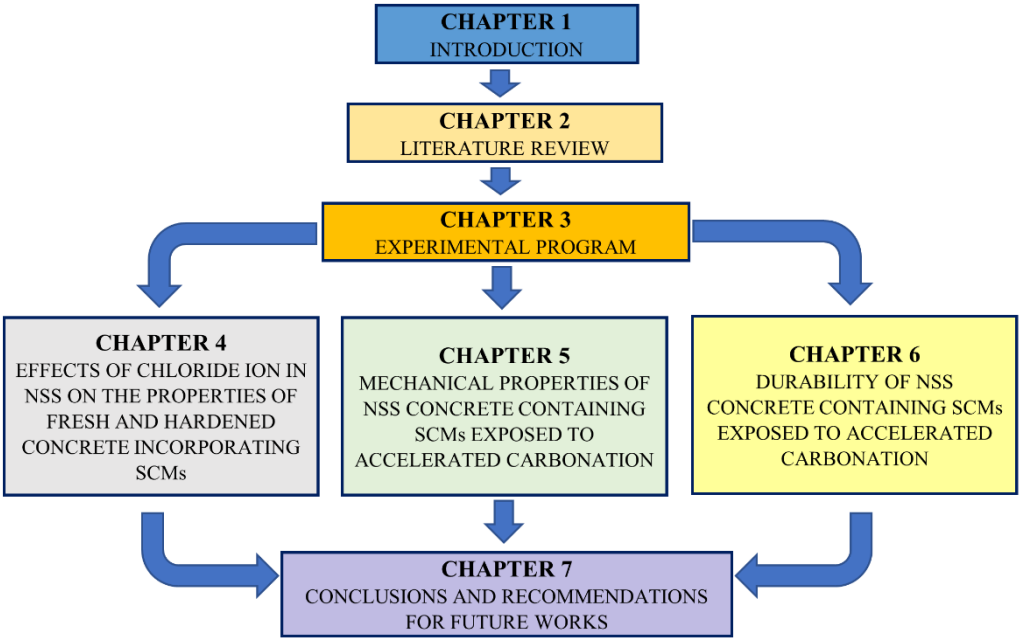

Fig. 1.1. Organization of dissertation

References of chapter 1:

[1] P. K. Mehta, P. J. M. Monteiro, Concrete: Microstructure, Properties, and Materials, Fourth Edition, (2014).

[2] F. J. Luo, L. He, Z. Pan, W. H. Duan, X. L. Zhao, F. Collins, Effect of very fine particles on workability and strength of concrete made with dune sand, Constr. Build. Mater. 47 (2013) 131–137.

[3] T. Nishida, N. Otsuki, H. Ohara, Z. M. Garba-Say, T. Nagata, Some considerations for applicability of seawater as mixing water in concrete, J. Mater. Civ. Eng. 27 (2015) 1–7.

[4] R. Zentar, V. Dubois, N.E. Abriak, Mechanical behaviour and environmental impacts of a test road built with marine dredged sediments, Resour. Conserv. Recycl. 52 (2008) 947–954.

[5] V. Dubois, N. E. Abriak, R. Zentar, G. Ballivy, The use of marine sediments as a pavement base material, Waste Manag. 29 (2009) 774–782.

[6] W. Liu, Y. J. Xie, B. Q. Dong, F. Xing, Study on characteristics of dredged marine sand and the mechanical properties of concrete made with dredged marine sand, Bull. Chin. Ceram. Soc. 33 (2014) 15–22.

[7] J. Limeira, M. Etxeberria, L. Agulló, D. Molina, Mechanical and durability properties of concrete made with dredged marine sand, Constr. Build. Mater. 25 (2011) 4165–4174.

[8] P. Ozer-Erdogan, H. M. Basar, I. Erden, L. Tolun, Beneficial use of marine dredged materials as a fine aggregate in ready-mixed concrete: Turkey example, Constr. Build. Mater. 124 (2016) 690–704.

[9] W. S. Deepak, Effect on compressive strength of concrete using sea sand as a partial replacement for fine aggregate, Int. J. Res. Eng. Technol. 04 (2016) 180–183.

[10] R. Mahendran, K. Godwin, T. G. Selvan, M. Murugan, Experimental study on concrete using sea sand as fine aggregate, 7 (2016) 4.

[11] S. K. Tulashie, F. Kotoka, D. Mensah, A. K. Kwablah, Investigation of the compressive strength of pit sand, and sea sand mortar prisms produced with rice husk ash as additive, Constr. Build. Mater. 151 (2017) 383–387.

[12] B. Lothenbach, K. Scrivener, R.D. Hooton, Supplementary cementitious materials, Cem. Concr. Res. 41 (2011) 1244–1256.

[13] M. C. G. Juenger, R. Siddique, Recent advances in understanding the role of supplementary cementitious materials in concrete, Cem. Concr. Res. 78 (2015) 71–80.

[14] M. A. Megat Johari, J. J. Brooks, S. Kabir, P. Rivard, Influence of supplementary cementitious materials on engineering properties of high strength concrete, Constr. Build. Mater. 25 (2011) 2639–2648.

[15] M. D. A. Thomas, R. D. Hooton, A. Scott, H. Zibara, The effect of supplementary cementitious materials on chloride binding in hardened cement paste, Cem. Concr. Res. 42 (2012) 1–7.

[16] P. Duan, Z. Shui, W. Chen, C. Shen, Effects of metakaolin, silica fume and slag on pore structure, interfacial transition zone and compressive strength of concrete, Constr. Build. Mater. 44 (2013) 1–6.

[17] F. Deschner, F. Winnefeld, B. Lothenbach, S. Seufert, P. Schwesig, S. Dittrich, F. Goetz-Neunhoeffer, J. Neubauer, Hydration of Portland cement with high replacement by siliceous fly ash, Cem. Concr. Res. 42 (2012) 1389–1400.

[18] E. Güneyisi, M. Gesoğlu, E. Booya, K. Mermerdaş, Strength and permeability properties of self-compacting concrete with cold bonded fly ash lightweight aggregate, Constr. Build. Mater. 74 (2015) 17–24.

[19] P. Sharmila, G. Dhinakaran, Compressive strength, porosity and sorptivity of ultra fine slag based high strength concrete, Constr. Build. Mater. 120 (2016) 48–53.

[20] A. Hadjsadok, S. Kenai, L. Courard, F. Michel, J. Khatib, Durability of mortar and concretes containing slag with low hydraulic activity, Cem. Concr. Compos. 34 (2012) 671–677.

[21] V. Shah, S. Bishnoi, Carbonation resistance of cements containing supplementary cementitious materials and its relation to various parameters of concrete, Constr. Build. Mater. 178 (2018) 219–232.

[22] E. Gruyaert, P. Van den Heede, N. De Belie, Carbonation of slag concrete: Effect of the cement replacement level and curing on the carbonation coefficient – Effect of carbonation on the pore structure, Cem. Concr. Compos. 35 (2013) 39–48.

[23] B. Šavija, M. Luković, Carbonation of cement paste: Understanding, challenges, and opportunities, Constr. Build. Mater. 117 (2016) 285–301.

[24] P. H. R. Borges, J. O. Costa, N. B. Milestone, C. J. Lynsdale, R. E. Streatfield, Carbonation of CH and C–S–H in composite cement pastes containing high amounts of BFS, Cem. Concr. Res. 40 (2010) 284–292.

[25] W. Liu, H. Cui, Z. Dong, F. Xing, H. Zhang, T.Y. Lo, Carbonation of concrete made with dredged marine sand and its effect on chloride binding, Constr. Build. Mater. 120 (2016) 1–9.

[26] H. Chang, Chloride binding capacity of pastes influenced by carbonation under three conditions, Cem. Concr. Compos. 84 (2017) 1–9.

[27] G. Villain, M. Thiery, G. Platret, Measurement methods of carbonation profiles in concrete: Thermogravimetry, chemical analysis and gammadensimetry, Cem. Concr. Res. 37 (2007) 1182–1192.

[28] B. Wu, G. Ye, Development of porosity of cement paste blended with supplementary cementitious materials after carbonation, Constr. Build. Mater. 145 (2017) 52–61.

[29] M. Auroy, S. Poyet, P. Le Bescop, J. M. Torrenti, T. Charpentier, M. Moskura, X. Bourbon, Comparison between natural and accelerated carbonation (3% CO2): Impact on mineralogy, microstructure, water retention and cracking, Cem. Concr. Res. 109 (2018) 64–80.

[30] V. T. Ngala, C. L. Page, Effects of carbonation on pore structure and diffusional properties of hydrated cement pastes, Cem. Concr. Res. 27 (1997) 995–1007.

[31] G. Rimmelé, V. Barlet-Gouédard, O. Porcherie, B. Goffé, F. Brunet, Heterogeneous porosity distribution in Portland cement exposed to CO2-rich fluids, Cem. Concr. Res. 38 (2008) 1038–1048.

[32] A. Morandeau, M. Thiéry, P. Dangla, Impact of accelerated carbonation on OPC cement paste blended with fly ash, Cem. Concr. Res. 67 (2015) 226–236.

[33] M. Auroy, S. Poyet, P. Le Bescop, J. M. Torrenti, T. Charpentier, M. Moskura, X. Bourbon, Impact of carbonation on unsaturated water transport properties of cement-based materials, Cem. Concr. Res. 74 (2015) 44–58.

[34] A. Fabbri, J. Corvisier, A. Schubnel, F. Brunet, B. Goffé, G. Rimmele, V. Barlet-Gouédard, Effect of carbonation on the hydro-mechanical properties of Portland cements, Cem. Concr. Res. 39 (2009) 1156–1163.

[35] M. Nedeljković, B. Šavija, Y. Zuo, M. Luković, G. Ye, Effect of natural carbonation on the pore structure and elastic modulus of the alkali-activated fly ash and slag pastes, Constr. Build. Mater. 161 (2018) 687–704.

[36] J. Xiao, C. Qiang, A. Nanni, K. Zhang, Use of sea-sand and seawater in concrete construction: Current status and future opportunities, Constr. Build. Mater. 155 (2017) 1101–1111.

CHAPTER 2. LITERATURE REVIEW

This chapter demonstrates a brief literature review on the effects of the usage of non-desalted sea sand (NSS) on the mechanical properties and durability of concrete. Additionally, the effects of supplementary cementitious materials (SCMs) and carbonation on the mechanical properties and chemical reaction of concrete are also presented.

2.1. Non-desalted sea sand concrete

2.1.1. Usage of non-desalted sea sand

The rapid growth of the world's population, as well as infrastructures has led to a remarkable increase in the construction industry in recent decades. Because of the lack of river sand (RS), NSS has been widely used as a raw material in industrial and residential buildings. More than 90% of the dredged NSS of the world has been used as construction material, among which about 20% is used for base and sub-base of pavement, and over 45% is used as fine aggregate in concrete production [1].

The exploitation and usage of marine aggregates have considerably taken place in different countries all over the world, with the largest producers being Japan, the Netherlands, and Hong Kong [2]. In many Asian countries, the extraction activities of marine sand have happened since the early 1970s. In Japan, marine sand has been mainly used as fine aggregate in the manufacturing of concrete since the 1970s [3]. As the report of Jianzhuang Xiao [1], approximately 8.54 million tons of marine sand was used in Japan for producing ready-mixed concrete in 2011. Additionally, approximately 3 million m^3 of marine aggregates are excavated annually in Turkey, whereas the total amount of marine sand exploited in 2011 was 30.5 million m^3 in China. It was estimated that the annual demand for marine sand in China would be over

55 million m^3 per year because of the massive reclamation projects such as new airports, buildings, apartments, seaports, roads, and other infrastructures [4].

Looking forward, marine aggregates will be expected to play an important role in the success of major infrastructure projects, especially in the construction industry. A huge dredged marine sand has been used widely in many fields such as beach replenishments, coastal protections, land reclamations, and civil constructions. As an example, for land reclamation, the Hong Kong international airport is located on a large artificial island of Chek Lap Kok which was built in 1998 with dredged marine aggregates [5]. According to the report of ICES WGEXT in 2017 [6], the most extracting country is the Netherlands with approximately 16 million tons of marine aggregates, followed by the United Kingdom, Denmark, and United States. While the United Kingdom uses most of the extracted marine aggregates for the construction industry, the Netherlands uses only approximately 40% for building purposes and the rest for beach replenishments or coastal protections [6,7].

The overview of marine sand extracted is presented in Fig 2.1 [2], where the dredged marine sand is mostly used as a raw material in many fields such as the construction industry, beach replenishment, shore protection, land reclamation, city expansion, etc.

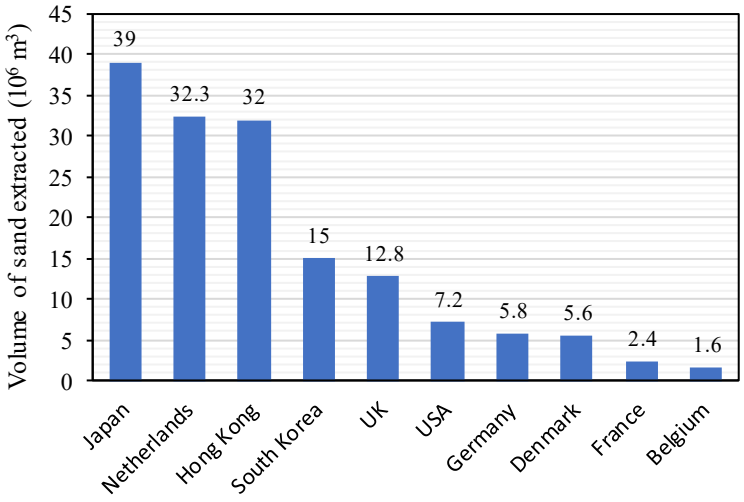

Fig. 2.1. Sand extracted from coastal areas around the world [2]

(Data sources: Japan, from 1998; Hong Kong, averaged over 1990-98; South Korea, averaged over 1993-95; Germany, from 2000; other countries, from 2000.)

2.1.2. Limitation of chloride ion content in reinforced concrete structure

Chloride ion in NSS is the primary reason for its limitation in the reinforced concrete structure. However, in case of unavoidable circumstances, NSS without treatments can be used as fine aggregate for concrete production, not only for plain concrete but also for reinforced concrete. Therefore, to control the corrosion of reinforced concrete caused by the direct use of NSS, many countries have established the limitation of chloride content in NSS. For example, Japanese code JASS 5 specifies that NSS is usable as a fine aggregate when the chloride ion content (calculated based on the content of sodium chloride) in NSS is less than 0.04% by mass of the dry sand and/or less than 0.3 kg/m^3 for all types of concrete [8]. Besides, the maximum permissiable chloride ion content of 0.3 kg/m^3 for ready-mixed concrete is also regulated by Japanese Industrial Standard (JIS) A 5308 [9]. On the other hand, British standard BS 882-1992 [10] has regulated the chloride content not only in the marine aggregate but also in coarse aggregate according to the type of concrete. In practice, the total chloride content in aggregates has been regulated for four applications of concrete: 0.01% for pre-stressed concrete and steam-

cured structural concrete, 0.03% for reinforced concrete made with sulfate-resisting Portland cement, 0.05% for structural concrete, and no regulation for other concrete without embedded steel bar. However, the BS EN 206 [11] which was published in 2013 to replace BS 882-1992 [10] has removed the limit values of the chloride content in marine aggregates. The total chloride content in concrete (expressed as the percentage of chloride ions by mass of cement) is used as an alternative parameter to control the chloride content from marine aggregates, water, and cement. Specifically, the maximum total chloride content in concrete shall not exceed 0.2%, 0.4%, and 1% for pre-stresses concrete, reinforced concrete, and concrete without embedded steel bar, respectively. In addition, according to Chinese standard JGJ 206 [12], marine sand cannot be used for pre-stressed concrete and the maximum permissible chloride content is 0.03 mass% of dry sand. While Japanese standard [8] and British standard [11] have regulated the chloride content in concrete without embedded steel bar, the current Hong Kong standard CS3 [13] has not limited the chloride content for concrete containing no embedded metal. It can be noticed that the limit values of chloride content are still significantly different among countries for plain and reinforced concrete. The comparison in the limitation of chloride ion content used for concrete among different countries was shown in Table 2.1.

Table 2.1. Limitation of chloride ion content in NSS among different countries

Country	Standard	Limit Cl^- in NSS %	Application
Japan	JASS 5	≤ 0.04	All concrete
British	BS 206	≤ 0.01	Pre-stresses concrete and steam-cured concrete
		≤ 0.03	Reinforced concrete using sulfate resisting Portland cement
		≤ 0.05	Reinforced concrete using other cement
		No limit	Other concrete without embedded metal
China	JGJ 206	0.03	Reinforced concrete using other cement
		Prohibition	Pre-stresses concrete and steam-cured concrete
Hong Kong	CS3	≤ 0.01	Pre-stresses concrete and steam-cured concrete
		≤ 0.03	Reinforced concrete using sulfate resisting Portland cement
		≤ 0.05	Reinforced concrete using other cement
		No limit	Other concrete without embedded metal

2.1.3. Mechanical properties and durability of non-desalted sea sand concrete

It should be noted that the NSS from different coastal areas will have different gradings. This is due to the formative condition of regions. The typical gradings of some different sea sands which were used as fine aggregate for concrete production are compared in Fig. 2.2 [14–17]. As shown in Fig. 2.2, there is a difference in the size distribution of NSS from various locations. Compared to the limit curves specified by JIS A 1102 [18], it should be noted that the gradings of NSS from some areas may not satisfactory and need a treatment before applying for concrete production. The variety in fineness modulus values is ranging from 1.57 to 2.85.

Additionally, the chloride ion content in NSS also varies with the sand extraction location, as shown in Table 2.2.

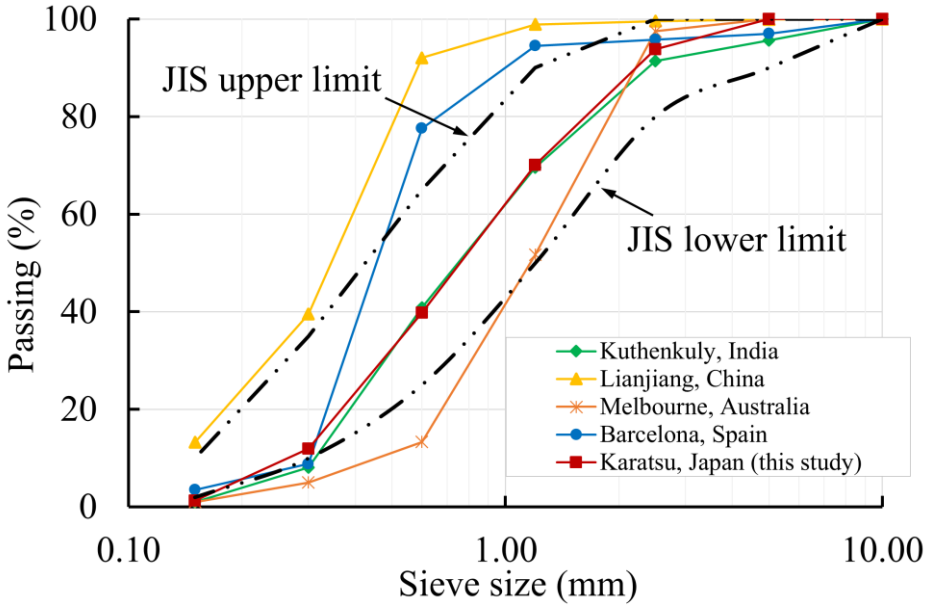

Fig. 2.2. Typical gradings of sea sands from different regions (synthesized from Ref. [14–17])

Table 2.2. Typical chloride ion content in sea sands of various regions

Region	Chloride ion content (mass% of dry sand) %	Ref.
Kuthenkuly, India	0.34	[14]
Lianjiang, china	0.289	[15]
Melbourne, Australia	0.13	[16]
Barcelona, Spain	0.10	[17]

The applicability of NSS as construction materials has been carried out by several researchers [15–17,19–23]. Zentar et al. [19] and Dubois et al. [20] have proposed that the dredged marine sand was a potential material in road construction for the base and sub-base of cement concrete pavement. There is a controversy in the conclusion related to the use of NSS for concrete production. Limeira et al. [17,21] concluded that NSS can be satisfactorily used as a fine

aggregate for plain concrete production when 15% to 50% of crushed limestone sand was replaced by NSS. For example, the normalized compressive strength of concrete with NSS compared to the reference concrete is shown in Fig. 2.3. [17]. Chen et al. [15] and Xu et al. [22] demonstrated that the interfacial transition zone (ITZ) of sulphoaluminate cement concrete with NSS was enhanced by the formation of Friedel's salt, leading to the improvement of its mechanical properties when compared with those of concrete with river sand. The improvement of ITZ was shown in Fig. 2.4 [15]. The residual strength of NSS concrete exposed to high temperature was generally similar to that of river sand concrete [16]. Yang et al. [23] investigated the alkali-activated slag concrete with NSS and reported that although its drying shrinkage was slightly higher, its chloride ion permeability resistance was better than that with the river sand concrete due to the more hydration products [23].

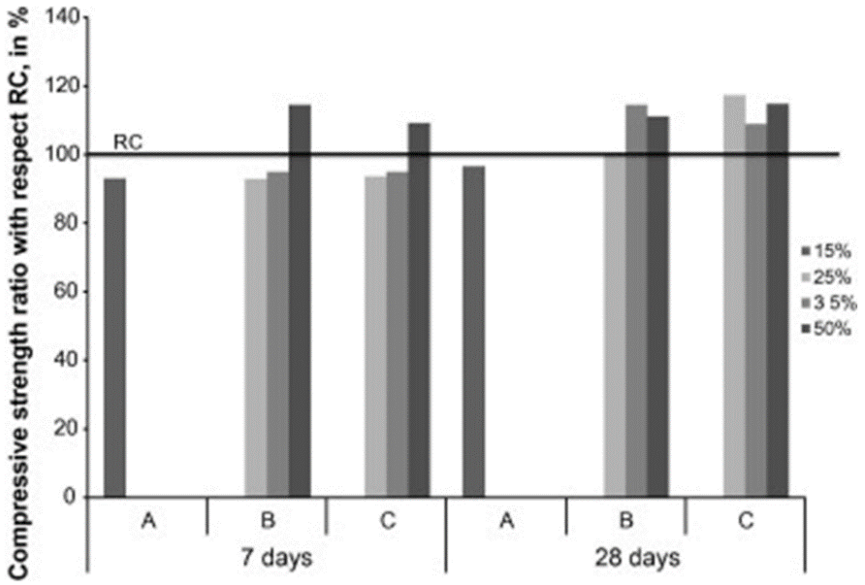

Fig. 2.3. Compressive strength ratio of NSS concretes (three types of NSS: A, B, C) with respect to that of reference concrete (RC) in % [17]

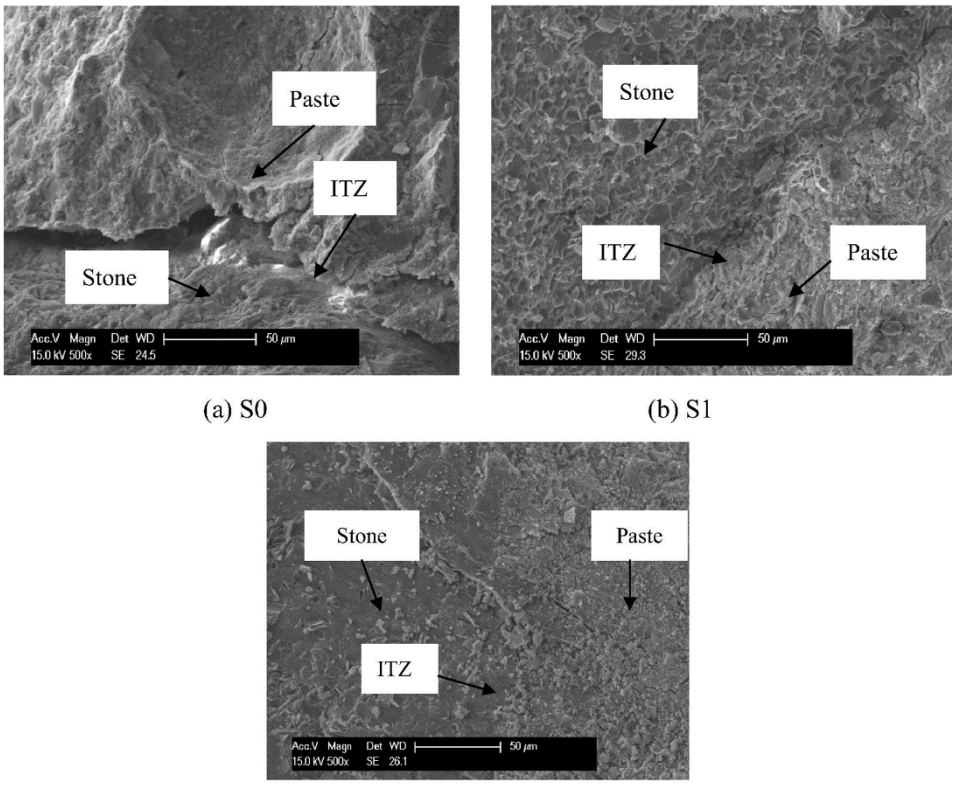

(a) S0 (b) S1

(c) S4

Fig. 2.4. Interfacial transition zone (ITZ) of concrete [15]; S0 denotes concrete made of Portland cement, river sand and fresh water; S1 denotes concrete made of sulphoaluminate cement, river sand and fresh water; S4 denotes concrete made of sulphoaluminate cement, marine sand and sea water.

Conversely, some researchers have adverse conclusions against the usage of NSS as a fine aggregate for concrete production [24–28]. Girish et al. [24] demonstrated that the compressive strength of NSS concrete at 28 days was lower than that of river sand concrete. It is also observed by other studies [25–27]. Tulashie et al. [27] has shown that the compressive strength of NSS cement mortar prisms decreases steeply on the 7^{th} and 28^{th} day (see Fig. 2.5), especially concrete containing rice husk. In addition, Çağatay [28] demonstrated that the usage of NSS for concrete production has a detrimental effect on the long-term compressive strength of concrete. Tulashie et al. [27] and Çağatay [28] also recommended that NSS should not be used as fine

aggregate for concrete production because of its adverse effects on the compressive strength of concrete.

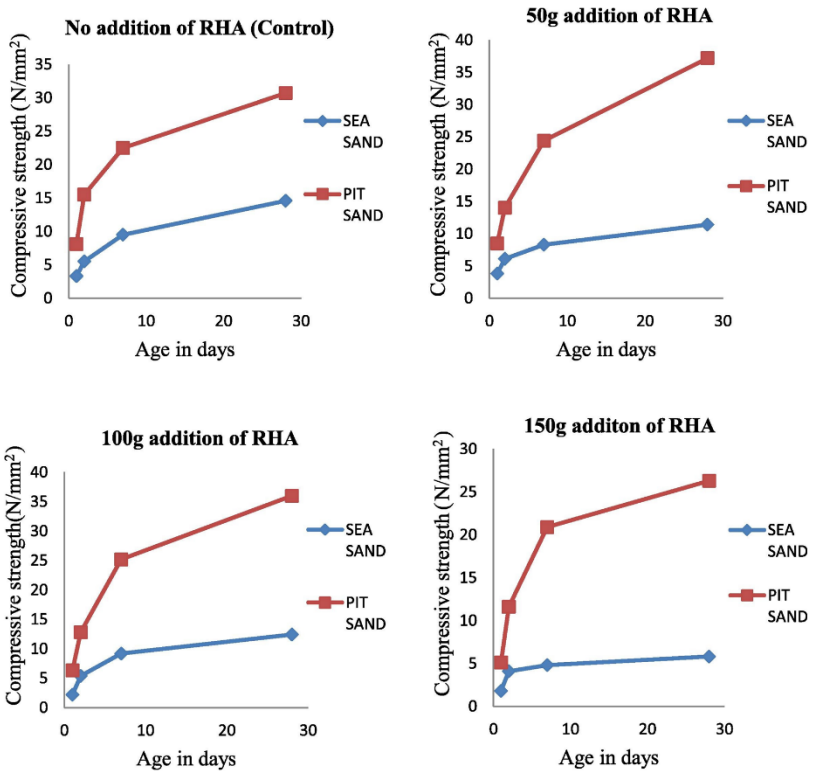

Fig. 2.5. Comparison of the compressive strength of pit sand and NSS cement mortar prisms [27]

Two popular factors that affect the durability of concrete are sulfate and carbonation. Yao [29] found that the sulfate resistance of NSS concrete was inferior to that of reference concrete. Meanwhile, Yang et al. [30] concluded that the new artificial reef concrete (NARC) preparing with sulphoaluminate cement, NSS, and seawater exhibited less compressive strength loss and mass change due to sulfate attack compared to ordinary Portland cement concrete (OPCC), as shown in Fig. 2.6. Regarding carbonation, Jiang et al. [31] claimed that the NSS concrete had the same carbonation depth development as that of river sand concrete. Kim et al. [32] claimed, after conducting the investigation for 15 years under natural carbonation condition, that the

carbonation depth of concrete increased as their chloride ion content increased. Conversely, Liu et al. [33] reported that the presence of chloride ion could reduce the carbonation coefficient of NSS concrete by 20%–50% in comparison with river sand concrete as shown in Fig. 2.7.

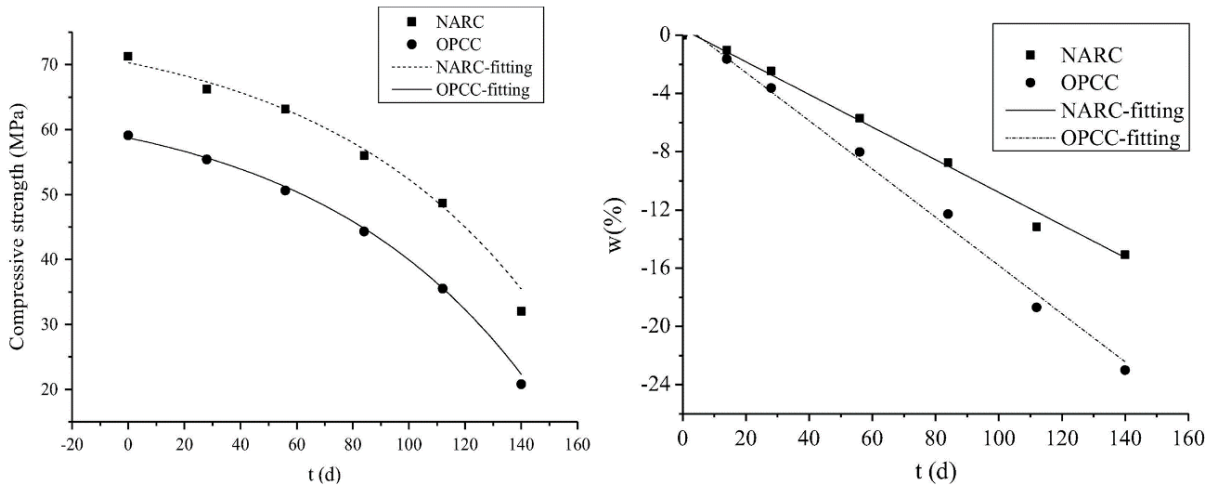

(a) Compressive strength loss (b) Mass change

Fig. 2.6. Compressive strength loss and mass change of concrete under the attack by biogenic sulfuric acid [30]

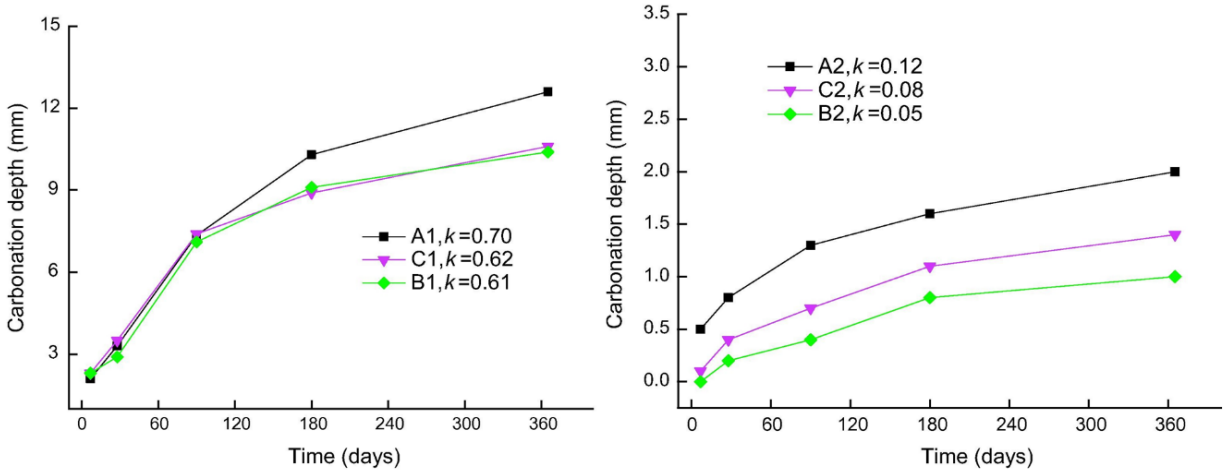

(a) Concretes with W/C=0.47, cement 360 kg/m^3 (b) Concretes with W/C =0.35, cement 460 kg/m^3

Fig. 2.7. Comparison of carbonation for concretes made with different sands [33]; For concretes with W/C=0.47, A_1, B_1, and C_1 were concretes made with river sand, dredged marine sand, and washed dredged marine sand, respectively; For concretes with W/C=0.35, A_2, B_2, and C_2 were concretes made with river sand, dredged marine sand, and washed dredged marine sand, respectively;

It is a fact that the chloride ion in NSS has a notable effect on the corrosion of steel bars in reinforced concrete. Dias et al. [34] concluded that the corrosion of steel bar became significant when the free chloride ion content in NSS concrete reached 0.3% by mass of cement after conducting the accelerated corrosion test and changing the chloride ion content in SS. Meanwhile, Liu et al. [35] illustrated that the steel bar in NSS concrete should be safe from corrosion when the free chloride ion content in NSS is less than 0.18% or the total chloride ion content in concrete is less than 0.34%. It means that if the chloride ion content in NSS reaches the limitation by current standards, NSS can be still safely used as fine aggregate in the reinforced concrete structure under normal atmospheric condition. On the other hand, several experiments on the availability of NSS concrete reinforced by fiber-reinforced polymer (FRP) bars instead of steel bars were carried out to avoid corrosion because FRP bars can show excellent corrosion resistance [36–40]. It was concluded that NSS can be a satisfactory

alternative material because FRP bars were not seriously damaged by chloride ions in comparison with steel bars. In addition, chloride ions in NSS could also improve the interfacial bonding performance between FRP bars and materials [36–39]. It can be clearly observed by Dong et al. [39] as shown in Fig. 2.8.

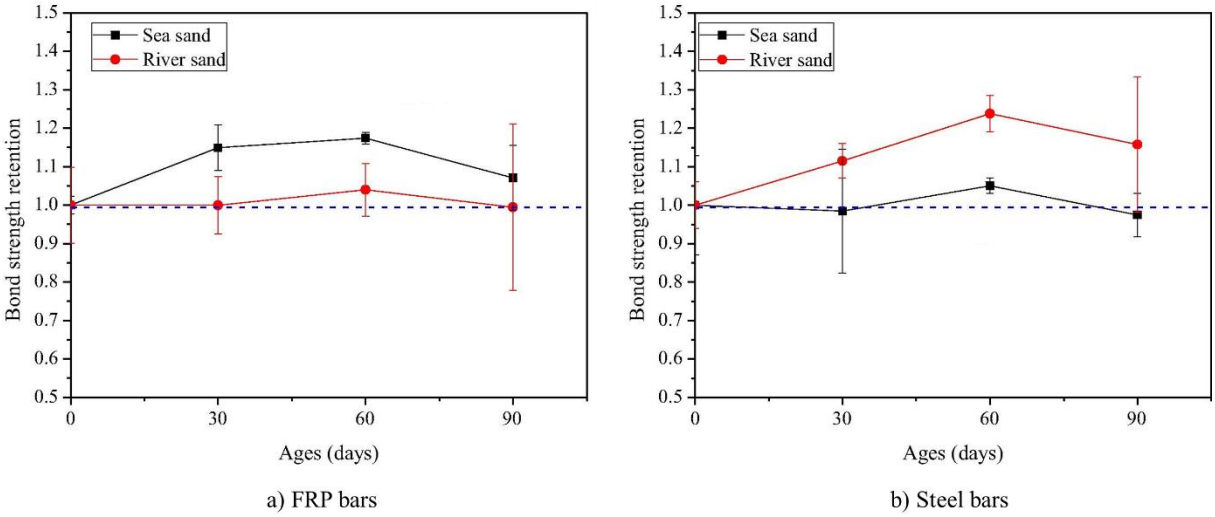

Fig. 2.8. Changes of bond strength in two types of concrete [39]

2.2. Effects of fly ash or ground granulated blast furnace slag on the properties of fresh and hardened concrete

The second most used substance in the world after water is cement. It is one of the most important and basic building materials for the infrastructure of modern society. The principal material made from cement is concrete that was applied in many construction fields such as dams, roads, railways, architectural innovative skyscrapers, high-rise apartments. In the year 2013, approximately 4 billion tons of cement were produced in the world [41]. The growing demand for concrete per year will lead to a remarkable increase in cement production. It is estimated that around 7% of the total global CO_2 emissions is due to the Portland clinker production which is the elementary cement component [42]. In recent years, the production of blended cement or the partial replacement of cement with supplementary cementitious materials

such as ground granulated blast furnace slag (BFS) or fly ash (FA) is widely used to eliminate the environmental impact. The utilization of SCMs could improve the mechanical properties, durability as well as chloride binding of concrete [43–58]. However, these mineral admixtures were very sensitive to the carbonation, leading to the significant influence of durability of concrete [59–65].

Fly ash is one of the residues which is generated by coal combustion for electricity and heat production, and it can either be siliceous (low calcium FA) or calcareous (high calcium FA), depending on the coal type, and consist primarily of glassy spheres with some crystalline matter and unburnt carbon [66]. Blast furnace slag is generated by melting the waste rock from iron ore (mainly silicon and aluminum compounds) at the temperature of 1300 ÷ 1500 °C, with calcium and magnesium compounds from the composition of fluxes (limestone, dolomite) and residues from the combustion of coke. Chemical and physical properties (including activity) of BFS depend on the type of raw material used (ore, fluxes, fuel) and the blast furnace process [66].

It was reported that concrete containing FA showed better workability due to the increased content of fine fraction in the concrete composition [43,54,55,66]. Meanwhile, the improvement in workability of concrete incorporating with BFS was most frequently associated with the smooth surface of slag grain (glassy phase) and less chemical activity compared to cement [43,54,55,67]. The presence of FA or BFS in concrete also contributed to a significant reduction of bleeding and segregation from the concrete mixture [55,67]. Moreover, the reduction of the kinetics of heat production rate was shown in Fig. 2.9 when cement was replaced by FA or BFS [68]. This can allow the concrete structure to avoid the cracks caused by thermal stresses.

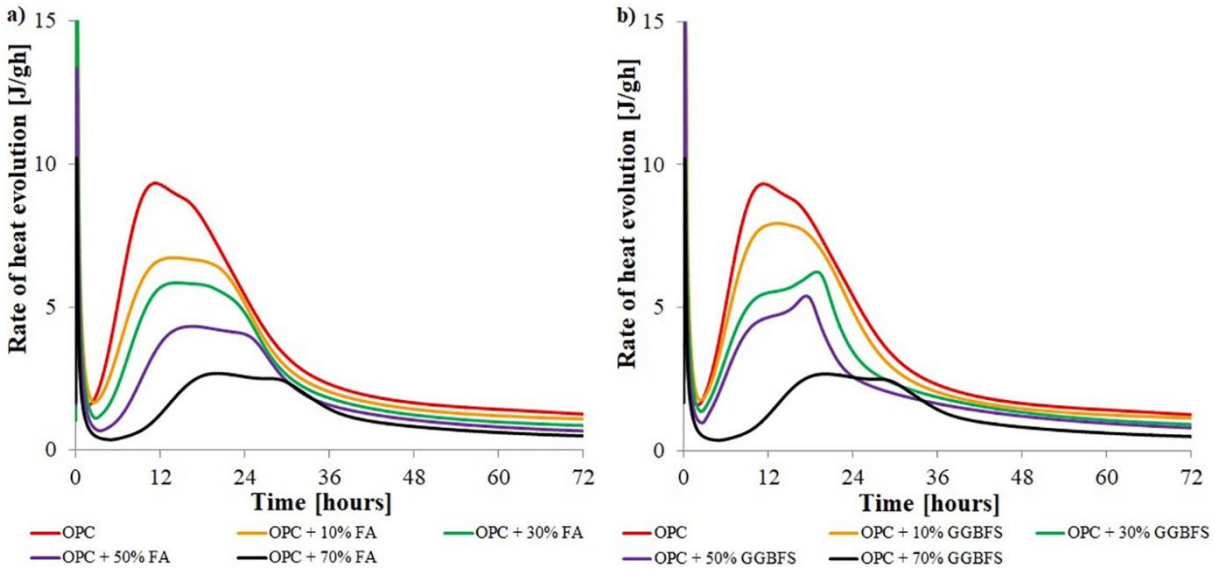

Fig. 2.9. Impact of FA (a) and BFS (b) replacement on heat release of cement [68]

A visible enhancement on long-term mechanical properties and durability of concrete mixtures containing FA or BFS was found by many studies [43–46,49,54,55,69]. Normally, when replacing a part of cement with FA or BFS, the early-age compressive strength of concrete was reduced due to the lower activity. The lower early compressive strength depends on many factors such as fineness, chemical composition, water to binder ratio and curing temperature. However, concrete with the proper addition of FA or BFS achieved later-age compressive strength similar to or even higher than those of concrete with Portland cement [43,54,55]. This fact is shown in Fig 2.10. This is due to the pozzolanic reaction effect of FA and hydraulicity of BFS. Calcium hydroxide, produced from the cement hydration, is consumed and formed calcium silicate hydrate (C–S–H) or calcium aluminate hydrate (C–A–H), as shown in Eqs. (2.1) and (2.2) [70]. On the other hand, the long-term durability of concrete containing FA or BFS increased. This is related to the progressive filling of the pores with the C-S-H phase from the pozzolanic reaction of FA or hydraulicity of BFS, leading to the improvement bonding between paste and aggregate and more compact microstructure [43–45,49,50,54,55].

$$xCa(OH)_2 + xSiO_2 + nH_2O = xCaO \cdot SiO_2 \cdot (x+n)H_2O \quad (2.1)$$

$$xCa(OH)_2 + xAl_2O_3 + nH_2O = xCaO \cdot Al_2O_3 \cdot (x+n)H_2O \quad (2.2)$$

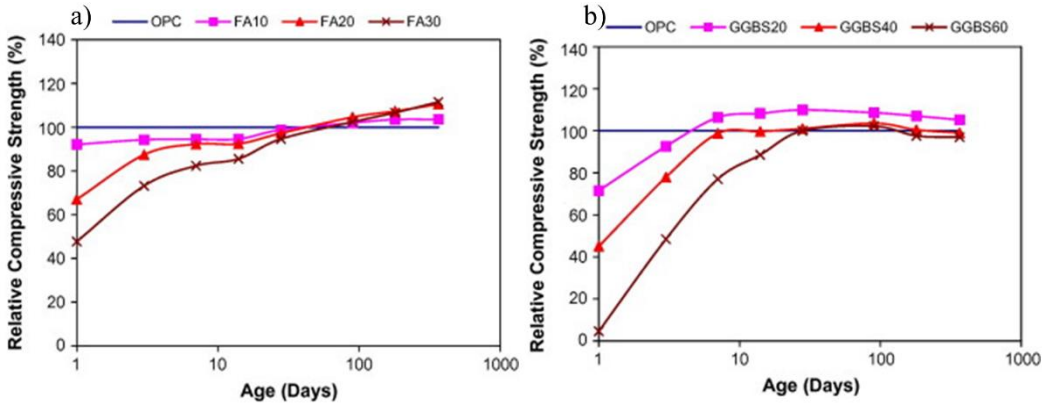

Fig. 2.10. Effect of FA (a) or BFS (b) on compressive strength of concrete [43]

2.3. Carbonation

Carbonation is a common factor that affects the mechanical properties and durability of concretes. It is a process of atmospheric carbon dioxide penetrating cementitious materials, dissolving in the pore solution to produce HCO_3^- and CO_3^{2-} ions, which react with Ca^{2+} from calcium hydroxide ($Ca(OH)_2$), calcium silicate hydrate (C–S–H), and the unreacted cement clinkers to precipitate as various forms of calcium carbonate ($CaCO_3$), silica gel and hydrated aluminum and iron oxides [59,60,62]. These chemical reactions are shown as the following Eqs:

$$Ca(OH)_2 + CO_2 \rightarrow CaCO_3 + H_2O \quad (2.3)$$

$$(CaO)_x(SiO_2)(H_2O)_y + xCO_2 \rightarrow xCaCO_3 + (SiO_2)(H_2O)_t + (y-t)H_2O \quad (2.4)$$

$$(CaO)_3(SiO_2) + (3-x)CO_2 + yH_2O \rightarrow (3-x)CaCO_3 + (CaO)_x(SiO_2)(H_2O)_y \quad (2.5)$$

$$(CaO)_2(SiO_2) + (2-x)CO_2 + yH2O \rightarrow (2-x)CaCO_3 + (CaO)_x(SiO_2)(H_2O)_y \quad (2.6)$$

2.3.1. Influence of carbonation on microstructure and mechanical properties of concrete

Carbonation reactions may change the structure and properties of concrete after long-term progression and thereby have an important impact on the mechanical properties of the material. Generally, $Ca(OH)_2$ is the first phase in hydrated cement paste which reacts with carbon dioxide, resulting in an initial reduction of overall porosity. The decrease in total porosity was attributed to the precipitation of calcium carbonate which can fill in the pore structure of concrete. It was demonstrated by Borges et al. [60] that the total porosity of concrete could be decreased even when containing BFS (see Fig. 2.11). Therefore, it is frequent to find a lower porosity and higher compressive strength due to the effect of carbonation [71–74] (see Fig. 2.12).

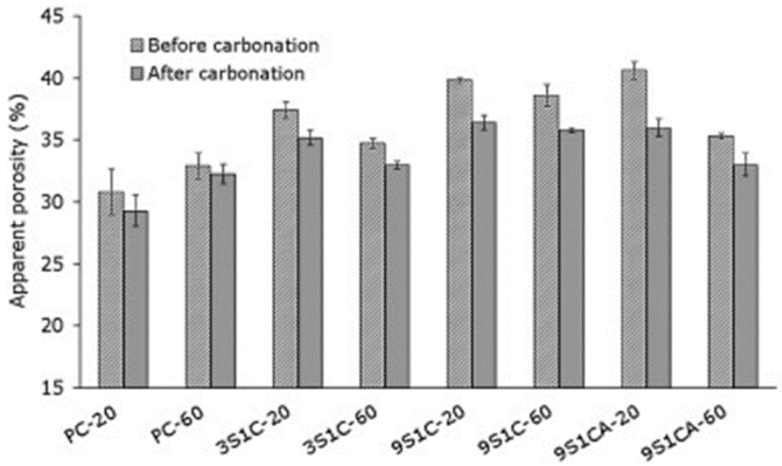

Fig. 2.11. Apparent porosity of pastes before and after carbonation [60];

XX-20 or 60: Samples cured under water at 20°C or 60°C; PC: Ordinary Portland cement; 3S1C: 75% BFS / 25% OPC; 9S1C: 90% BFS / 10% OPC; 9S1CA: 90% BFS / 10% OPC + activated by Na_2SiO_3

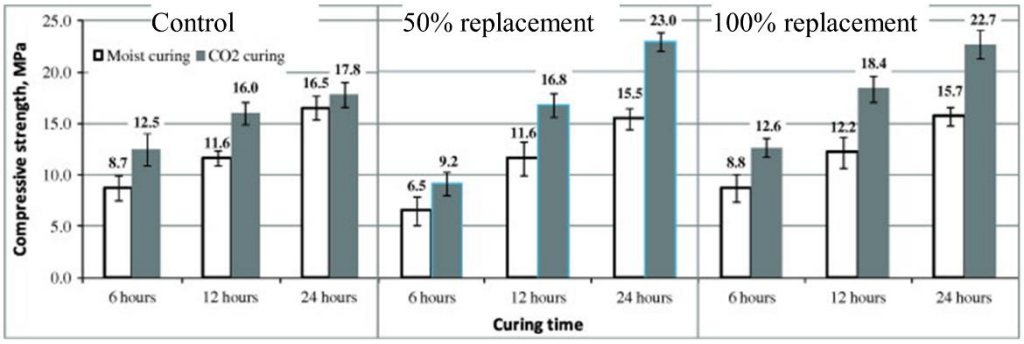

Fig. 2.12. Effect of curing condition on compressive strength of concrete containing recycled aggregates [74]

However, when the $Ca(OH)_2$ is further depleted and covered by the formation of $CaCO_3$, the interlayer Ca^{2+} from C–S–H also reacts with carbon dioxide [60]. The removal of interlayer Ca^{2+} ions creates an excess of negative charges, which are balanced through the subsequent formation of Si-OH groups, leading to the formation of silica gel and an increase in the mean silicate chain length, thus pulling them closer together leading to shrinkage. As a result, carbonation also causes the polymerization of the silicate chains in C–S–H, which may result in a volumetric decrease (shrinkage), cracking, and coarsening the capillary pore (see Fig. 2.13). Maruyama et al. [75] reported that the increase in the number of voids due to the formation of internal cracks mainly caused a decrease in the modulus of elasticity of concrete. The reduction in modulus of elasticity was also found in the carbonated blended OPC and BFS cement paste by Çopuroğlu et al. [76]. Morandeau et al. [64] demonstrated that the total porosity of cement pastes blended with FA was significantly decreased by the carbonation of $Ca(OH)_2$, whereas its capillary pores (typically greater than 50 μm [64]) were increased due to the carbonation of calcium silicate hydrates (C–S–H) gel that was formed from the pozzolanic reaction of FA.

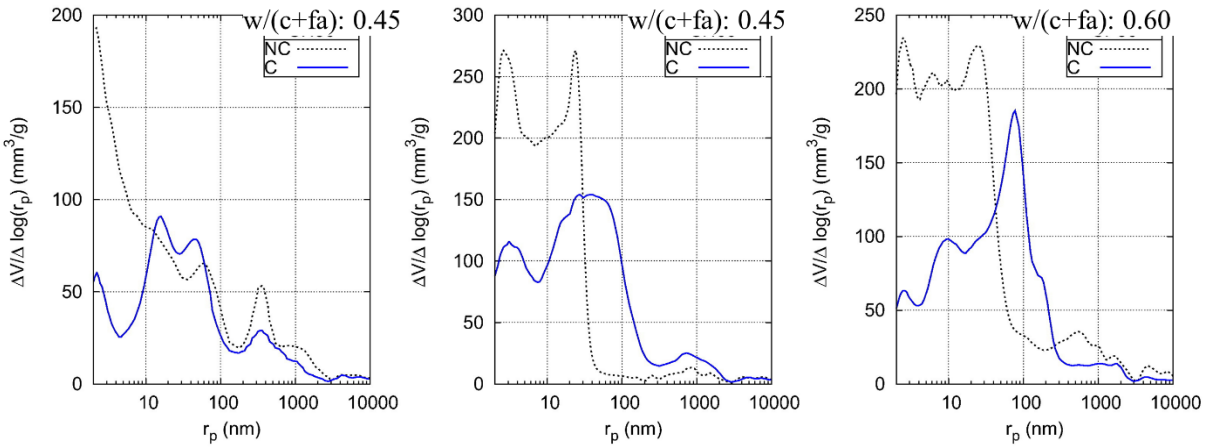

a) OPC + 30% FA b) OPC +60% FA c) OPC +30% FA

Fig. 2.13. The average pore size distribution of non-carbonation and carbonation concrete [64]

2.3.2. Influence of carbonation on the durability of concrete

Many researchers reported that concrete containing SCMs was very sensitive to carbonation. For example, Borges et al. [60] illustrated that the carbonation rate increased with the increasing amount of BFS in the mixes, as shown in Fig. 2.14. The carbonation resulted in not only the change in microstructure of concrete [60,64,65,77–80], but also the formation of microcracks [60,65,81,80,82,83]. As a consequence, the carbonation process affects the durability of concrete. Some previous studies reported that the precipitation of $CaCO_3$ could lead to the porosity clogging and then to a decrease in transport properties [84–86]. For example, Fig. 2.15 shows the decrease in water permeability of mortar under carbonation in comparison with that of mortar under non-carbonation regardless of water to cement ratio [84].

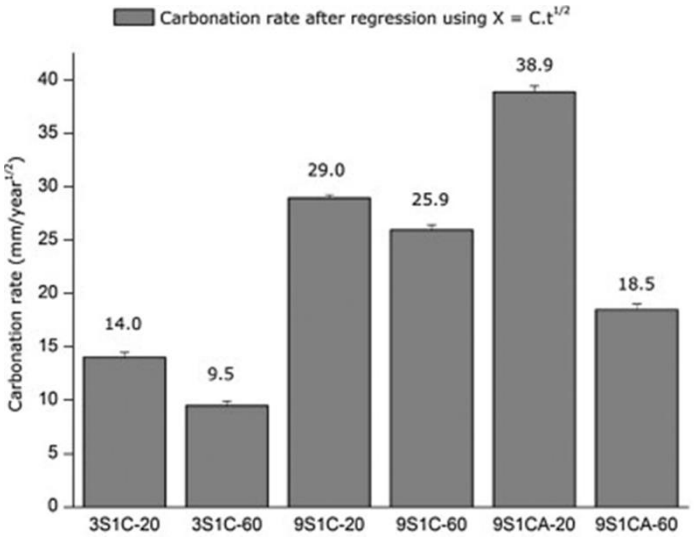

Fig. 2.14. Carbonation rate for BFS:OPC pastes [60];

XX-20 or 60: Samples cured under water at 20°C or 60°C; 3S1C: 75% BFS / 25% OPC;

9S1C: 90% BFS / 10% OPC; 9S1CA: 90% BFS / 10% OPC + activated by Na_2SiO_3

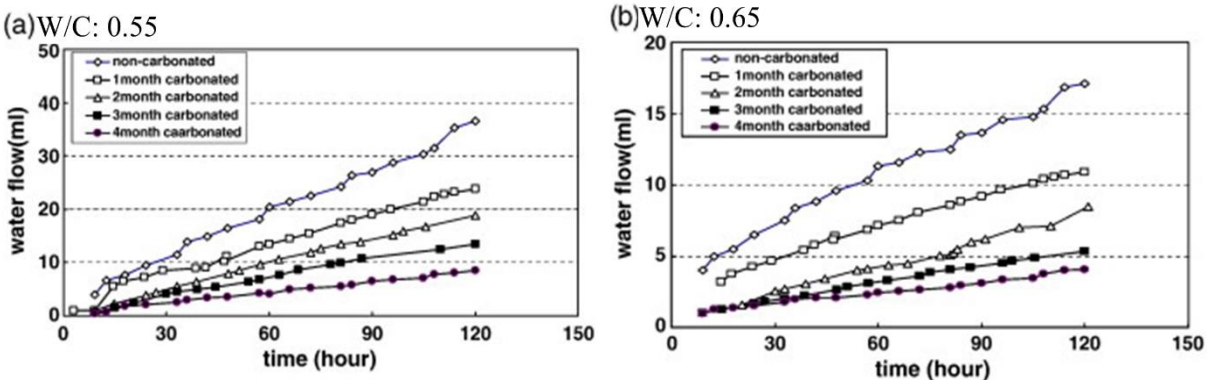

Fig. 2.15. Change in water permeability with time under carbonation [84]

On the other hand, the adverse effects of carbonation on transport properties of concrete were reported by many studies, especially concrete containing SCMs [60,64,65]. That is a significant increase in permeability and/or diffusivity of concrete after carbonation. For example, Auroy et al. [65] found a remarkable increase in air permeability of concrete containing BFS despite the fall of porosity (see Fig. 2.16). The reason was attributed to the coarsening of the pore structure [64,79] while that was recently explained by the formation of

cracks [60,65,78]. The development of cracks due to carbonation was observed in hardened cement paste by using computed tomography as shown in Fig. 2.17 [83]. It can be seen that the increase in the volume and surface of cracks can be clearly distinguished with the extension of the carbonation time.

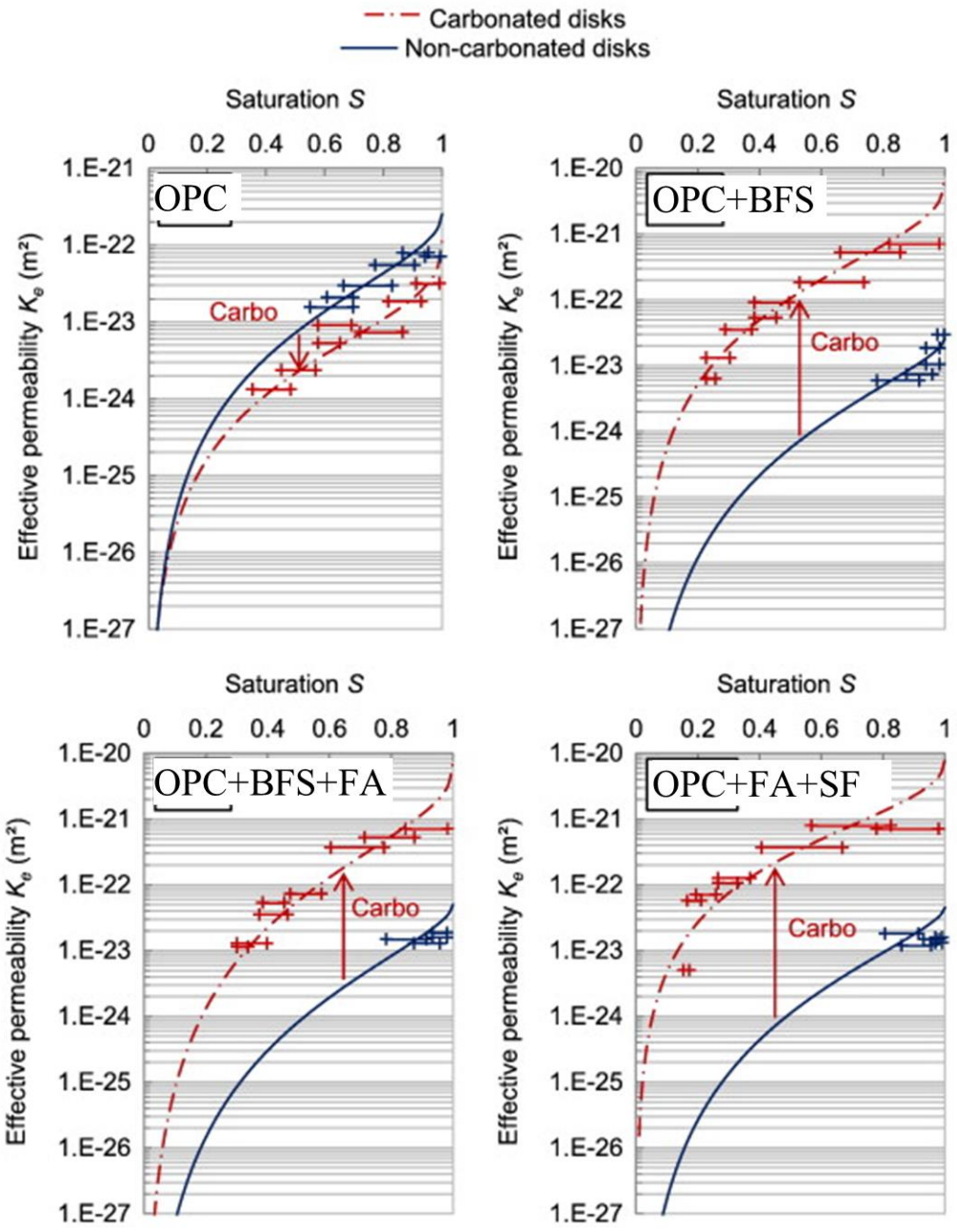

Fig. 2.16. Impact of carbonation on the effective permeability (K_e) [65]

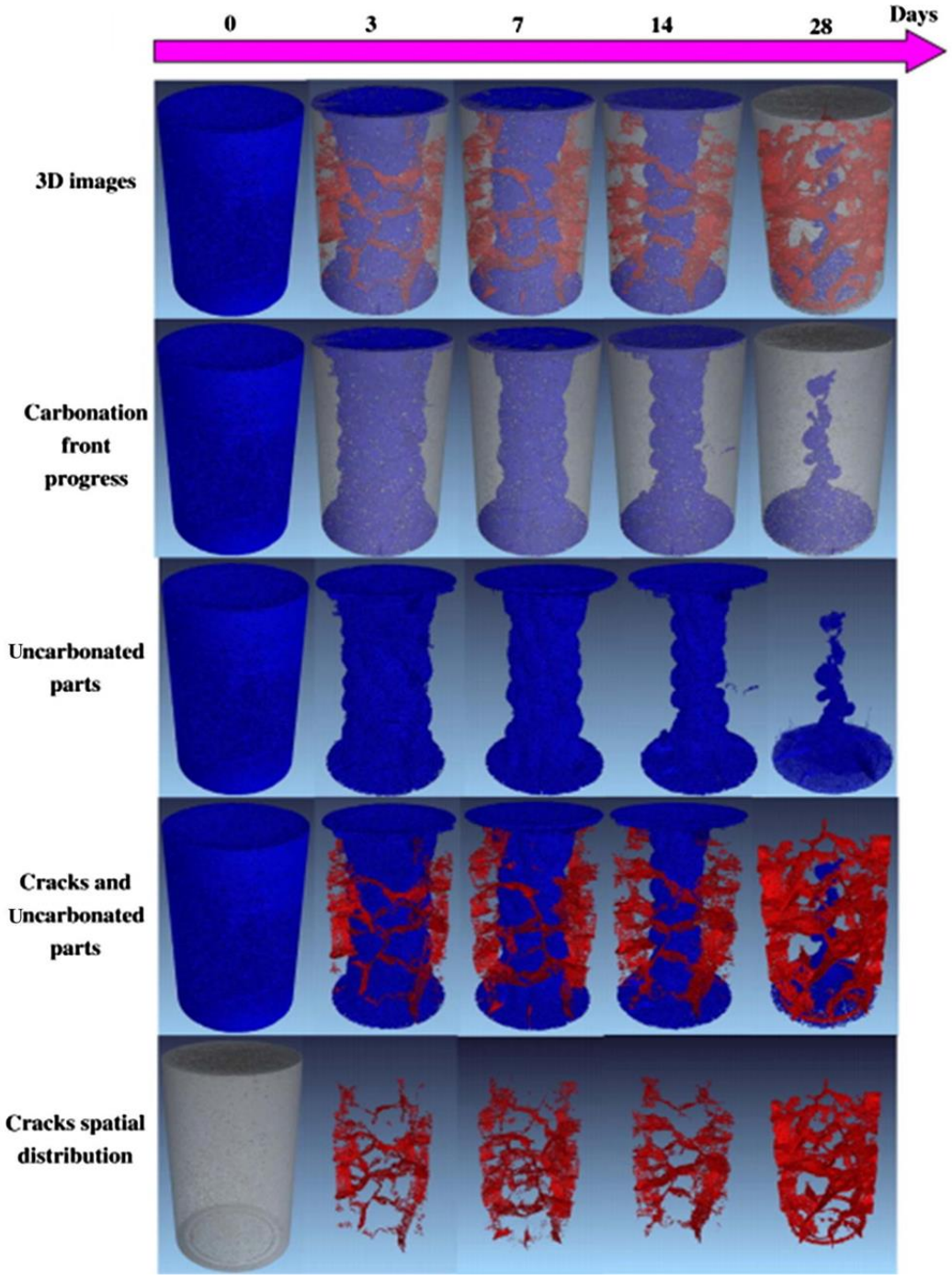

Fig. 2.17. 3D images of carbonation front progress and cracks spatial distribution with different carbonation times [83]

2.3.3. Influence of carbonation on chloride binding of concrete

Moreover, the addition of SCMs such as FA and BFS in concrete could increase the chloride binding performance of concrete due to the increase in Al_2O_3 content [56,58,63,87].

Normally, there are two types of mechanism of chloride binding: physical and chemical binding [87]. The physical binding was the adsorption of chloride ions onto cement hydrates due to their high specific surface values (mostly on C–S–H) and chemical binding was the reaction between chloride ions and AFm compound which refers to a family of hydrated calcium aluminates in cement matrix.. However, these binding mechanisms are changed by carbonation. The changes in chloride binding induced by carbonation are particularly significant when the mixture contains SCMs because during the carbonation process, the dissolution can affect not only $Ca(OH)_2$ but also C–S–H, which weaken the physical chloride binding capacity. Meanwhile, the chemical chloride binding capacity was also reduced due to the decomposition of the solid Friedel's salt in carbonated concrete [33,87,88]. For example, the chloride binding of pastes with different water to cement ratios, as well as pastes containing BFS or FA, is shown in Fig. 2. 18. It is clear that the addition of FA or BFS effectively improved chloride binding capacity under non-carbonation, whereas there is an obvious decrease in the chloride binding capacity of carbonated pastes, especially pastes incorporating FA and BFS in comparison with paste without SCMs [87].

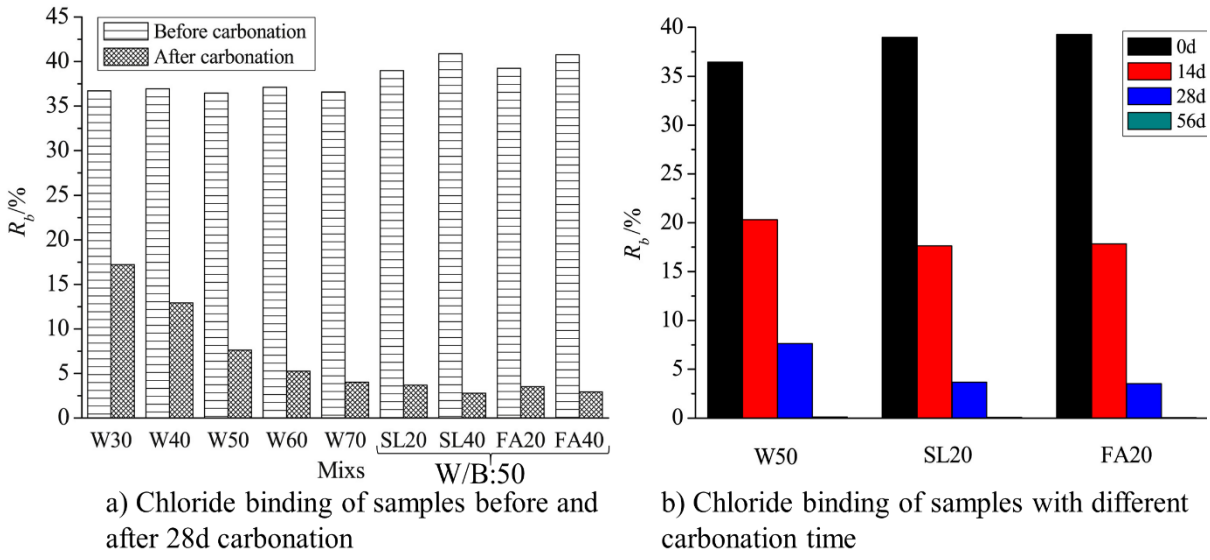

a) Chloride binding of samples before and after 28d carbonation

b) Chloride binding of samples with different carbonation time

Fig. 2. 18. Chloride binding of samples containing SCMs under carbonation [87]

2.4. Summary

Although NSS concrete has been investigated, there is controversy in the application of NSS for concrete production among researchers. Besides, previous studies also demonstrated that SCMs can effectively improve the mechanical performance of concrete. Moreover, carbonation causes some disadvantages; however, most researchers evaluated the feasibility of NSS for concrete production without considering the effect of carbonation. Until now, there is less study related to the effect of chloride ion in NSS on mechanical properties and durability of concrete exposed to carbonation, especially when concrete simultaneously incorporates SCMs. Therefore, the effects of chloride ion in NSS on the fresh properties (i.e. slump and air content) as well as mechanical properties (i.e. compressive strength and modulus of elasticity) and durability (i.e. carbonation resistance, water permeability, sorptivity, and chloride binding) of NSS concrete containing FA and BFS under considering the carbonation were investigated to fill this knowledge gap as well as to extensively verify the applicability of NSS for concrete production.

References of chapter 2:

[1] J. Xiao, C. Qiang, A. Nanni, K. Zhang, Use of sea-sand and seawater in concrete construction: Current status and future opportunities, Construction and Building Materials. 155 (2017) 1101–1111.

[2] E. Garel, W. Bonne, M.B. Collins, C. Peffer, Offshore sand and gravel mining, in: Encyclopedia of Ocean Sciences (Third Edition), Academic Press, Oxford, 2019: pp. 655–662.

[3] Hashida M., Matsunaga N., Komatsu T., Present situation of sea-sand mining in Kyushu island, Japan and its influence on coastal environment, Coastal Engineering. (1992) 3331–3342.

[4] M. Zhao, D. Yang, P. Wang, P. Shi, A market-based approach to marine sand resource management in the Pearl River estuary, China, Ocean & Coastal Management. 105 (2015) 56–64.

[5] European Space Agency (ESA), Earth watching, (2013). https://earth.esa.int/web/earth-watching/historical-views/content/-/article/hong-kong-airport-march-2013.

[6] ICES, Interim Report of the Working Group on the Effects of Extraction of Marine Sediments on the Marine Ecosystem (WGEXT), ICES-International Council for the Exploration of the Sea, Norwich, UK, 2017.

[7] Crown Estate, Marine aggregates information centre, (2020). http://www.marineaggregates.info/index.php.

[8] JASS 5, Japanese architectural standard specification for reinforced concrete work, Architectural Institute of Japan, Tokyo, 40 (2002) 19–27.

[9] JIS A 5308, Ready-mixed concrete, Japanese Standards Association, Tokyo, (2019).

[10] BS 882-1992. Specification for aggregates from natural sources for concrete, British Standard, London, 1992.

[11] BS EN 206-2013. Concrete-Specification, performance, production and conformity, Bristish standard, London, 2013.

[12] JGJ 206-2010. Technical code for application of sea sand concrete, Chinese Industral Standard, 2010.

[13] CS3-2013. Aggregates for concrete. Construction standard, Standing Committee on concrete technology, Hong kong, 2013.

[14] S. Luhar, U. Khandelwal, A study on durability of dredged marine sand concrete, International Journal of Engineering Research and Reviews. 3 (2015) 56–76.

[15] C. Chen, T. Ji, Y. Zhuang, X. Lin, Workability, mechanical properties and affinity of artificial reef concrete, Construction and Building Materials. 98 (2015) 227–236.

[16] Y. L. Li, X. L. Zhao, R. K. Singh Raman, S. Al-Saadi, Thermal and mechanical properties of alkali-activated slag paste, mortar and concrete utilising seawater and sea sand, Construction and Building Materials. 159 (2018) 704–724.

[17] J. Limeira, M. Etxeberria, L. Agulló, D. Molina, Mechanical and durability properties of concrete made with dredged marine sand, Construction and Building Materials. 25 (2011) 4165–4174.

[18] JIS A 1102, Method of test for sieve analysis of aggregates, Japanese Standards Association, Tokyo, 2014.

[19] R. Zentar, V. Dubois, N. E. Abriak, Mechanical behaviour and environmental impacts of a test road built with marine dredged sediments, Resources, Conservation and Recycling. 52 (2008) 947–954.

[20] V. Dubois, N. E. Abriak, R. Zentar, G. Ballivy, The use of marine sediments as a pavement base material, Waste Management. 29 (2009) 774–782.

[21] J. Limeira, L. Agullo, M. Etxeberria, Dredged marine sand in concrete: An experimental section of a harbor pavement, Construction and Building Materials. 24 (2010) 863–870.

[22] Q. Xu, T. Ji, Z. Yang, Y. Ye, Preliminary investigation of artificial reef concrete with sulphoaluminate cement, marine sand and sea water, Construction and Building Materials. 211 (2019) 837–846.

[23] S. Yang, J. Xu, C. Zang, R. Li, Q. Yang, S. Sun, Mechanical properties of alkali-activated slag concrete mixed by seawater and sea sand, Construction and Building Materials. 196 (2019) 395–410.

[24] C.G. Girish, D. Tensing, K.L. Priya, Dredged offshore sand as a replacement for fine aggregate in concrete, Int. J. Eng. Sci. Emerg. Technol. 8 (2015) 88–95.

[25] W. S. Deepak, Effect on compressive strength of concrete using sea sand as a partial replacement for fine aggregate, International Journal of Research in Engineering and Technology. 04 (2016) 180–183.

[26] R. Mahendran, K. Godwin, T. G. Selvan, M. Murugan, Experimental study on concrete using sea sand as fine aggregate, 7 (2016) 4.

[27] S. K. Tulashie, F. Kotoka, D. Mensah, A. K. Kwablah, Investigation of the compressive strength of pit sand, and sea sand mortar prisms produced with rice husk ash as additive, Construction and Building Materials. 151 (2017) 383–387.

[28] İ. H. Çağatay, Experimental evaluation of buildings damaged in recent earthquakes in Turkey, Engineering Failure Analysis. 12 (2005) 440–452.

[29] H. H. Yao, Study on the mechanical properties and durability of sea sand concrete, Qingdao University of Technology, 2011.

[30] Y. Yang, T. Ji, X. Lin, C. Chen, Z. Yang, Biogenic sulfuric acid corrosion resistance of new artificial reef concrete, Construction and Building Materials. 158 (2018) 33–41.

[31] Z. Jiang, T.J. Zhao, X.C. Song, Study on carbonation performance of sea sand concrete, Engineering and Constructions. 41 (2009) 11–14.

[32] D. G. Kim, M. S. Cho, J. S. Lee, The effects of chloride on durability of concrete mixed with sea sand, 3 (2013) 325–331.

[33] W. Liu, H. Cui, Z. Dong, F. Xing, H. Zhang, T.Y. Lo, Carbonation of concrete made with dredged marine sand and its effect on chloride binding, Construction and Building Materials. 120 (2016) 1–9.

[34] W. P. S. Dias, G. A. P. S. N. Seneviratne, S. M. A. Nanayakkara, Offshore sand for reinforced concrete, Construction and Building Materials. 22 (2008) 1377–1384.

[35] W. Liu, R. Huang, J. Fu, W. Tang, Z. Dong, H. Cui, Discussion and experiments on the limits of chloride, sulphate and shell content in marine fine aggregates for concrete, Construction and Building Materials. 159 (2018) 725–733.

[36] F. Guo, S. Al-Saadi, R. K. Singh Raman, X. L. Zhao, Durability of fiber reinforced polymer (FRP) in simulated seawater sea sand concrete (SWSSC) environment, Corrosion Science. 141 (2018) 1–13.

[37] F. Y. Liao, C. Hou, W. J. Zhang, J. Ren, Experimental investigation on sea sand concrete-filled stainless steel tubular stub columns, Journal of Constructional Steel Research. 155 (2019) 46–61.

[38] Q. Zhang, J. Xiao, Q. Liao, Z. Duan, Structural behavior of seawater sea-sand concrete shear wall reinforced with GFRP bars, Engineering Structures. 189 (2019) 458–470.

[39] Z. Dong, G. Wu, Y. Xu, Experimental study on the bond durability between steel-FRP composite bars (SFCBs) and sea sand concrete in ocean environment, Construction and Building Materials. 115 (2016) 277–284.

[40] Y. L. Li, X. L. Zhao, R. K. Singh Raman, S. Al-Saadi, Tests on seawater and sea sand concrete-filled CFRP, BFRP and stainless steel tubular stub columns, Thin-Walled Structures. 108 (2016) 163–184.

[41] E. Aprianti, P. Shafigh, R. Zawawi, Z. F. Abu Hassan, Introducing an effective curing method for mortar containing high volume cementitious materials, Construction and Building Materials. 107 (2016) 365–377.

[42] K. H. Yang, Y. B. Jung, M. S. Cho, S. H. Tae, Effect of supplementary cementitious materials on reduction of CO2 emissions from concrete, Journal of Cleaner Production. 103 (2015) 774–783.

[43] M. A. Megat Johari, J. J. Brooks, S. Kabir, P. Rivard, Influence of supplementary cementitious materials on engineering properties of high strength concrete, Construction and Building Materials. 25 (2011) 2639–2648.

[44] S. Cheng, Z. Shui, T. Sun, R. Yu, G. Zhang, Durability and microstructure of coral sand concrete incorporating supplementary cementitious materials, Construction and Building Materials. 171 (2018) 44–53.

[45] P. Duan, Z. Shui, W. Chen, C. Shen, Effects of metakaolin, silica fume and slag on pore structure, interfacial transition zone and compressive strength of concrete, Construction and Building Materials. 44 (2013) 1–6.

[46] J. Xie, J. Wang, R. Rao, C. Wang, C. Fang, Effects of combined usage of GGBS and fly ash on workability and mechanical properties of alkali activated geopolymer concrete with recycled aggregate, Composites Part B: Engineering. 164 (2019) 179–190.

[47] A. Oner, S. Akyuz, An experimental study on optimum usage of GGBS for the compressive strength of concrete, Cement and Concrete Composites. 29 (2007) 505–514.

[48] J. Liu, G. Ou, Q. Qiu, X. Chen, J. Hong, F. Xing, Chloride transport and microstructure of concrete with/without fly ash under atmospheric chloride condition, Construction and Building Materials. 146 (2017) 493–501.

[49] A. Hadjsadok, S. Kenai, L. Courard, F. Michel, J. Khatib, Durability of mortar and concretes containing slag with low hydraulic activity, Cement and Concrete Composites. 34 (2012) 671–677.

[50] G. Li, A. Zhang, Z. Song, S. Liu, J. Zhang, Ground granulated blast furnace slag effect on the durability of ternary cementitious system exposed to combined attack of chloride and sulfate, Construction and Building Materials. 158 (2018) 640–648.

[51] A.C.I. Committee 226, Ground Granulated Blast-Furnace Slag as a Cementitious Constituent in Concrete, MJ. 84 (1987) 327–342.

[52] S. C. Pal, A. Mukherjee, S. R. Pathak, Investigation of hydraulic activity of ground granulated blast furnace slag in concrete, Cement and Concrete Research. 33 (2003) 1481–1486.

[53] R. Siddique, Performance characteristics of high-volume Class F fly ash concrete, Cement and Concrete Research. 34 (2004) 487–493.

[54] M. C. G. Juenger, R. Siddique, Recent advances in understanding the role of supplementary cementitious materials in concrete, Cement and Concrete Research. 78 (2015) 71–80.

[55] B. Lothenbach, K. Scrivener, R.D. Hooton, Supplementary cementitious materials, Cement and Concrete Research. 41 (2011) 1244–1256.

[56] M. D. A. Thomas, R. D. Hooton, A. Scott, H. Zibara, The effect of supplementary cementitious materials on chloride binding in hardened cement paste, Cement and Concrete Research. 42 (2012) 1–7.

[57] G. Hannesson, K. Kuder, R. Shogren, D. Lehman, The influence of high volume of fly ash and slag on the compressive strength of self-consolidating concrete, Construction and Building Materials. 30 (2012) 161–168.

[58] M. Saillio, V. Baroghel-Bouny, F. Barberon, Chloride binding in sound and carbonated cementitious materials with various types of binder, Construction and Building Materials. 68 (2014) 82–91.

[59] B. Šavija, M. Luković, Carbonation of cement paste: Understanding, challenges, and opportunities, Construction and Building Materials. 117 (2016) 285–301.

[60] P. H. R. Borges, J. O. Costa, N. B. Milestone, C. J. Lynsdale, R. E. Streatfield, Carbonation of CH and C–S–H in composite cement pastes containing high amounts of BFS, Cement and Concrete Research. 40 (2010) 284–292.

[61] E. Gruyaert, P. Van den Heede, N. De Belie, Carbonation of slag concrete: Effect of the cement replacement level and curing on the carbonation coefficient – Effect of carbonation on the pore structure, Cement and Concrete Composites. 35 (2013) 39–48.

[62] V. Shah, S. Bishnoi, Carbonation resistance of cements containing supplementary cementitious materials and its relation to various parameters of concrete, Construction and Building Materials. 178 (2018) 219–232.

[63] M. Jin, S. Gao, L. Jiang, H. Chu, M. Lu, F. F. Zhi, Degradation of concrete with addition of mineral admixture due to free chloride ion penetration under the effect of carbonation, Corrosion Science. 138 (2018) 42–53.

[64] A. Morandeau, M. Thiéry, P. Dangla, Impact of accelerated carbonation on OPC cement paste blended with fly ash, Cement and Concrete Research. 67 (2015) 226–236.

[65] M. Auroy, S. Poyet, P. Le Bescop, J. M. Torrenti, T. Charpentier, M. Moskura, X. Bourbon, Impact of carbonation on unsaturated water transport properties of cement-based materials, Cement and Concrete Research. 74 (2015) 44–58.

[66] Z. Giergiczny, Fly ash and slag, Cement and Concrete Research. 124 (2019) 105826.

[67] D. Jiao, C. Shi, Q. Yuan, X. An, Y. Liu, H. Li, Effect of constituents on rheological properties of fresh concrete-A review, Cement and Concrete Composites. 83 (2017) 146–159.

[68] M. Batog, Z. Giergiczny, Influence of mass concrete constituents on its properties, Construction and Building Materials. 146 (2017) 221–230.

[69] E. Sakai, S. Miyahara, S. Ohsawa, S. H. Lee, M. Daimon, Hydration of fly ash cement, Cement and Concrete Research. 35 (2005) 1135–1140.

[70] D. Zhang, J. Zhao, D. Wang, C. Xu, M. Zhai, X. Ma, Comparative study on the properties of three hydraulic lime mortar systems: Natural hydraulic lime mortar, cement-aerial lime-based mortar and slag-aerial lime-based mortar, Construction and Building Materials. 186 (2018) 42–52.

[71] J. M. Chi, R. Huang, C. C. Yang, Effects of carbonation on mechanical properties and durability of concrete using accelerated testing method, Journal of Marine Science and Technology. 10 (2002) 14–20.

[72] M. A. Sanjuán, C. Andrade, M. Cheyrezy, Concrete carbonation tests in natural and accelerated conditions, Advances in Cement Research. 15 (2003) 171–180.

[73] C. F. Chang, J. W. Chen, Strength and Elastic Modulus of Carbonated Concrete, MJ. 102 (2005) 315–321.

[74] B. Zhan, C. Poon, C. Shi, CO2 curing for improving the properties of concrete blocks containing recycled aggregates, Cement and Concrete Composites. 42 (2013) 1–8.

[75] I. Maruyama, H. Sasano, Y. Nishioka, G. Igarashi, Strength and Young's modulus change in concrete due to long-term drying and heating up to 90°C, Cement and Concrete Research. 66 (2014) 48–63.

[76] O. Çopuroğlu, E. Schlangen, Modeling of frost salt scaling, Cement and Concrete Research. 38 (2008) 27–39.

[77] B. Wu, G. Ye, Development of porosity of cement paste blended with supplementary cementitious materials after carbonation, Construction and Building Materials. 145 (2017) 52–61.

[78] M. Auroy, S. Poyet, P. Le Bescop, J. M. Torrenti, T. Charpentier, M. Moskura, X. Bourbon, Comparison between natural and accelerated carbonation (3% CO2): Impact on mineralogy, microstructure, water retention and cracking, Cement and Concrete Research. 109 (2018) 64–80.

[79] V. T. Ngala, C. L. Page, Effects of carbonation on pore structure and diffusional properties of hydrated cement pastes, Cement and Concrete Research. 27 (1997) 995–1007.

[80] G. Rimmelé, V. Barlet-Gouédard, O. Porcherie, B. Goffé, F. Brunet, Heterogeneous porosity distribution in Portland cement exposed to CO2-rich fluids, Cement and Concrete Research. 38 (2008) 1038–1048.

[81] M. Nedeljković, B. Šavija, Y. Zuo, M. Luković, G. Ye, Effect of natural carbonation on the pore structure and elastic modulus of the alkali-activated fly ash and slag pastes, Construction and Building Materials. 161 (2018) 687–704.

[82] A. Fabbri, J. Corvisier, A. Schubnel, F. Brunet, B. Goffé, G. Rimmele, V. Barlet-Gouédard, Effect of carbonation on the hydro-mechanical properties of Portland cements, Cement and Concrete Research. 39 (2009) 1156–1163.

[83] J. Han, W. Sun, G. Pan, W. Caihui, Monitoring the evolution of accelerated carbonation of hardened cement pastes by X-ray computed tomography, J. Mater. Civ. Eng. 25 (2013) 347–354.

[84] H. W. Song, S. J. Kwon, Permeability characteristics of carbonated concrete considering capillary pore structure, Cement and Concrete Research. 37 (2007) 909–915.

[85] W. P. S. Dias, Reduction of concrete sorptivity with age through carbonation, Cement and Concrete Research. 30 (2000) 1255–1261.

[86] P. J. Dewaele, E. J. Reardon, R. Dayal, Permeability and porosity changes associated with cement grout carbonation, Cement and Concrete Research. 21 (1991) 441–454.

[87] H. Chang, Chloride binding capacity of pastes influenced by carbonation under three conditions, Cement and Concrete Composites. 84 (2017) 1–9.

[88] G. Villain, M. Thiery, G. Platret, Measurement methods of carbonation profiles in concrete: Thermogravimetry, chemical analysis and gammadensimetry, Cement and Concrete Research. 37 (2007) 1182–1192.

CHAPTER 3. EXPERIMENTAL PROGRAM

This chapter illustrates the experimental program of the present study, including the materials, mixture proportions, the mixing and casting progress, and the curing conditions. All the measurements were performed to study the effects of chloride ion in NSS, carbonation, and SCMs on the mechanical properties and durability of NSS concrete.

3.1. Materials

3.1.1. Cementitious materials

Ordinary Portland cement (OPC), fly ash (FA) type II, and ground granulated blast furnace slag (BFS) 4000, as classified by Japanese Industrial Standard JIS R5210 [1], JIS A 6201 [2] and JIS A 6206 [3], respectively, were used as cementitious materials in this study. There are four types of low-calcium FA as well as BFS specified by the JIS, with FA type II and BFS 4000 being the most used in Japan. Therefore, the reference to FA and BFS in this manuscript will be with regard to type II and 4000, respectively. The specific surface areas of OPC, FA, and BFS were 3340, 3550, and 4170 cm^2/g, respectively, and their densities are 3.16, 2.24, and 2.91 g/cm^3, respectively. The chemical compositions of cementitious materials are shown in Table 3.1. The calcium oxide (CaO) content in BFS was much higher than that in FA and less than that in OPC. The mineralogical compositions of the cementitious materials were determined using X-ray diffraction (XRD), as shown in Fig. 3.1. XRD analysis indicated that OPC mainly comprised alite (C_3S), belite (C_2S), celite (C_3A), and ferrite (C_4AF) and that crystalline phases of quartz, mullite, and hematite were observed in FA, as shown in Figs. 3.1(a) and (b), respectively. Blast furnace slag showed an amorphous hump with a peak at around 28–33° that mainly consisted of a glassy phase (Fig. 3.1(c)).

Table 3.1. Chemical composition of cementitious materials

Materials	Chemical composition (% by mass)									
	CaO	SiO_2	Al_2O_3	Fe_2O_3	MgO	SO_3	Na_2O	K_2O	Cl	LOI
OPC	64.79	19.89	5.19	3.07	1.26	1.95	0.31	0.36	0.01	2.65
FA	1.47	59.40	29.37	5.77	0.80	–	–	1.10	–	2.90
BFS	43.78	34.45	14.06	0.27	5.84	–	0.24	0.23	0.00	0.05

– Not measured

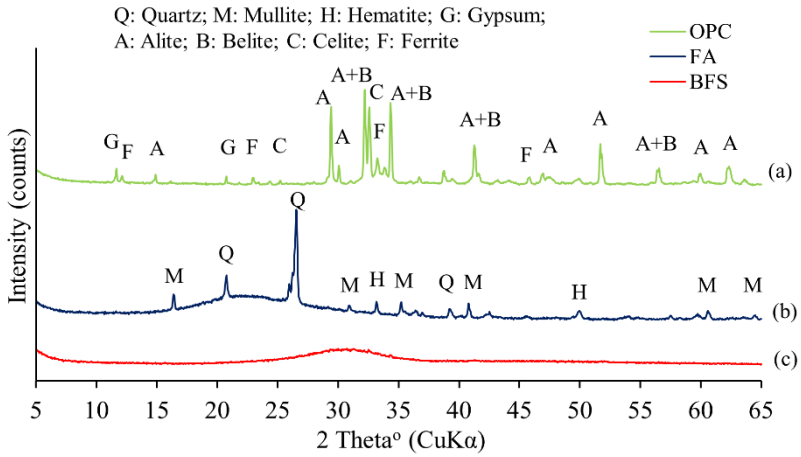

Fig. 3.1. X-ray diffraction patterns of cementitious materials

3.1.2. Aggregates

Gravel (G), with a particle size of 5–20 mm, saturated surface-dry condition density of 2.62 g/cm^3, and water absorption of 0.67%, was used as coarse aggregate. The non-desalted sea sand (NSS) used as fine aggregate in this study was sourced from the Karatsu harbor in Saga prefecture, Japan. Desalted sea sand (DSS), obtained by removing salts from the NSS, was used as a reference. The mineralogical analysis for NSS and DSS was conducted by X-ray diffraction. The results show that the main phases of NSS and DSS were almost the same and were quartz,

feldspar, and calcite. The chemical compositions of DSS and NSS were analysed by an energy dispersive X-ray spectrometry, and the concentration of chloride and sulfate ions in NSS and DSS were measured by employing ion chromatography. The sample preparation for ion chromatography measurement was prepared by referring to JIS A 1154 [4]. The sample preparation is mentioned more detail in Section 3.3.10. The physical properties and chemical compositions of the fine aggregates are presented in Tables 3.2 and 3.3. The particle size distribution of DSS and NSS in this study was within the limit according to JIS A 1102 [5]. However, their composition and characteristics may be different compared to those from other locations which were reported in a previous study [6].

Table 3.2. Physical properties of fine aggregates

Type of sand	Residue on each sieve size (%)							Fineness modulus	Density (g/cm^3)	Water absorption (%)
	5.0	2.5	1.2	0.6	0.3	0.15	< 0.15			
NSS	0.0	6.2	23.7	30.3	27.9	10.6	1.3	2.83	2.60	1.33
DSS	0.3	8.3	21.8	28.7	32.8	7.1	1.0	2.89	2.60	1.31

Table 3.3. Chemical composition of fine aggregates

Type of sand	Chemical composition (% by mass)							
	SiO_2	Al_2O_3	K_2O	CaO	Fe_2O_3	MgO	Cl^- (%)	SO_4^{2-} (%)
NSS	81.60	8.39	4.07	3.67	1.60	0.56	0.1968	0.0860
DSS	83.52	7.37	3.46	3.49	1.24	0.42	0.0054	0.0090

3.1.3. Water and admixtures

Tap water (W) was used for casting concrete specimens. The commercially available water-reducing agent (WRA) SV10L (its components include lignosulfonate, oxycarboxylic acid salt,

and polycarboxylic acid manufactured by Flowric Co.,Ltd., Japan) and air-entraining agent (AE) AE6 (an anionic surfactant manufactured by Flowric Co.,Ltd., Japan) were used to obtain mixtures with the desired slump and air content of 150 ± 20 mm and 2.0 ± 0.5%, respectively.

3.2. Mixture proportions and specimen preparation

3.2.1. Mixture proportions

Six different mixture proportions of concrete were prepared with a constant water-to-cementitious materials ratio of 0.50, to represent the common concretes used for structures in the marine environment such as breakwater or artificial reef. The expected compressive strength of concrete in this study at the age of 28 days was 40 N/mm^2. Ordinary Portland cement was partially replaced by 15% FA or 45% BFS by mass. These replacement ratios were chosen to obtain almost the same compressive strength level at the age of 28 days as the reference concrete. Further details are shown in Table 3.4. Desalted sea sand is accepted in Japan for use as fine aggregate in concrete production when the chloride ion content is less than 0.04% by mass of the dry sand and/or less than 0.3 kg/m^3 in the concrete [7]; therefore, concrete specimens with OPC and DSS were considered as the reference in this study.

Table 3.4. Mixture proportion of concrete (kg/m^3)

Concrete mixtures	OPC–DSS	OPC–NSS	FA15–DSS	FA15–NSS	BFS45–DSS	BFS45–NSS
OPC (kg/m^3)	350	350	298	298	193	193
W (kg/m^3)	175	175	175	175	175	175
FA (kg/m^3)	–	–	53	53	–	–
BFS (kg/m^3)	–	–	–	–	158	158
DSS (kg/m^3)	847	–	838	–	841	–
NSS (kg/m^3)	–	847	–	838	–	841
G (kg/m^3)	966	966	956	956	960	960
WRA (g/m^3)	700	700	595	595	385	385
AE (g/m^3)	1.75	1.75	23.80	23.80	0.96	0.96

3.2.2. Casting

All the aggregates were prepared under saturated surface-dry conditions and stored at 20 °C for at least 24 h before mixing to reduce the effect of temperature on the fresh concrete. Each mixture was mixed using a 100-L pan mixer that was prewetted by the corresponding mortar to avoid moisture and other materials loss during mixing. The mixing procedure was conducted as follows; first, the cementitious materials and the fine aggregate were mixed for 30 s. After that, while the mixer was running, the required water containing WRA and AE was slowly poured into the dry mixture for 30 s. The mixture was continuously mixed for 30 s before stopping to mix by hand for 60 s. Then, coarse aggregate was added to the mixer and the concrete mixture was mixed for 60 s. After that, the mixer was rested for 60 s for scraping the sticky concrete on the sides of the pan. To get a more homogenous concrete mixture, the mixer was rotated again for 60 s before finishing. The mixing procedure is shown in Fig. 3.2.

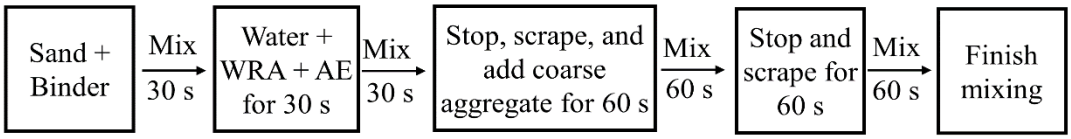

Fig. 3.2. Mixing procedure

3.2.3. Specimen preparation

After mixing, the fresh concrete was divided into two parts: one part was used to measure the properties of the fresh concrete with time; the other was cast into cylindrical plastic molds with 100 mm diameter and 200 mm height and prismatic molds with dimensions of 100×100×400 mm, in two layers and compacted to reduce air voids. The surfaces of the specimens were smoothed and hermetically sealed with aluminum adhesive tape to prevent excessive water evaporation and carbonation. It is noted that the aluminum tape had an acrylic adhesive layer which prevented the aluminum to directly contact and react with the cement paste. Before being subjected to accelerated carbonation, all concrete specimens were sealed for 28 days at 20 ± 2 ºC to minimize the effect of carbonation on the cement hydration, pozzolanic reaction of FA, and hydraulicity of BFS.

The cylindrical specimens were used for mechanical properties, permeability, and sorptivity tests. After sealed curing for 28 days, the cylindrical specimens were divided into two groups. One group was cured under sealed conditions while the other group was cured under carbonation conditions until the designated ages. The cylindrical specimens under sealed condition were continued to be placed at 20 ± 2 ºC, whereas those under carbonation condition were completely demolded and put in an accelerated carbonation chamber (see Fig. 3.3). The CO_2 concentration in the chamber was 5%, and the temperature and relative humidity (R.H.) were 20 ± 2 ºC and 60% ± 5%, respectively. The CO_2 concentration was set based on previous

studies [9, 10] for the purpose of obtaining experimental results in a short period. It should be noted that results may differ from that under natural carbonation.

For permeability and sorptivity tests, the specimens having 100 mm diameter and 50 mm height were prepared from cutting three parts of the cylindrical specimens. It is noted that thin sections approximately 15 mm from both ends of cylindrical specimens were discarded to eliminate the influence of the distribution of coarse aggregates and mortar during casting. This preparation was conducted at the designated ages for the samples under sealed condition. Meanwhile, those under carbonation condition were prepared after sealed curing for 28 days and thereby put in an accelerated carbonation chamber (see Fig. 3.3).

One surface (100 x 400 mm) of the prismatic specimens was exposed after 28 days of sealed curing and the specimens were placed in the accelerated carbonation chamber. These specimens were later used for measurement of carbonation depth (See Fig.3.3). The experiment timeline of this study is shown in Fig. 3.4.

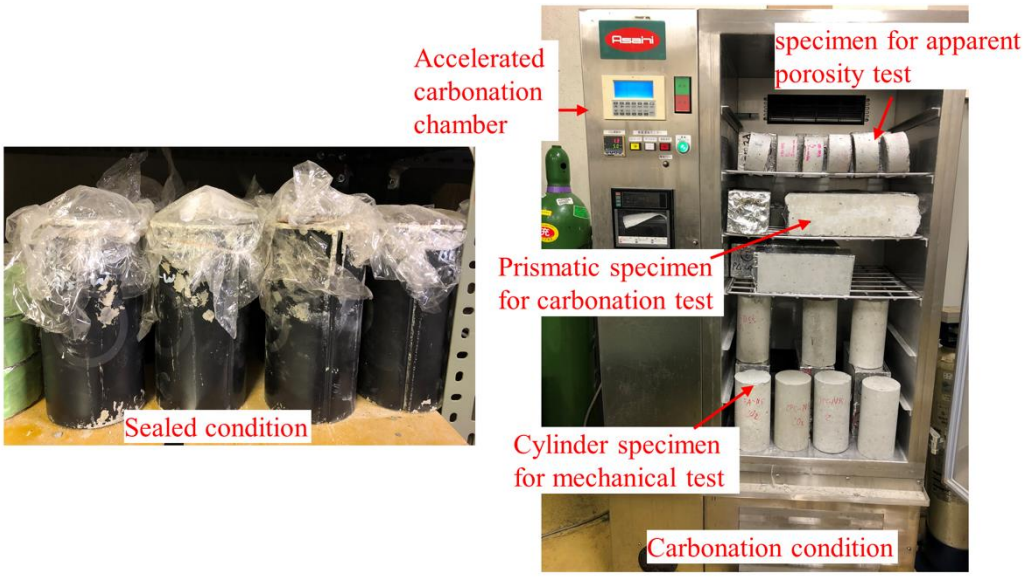

Fig. 3.3. Specimens preparation

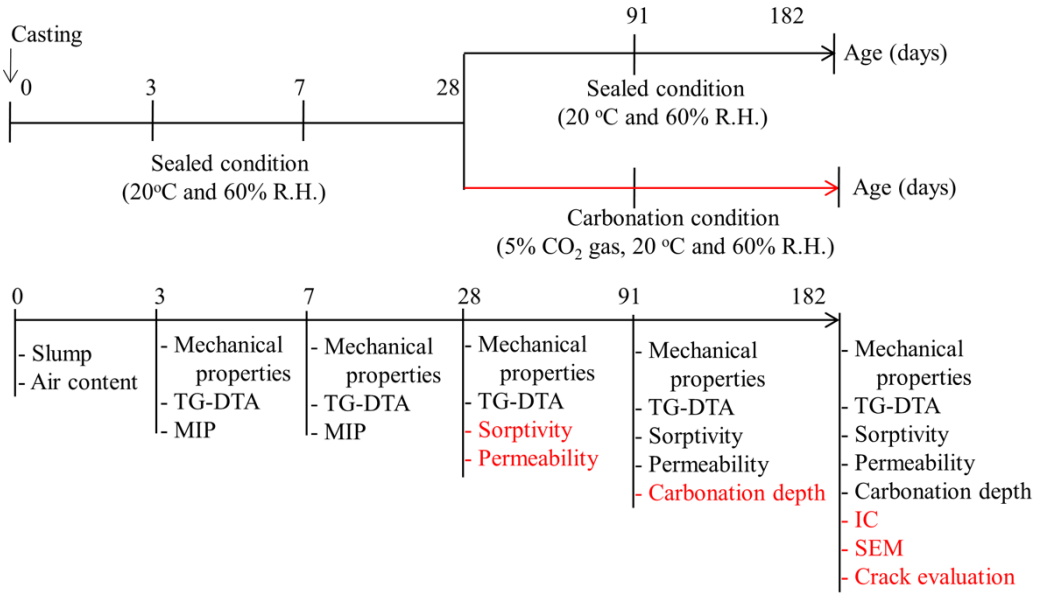

Fig. 3.4. Experimental timeline; TG-DTA: thermal gravimetry and differential thermal analysis; MIP: mercury intrusion porosimetry; IC: ion chromatography; SEM: scanning electron microscopy;

3.3. Experimental methods

3.3.1. Slump and air content

Slump and air content of fresh concrete were measured according to JIS A 1101 [10] and JIS A 1128 [11], respectively (see Fig. 3.5.). The air content was determined using a pressure air meter. To investigate the effect of chloride ion and SCMs on the workability, the initial slump and air content of fresh concrete were measured immediately after mixing, the retentions in slump and air content were determined at 30 and 60 min after mixing.

a) Slump test b) Air content test

Fig. 3.5. Slump and air content measurements

3.3.2. Compressive strength and modulus of elasticity

Mechanical properties, compressive strength and modulus of elasticity, of the hardened concrete cured at 20 °C under sealed condition were determined using cylindrical specimens (ϕ 100 mm × 200 mm) at ages of 3, 7, 28, 91, and 182 days, whereas those of carbonated samples were determined at the ages of 91 and 182 days. These tests were conducted by using an automatic compression machine with a loading capacity of 1000 kN, in accordance with JIS A 1108 [12] and JIS A 1149 [13], respectively. The tests were carried out at a constant loading rate of 1.5 kN/s. Two strain gauges were attached along the vertical direction of specimens to measure the strain during the loading. The reported values were obtained as the averages for three specimens of each mixture at each testing day. This test set up is shown in Fig. 3.6.

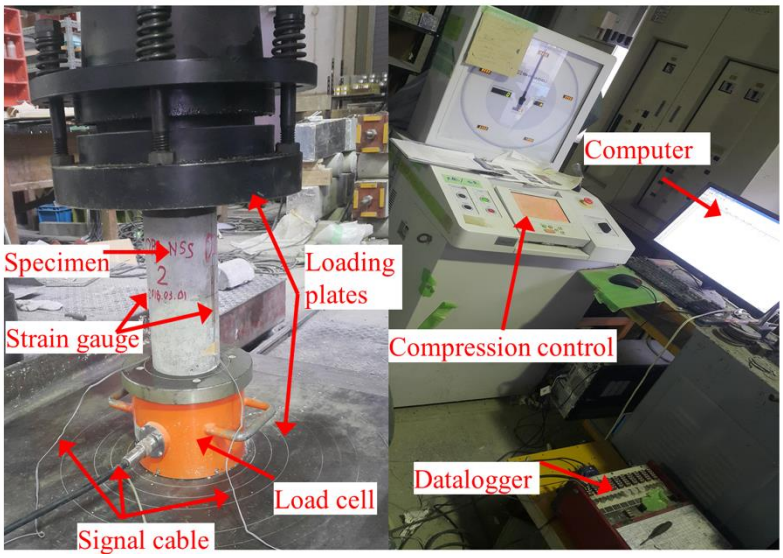

Fig. 3.6. Mechanical properties measurement

3.3.3. Carbonation depth

After 1, 4, 9, 13, and 22 weeks of accelerated carbonation, the prismatic specimens were split at approximately 50 mm from the side edge perpendicular to the exposed surface for measuring carbonation depth. Then, the freshly broken surface with dimensions of 100×100 of remained part of the prismatic specimen was covered with aluminum adhesive tape and the remaining part of the specimen was placed back in the carbonation chamber for testing at later ages. The carbonation depth was measured by spraying phenolphthalein solution onto the freshly broken surface (see Fig. 3.7) of the 50 mm wide block. The value of carbonation depth was calculated as the average of ten measurements by using an electronic calliper with an accuracy of 0.01 mm.

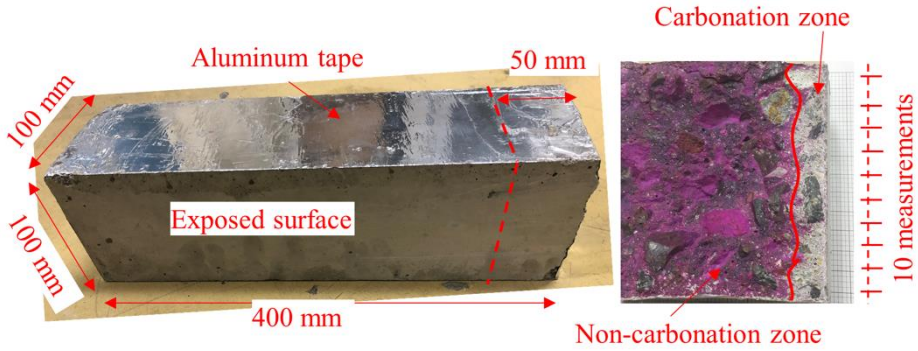

Fig. 3.7. Carbonation depth measurement

3.3.4. Permeability

The aim of water permeability test is to measure the inter-connected pores in the cement matrix. The permeability was measured on concrete specimens at 28, 91, and 182 days under sealed and carbonation conditions according to ASTM C642 [14]. The average of the measurements from three samples were reported.

The sample for permeability test was firstly dried in an oven at 105 ± 5 °C for 24 h. The mass of dried sample (m_d) was measured after cooling at 20 ± 2 °C. Then, it was immersed in water at 20 ± 2 °C for 48 h. The mass of saturated sample (m_s) was measured after boiling in tap water for 5 h to fully fill all the open porosity and cooling down for 14 h at 20 °C. Finally, the sample was suspended in water and its mass (m_w) was measured, as shown in Fig. 3.8. The water absorption and apparent porosity were calculated following Eqs. (3-1) and (3-2), respectively.

$$\text{Water absorption}, \% = \left(\frac{m_s - m_d}{m_d}\right) \times 100 \quad (3\text{-}1)$$

$$\text{Apparent porosity}, \% = \left(\frac{m_s - m_d}{m_s - m_w}\right) \times 100 \quad (3\text{-}2)$$

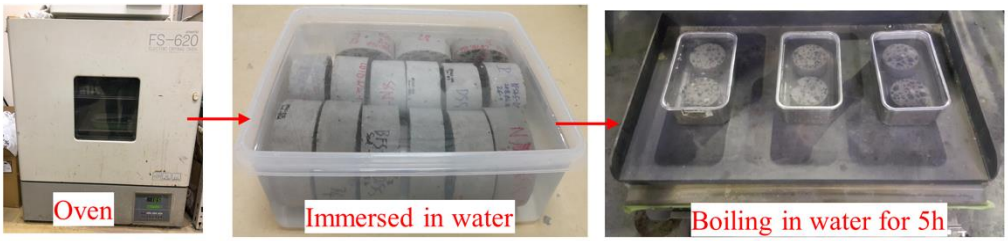

Fig. 3.8. Permeability measurement

3.3.5. Sorptivity

The sorptivity test is to determine the absorption and transmittance of fluids into the body of material by capillary suction. The sorptivity test was conducted on concrete specimens at 28, 91, and 182 days under sealed and carbonation conditions according to ASTM C1585 [15]. All the values reported here are the average from three samples.

The carbonation process can dry concrete specimens, leading to the difference in the moisture of specimens between sealed and carbonation conditions. To achieve the homogeneous moisture and constant mass, all the samples under both sealed and carbonation conditions were preprocessed in the environmental chamber at 50 ± 2 ºC and 80% ± 3% R.H. for 3 days, and then cooled to 20 ºC in a sealed container for 15 days. Then, the curved surface of cylindrical sample was coated with aluminum adhesive tape, whereas one of the flat surfaces was covered with a plastic sheet to avoid evaporation and any flow of water into the sample, except through the exposed flat surface. The initial mass of the sample was measured, and then the sample was partially immersed in water with level 2–3 mm, as shown in Fig. 3.9. During the sorptivity test, the mass of the specimen was determined at various times up to 6 h. The cumulative water absorption (I) was calculated by Eq. (3-3). Meanwhile, the sorptivity coefficient (S) was related to the cumulative water absorption and square root of elapsed time ($t^{0.5}$) and can be calculated using Eq. (3-4).

$$I = \frac{\Delta m_t}{a \times d} \tag{3-3}$$

$$S = \frac{I}{t^{0.5}} \quad (3\text{-}4)$$

Where, Δm_t is the gain in mass of the sample at the time t (g); a is the cross-sectional area of the sample (mm^2), and d is the density of water (g/mm^3).

Fig. 3.9. Sorptivity measurement

3.3.6. Thermal gravimetry and differential thermal analysis (TG-DTA)

Thermal gravimetry and differential thermal analysis (TG-DTA) was used to determine amounts of $Ca(OH)_2$ (CH) and $CaCO_3$ (CC) in concrete, as shown in Fig. 3.10. The individual measurements were carried out for each specimen, as also mentioned in the previous studies [16,17]. The heating rate was 10 °C/min from room temperature (i.e., approximately 20 °C) to 1000 °C under a nitrogen atmosphere to prevent carbonation. The sample without coarse aggregate from the core of concrete specimen after compressive strength test and from the carbonated area after carbonation depth measurement was collected to represent for non-carbonation and carbonation areas, respectively. After that, all the samples were immediately soaked in acetone for 24 h to stop further hydration and carbonation. The sample was then dried in a vacuum desiccator for 24 h and ground into powder particles with a maximum size of 150 μm for TG-DTA. The CH content of paste in sample was determined based on the ignited mass of paste in sample and the mass loss of dehydration of CH in the sample obtained from the TGA

curve between the initial and final temperatures of the corresponding DTA peaks between 400 and 500 °C. The amount of CC of paste in sample was also calculated from the ignited mass of paste in sample and the mass loss of CO_2 in the decarbonation between 550 and 800 °C. Additionally, a chemical test was also performed to measure the aggregate and paste content in sample based on the reports of the Japan Cement Association [18,19]. After grinding, approximately 1 g of powder was poured into 250 ml of 0.1 M HCl solution. The solution was then stirred for approximately 20 min by using a magnet machine with rotation speed of 300 rpm (rounds per minute) and 30 °C. Thereafter, the solution was filtered to obtain the solid powder using filter paper. Subsequently, solid powder was heated up to 1000 °C in an electric furnace for approximately 7 h to eliminate free and chemically bound water. The mass of residual solid powder after ignition was measured. The aggregate content in sample was directly calculated based on the mass loss of sample before and after ignition, whereas the paste content was determined by combining the chemical and TG-DTA tests. Finally, the CH and CC contents of paste in sample as a percentage of cement content was calculated based on considering the quantitative determination of aggregate and paste in the sample as the following Eqs. (3-5) and (3-6) which were referred to the previous studies [16,20]. The cement hydration produced CH, which was probably consumed by carbonation and pozzolanic reaction, whereas the carbonation of cement hydration products (i.e., CH and calcium silicate hydrate (C–S–H)) mostly generated CC. Therefore, based on the reduction in the amount of CH between sealed and carbonation conditions, the amount of CC formed from CH was calculated. Meanwhile, that from C–S–H was determined by the difference in the amount of CC between measuring in sample and converting from the amount of carbonated CH.

$$CH = \frac{CH^{TG-DTA}}{r \times B} \times 100 \quad (3\text{-}5)$$

$$CC = \frac{CC^{TG-DTA}}{r \times B} \times 100 \quad (3\text{-}6)$$

where CH and CC are the percentages of CH and CC of the paste in the sample based on the cement mass%, B is the amount of cementitious materials in the sample (mass%), CH^{TG-DTA} and CC^{TG-DTA} are the amounts of CH and CC (mass%) of the paste in the sample as determined from TG-DTA analysis, and r is the mass ratio of cement in the cementitious materials (r = 1 for OPC concrete, r = 0.85 for FA concrete, and r = 0.55 for BFS concrete).

Fig. 3.10. TG-DTA measurement

3.3.7. Mercury intrusion porosimetry (MIP)

The pore volumes of test specimens were determined by mercury intrusion porosimetry (MIP), as shown in Fig. 3.11. A previous study [21] proved that cored and crushed concrete samples provided virtually identical MIP results; therefore, even if compressive strength test affected the microstructure, the crushed concrete sample without coarse aggregate could be used after the compressive strength test to measure the pore volume by MIP. After the compressive strength test, mortar samples from the cores of broken concrete specimens were selected and carefully cut into small pieces with a size range of 2.5–5.0 mm. The samples were then immersed in acetone to stop further hydration. Before measurement, the samples were dried in a vacuum desiccator for 24 h. The sample mass for a MIP measurement was approximately 1.5 g. All the results of the pore volumes were individual measurements. It is noted that mortar (cement paste and fine aggregate) was used as the samples for individual

measurements which were also carried out via MIP test in the previous studies [16,20]. The MIP apparatus used in this study operated at a maximum pressure of 414 × 10^8 N/m^2. The pore size distribution of samples was determined over a diameter range of 0.003–200 μm.

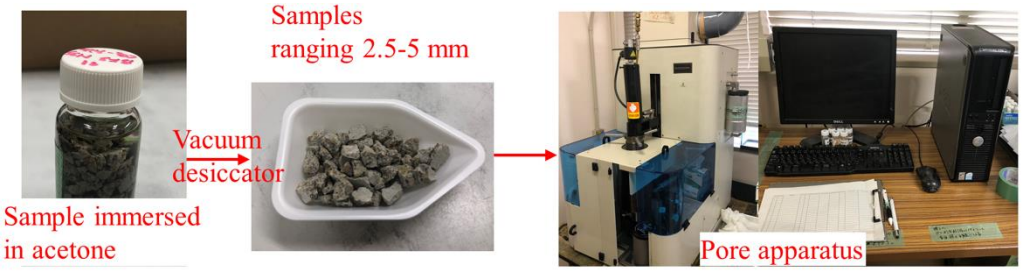

Fig. 3.11. Pore structure measurement

3.3.8. Scanning electron microscopy (SEM)

Scanning electron microscopy (SEM) analysis was used to identify the peculiar morphological characteristics of samples and to strengthen the arguments provided in discussions. The SEM test was performed on the samples at 182 days, as shown in Fig. 3.12. While the samples from the core of specimen under sealed condition were chosen, those from the carbonated area of the prismatic fragment was collected to represent carbonation condition. Then, the samples were carefully crushed into the size of approximately 5 mm and immersed in acetone to stop hydration. Before testing, the samples were dried for 24 h in a vacuum desiccator. An acceleration voltage of 15 kV and magnification of 500 was applied to all samples after coating with platinum.

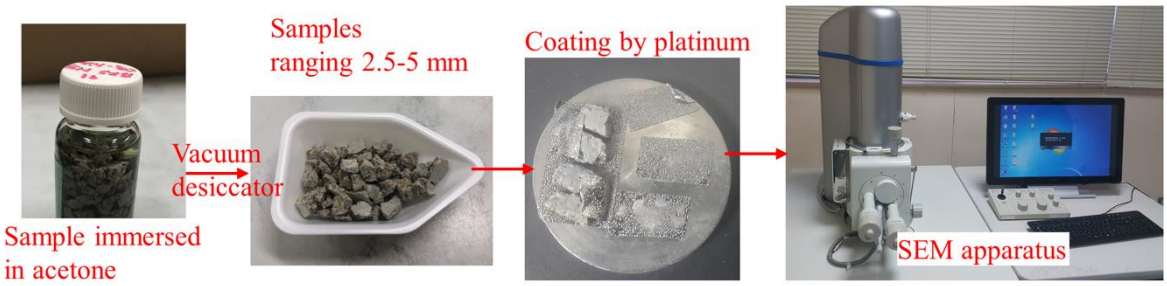

Fig. 3.12. Microstructure measurement by SEM

3.3.9. Crack evaluation by visual observation

Cracks with a width of approximately 0.1 mm were formed on the surface of concrete specimens under carbonation condition. Therefore, crack visual observation was carried out to detect its distribution. One specimen (prepared similar to the specimens prepared for apparent porosity test as mentioned in section 3.2.3) at 182 days of each mixture under both conditions was randomly chosen to impregnate with a fluid resin containing a fluorescent dye. Then, the specimens were subjected to the light of the ultraviolet lamp to detect cracks by visual observation and take images with a digital camera, as shown in Fig. 3.13. Because the fluorescent resin included very low viscosity epoxy, the specimen immersed in fluorescent resin was placed in a vacuum for 2 h to increase the penetration depth of fluorescent resin. When the fluorescent resin hardened, the remained fluorescent resin on the surface of the specimen was cut to provide a test surface.

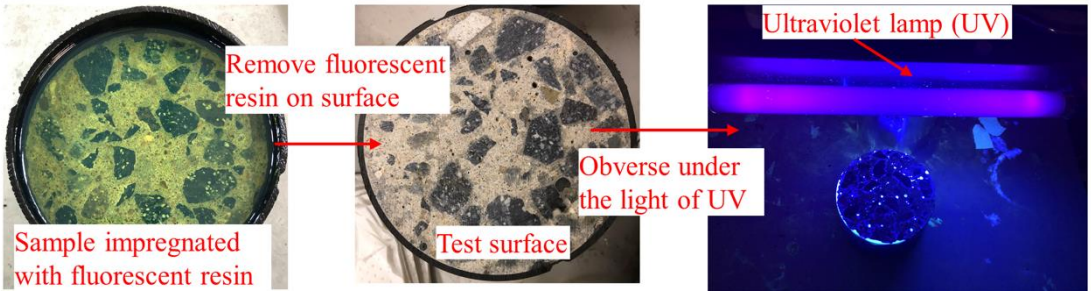

Fig. 3.13. Crack evaluation

3.3.10. Chloride ion content in hardened concrete

To evaluate the effect of carbonation on chloride binding, the samples without coarse aggregate were taken from the carbonated zone after measuring carbonation depth. Meanwhile, that from the core of broken concrete specimens, which were stored under sealed condition, was collected after compressive strength test for comparison. Before measuring, the sample was ground into fine powder and sieved through a 150 μm sieve. For measuring free chloride ion content, the approximate 5 g of the powder was dissolved in 100 mL pure water and stirred for 30 min by using a magnetic stirrer with the rotation speed of 300 rpm (revolutions per minute) and temperature of 50 ºC. For measuring the total chloride ion content, approximately 1 g of the powder was dissolved in 50-mL of 2 mol HNO_3 and boiled for 5 min to completely extract the chloride ion from the powder. For the sample containing FA or BFS, it is noted that 1 mL of H_2O_2 (hydrogen peroxide) was added in the solution to completely extract chloride ions from the hardened sample. After boiling, the solutions containing samples were filtered using filter paper. Subsequently, total volume of 200-mL solution was obtained by adding 150-mL pure water. Then, the solutions obtained after filtering were used to determine the free and total chloride ion content, as shown in Fig. 3.14. An ion chromatography apparatus I1000 was employed to determine the total and free chloride ions in the concrete according to JIS A1154 [4].

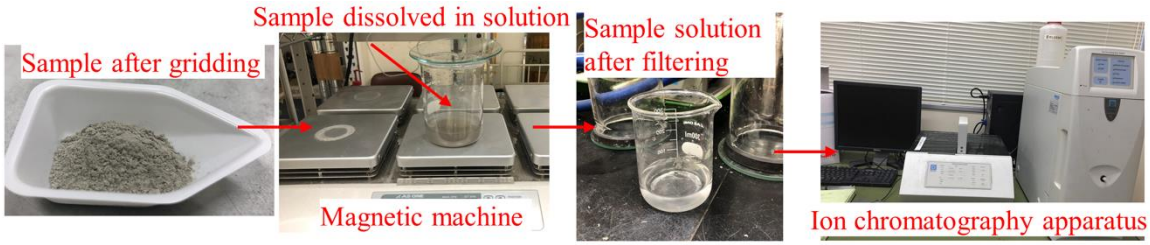

Fig. 3.14. Chloride ion measurement

3.4. Summary

The experiments conducted in this study are summarised in Fig 3.15. They are discussed in detail in the following chapters.

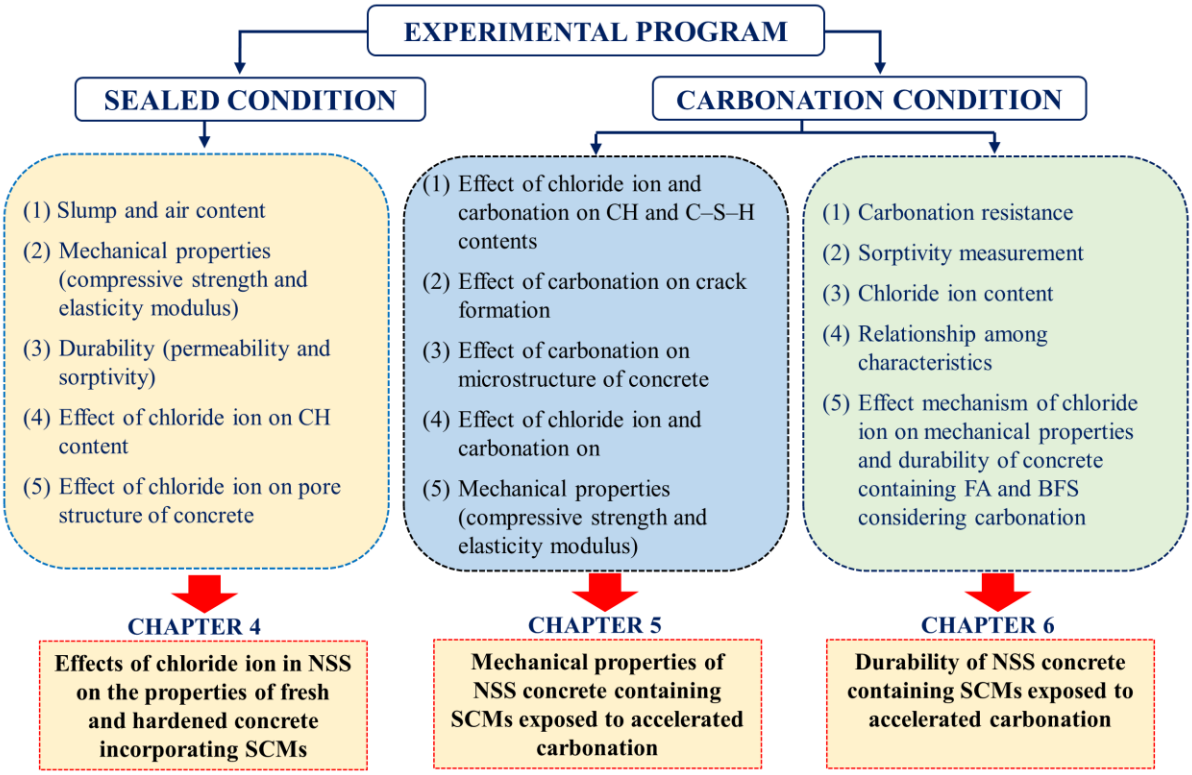

Fig. 3.15. Outline of the experimental program

References of chapter 3:

[1] JIS R 5210, Portland cement, Japanese Standards Association, Tokyo, (2009).

[2] JIS A 6201, Fly ash for use in concrete, Japanese Standards Association, Tokyo, (2015).

[3] JIS A 6206, Ground granulated blast-furnace slag for concrete, Japanese Standards Association, Tokyo, (2013).

[4] JIS A 1154, Concentration of chloride ions contained in hardened concrete, Japanese Standards Association, Tokyo, (2012).

[5] JIS A 1102, Method of test for sieve analysis of aggregates, Japanese Standards Association, Tokyo, 2014.

[6] J. Xiao, C. Qiang, A. Nanni, K. Zhang, Use of sea-sand and seawater in concrete construction: Current status and future opportunities, Construction and Building Materials. 155 (2017) 1101–1111.

[7] JASS 5, Japanese architectural standard specification for reinforced concrete work, Architectural Institute of Japan, Tokyo, 40 (2002) 19–27.

[8] P. H. R. Borges, J. O. Costa, N. B. Milestone, C. J. Lynsdale, R. E. Streatfield, Carbonation of CH and C–S–H in composite cement pastes containing high amounts of BFS, Cement and Concrete Research. 40 (2010) 284–292.

[9] C. D. Atiş, Accelerated carbonation and testing of concrete made with fly ash, Construction and Building Materials. 17 (2003) 147–152.

[10] JIS A 1101, Method of test for slump of Concrete, Japanese Standards Association, Tokyo, (2014).

[11] JIS A 1128, Method of test for air content of fresh concrete by pressure method, Japanese Standards Association, Tokyo, (2005).

[12] JIS A 1108, Method of test for compressive strength of concrete, Japanese Standards Association, Tokyo, (2006).

[13] JIS A 1149, Method of test for static modulus of elasticity of concrete, Japanese Standards Association, Tokyo, (2010).

[14] ASTM C642-13, Test method for density, absorption, and voids in hardened concrete, ASTM International, West Conshohocken, 2013.

[15] ASTM C1585-13, Test method for measurement of rate of absorption of aater by hydraulic-cement concretes, ASTM International, West Conshohocken, 2013.

[16] P. T. Bui, Y. Ogawa, K. Nakarai, K. Kawai, R. Sato, Internal curing of Class-F fly-ash concrete using high-volume roof-tile waste aggregate, Mater Struct. 50 (2017) 203.

[17] P. T. Bui, Y. Ogawa, K. Nakarai, K. Kawai, Effect of internal alkali activation on pozzolanic reaction of low-calcium fly ash cement paste, Mater Struct. 49 (2016) 3039–3053.

[18] Japan Cement Association Joint Research Report on Mixture Proportion Estimation of Hardened Concrete, Report of Technical Committee on Concrete, F-18 (In Japanese), 1967.

[19] Japan Cement Association Joint Research Report on Mixture Proportion Estimation of Hardened Concrete (Part 2), Report of Technical Committee on Concrete, F-23 (In Japanese), 1971.

[20] L. S. Ho, K. Nakarai, Y. Ogawa, T. Sasaki, M. Morioka, Effect of internal water content on carbonation progress in cement-treated sand and effect of carbonation on compressive strength, Cement and Concrete Composites. 85 (2018) 9–21.

[21] R. Kumar, B. Bhattacharjee, Study on some factors affecting the results in the use of MIP method in concrete research, Cement and Concrete Research. 33 (2003) 417–424.

CHAPTER 4. EFFECTS OF CHLORIDE ION IN NSS ON THE PROPERTIES OF FRESH AND HARDENED CONCRETE INCORPORATING SCMs

This chapter discusses the effect of chloride ion in non-desalted sea sand (NSS) on the properties of fresh and hardened concrete containing supplementary cementitious materials (SCMs) under sealed condition to extensively verify the application of NSS for concrete production. The effect of chloride ion on the variation of slump and air content of fresh concrete was observed for 60 min. Meanwhile, the effect of chloride ion on compressive strength, modulus of elasticity, permeability, and sorptivity of hardened concrete containing SCMs was investigated after 91 days of curing under sealed condition. Moreover, the pore structure and portlandite (CH) content in concrete were also measured to explain the mechanism.

4.1. Properties of fresh concrete

4.1.1. Slump

Figure 4.1 exhibits the slump variation of all the fresh concrete mixtures with time. In this study, the addition of water-reducing agent (WRA) and air-entraining agent (AE) to all the mixtures with DSS helped to control the initial slump to 150 ± 20 mm. The same dosages of WRA and AE were used for both desalted sea sand (DSS) and NSS concretes containing the same binder, as given in Table 3.3; however, their dosages differed between the OPC, FA15, and BFS45 mixtures. Initial slumps of concretes made with NSS were considerably lower than those made with DSS, despite the same dosages of WRA and AE, except for FA replacement. It is different from the results of Liu et al. [1] which showed that the slump of fresh NSS concrete was unnoticeably different compared with that of river sand (RS) concrete. It may be

due to the various chemical composition (e.g., chloride ion content) and characteristics (e.g., surface texture, particle size) of NSS from different regions. The difference in initial slump between NSS and DSS concretes is probably due to the fine particles of NSS. The desalination process is believed to decrease the amount of fine particles in DSS, as reported by Erdogan et al. [2]. The mass of fine particles passing 0.30 mm in NSS was slightly higher than that in DSS, as seen in Table 3.2 (see Section 3.1.2). In particular, the amount of fine particles passing 0.30 mm was 11.9% for NSS, whereas that was 8.1% for DSS; Fine particles can increase the water demand of concrete which leads to the decrease in the fluidity of fresh concrete. Initial slumps of concretes made with NSS were therefore lower than those of concretes made with DSS.

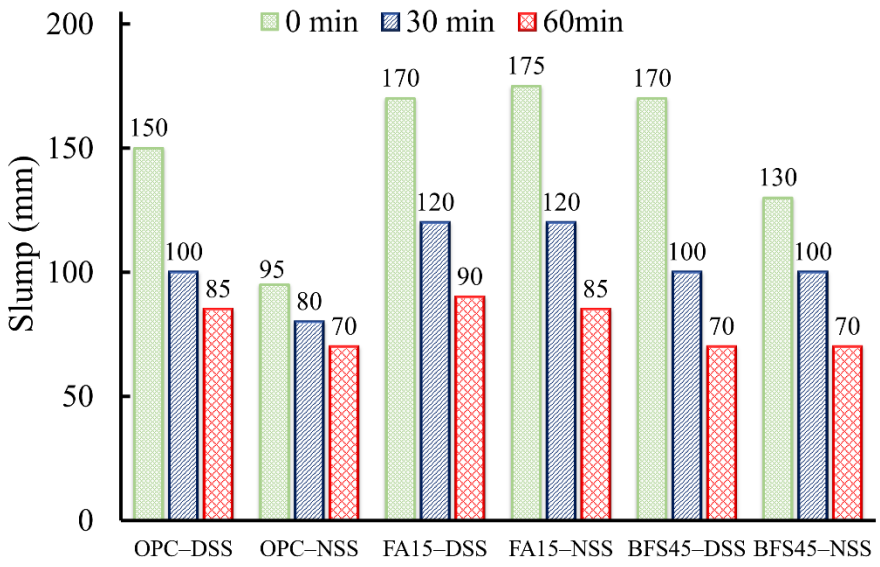

Fig. 4.1. Slump variances of concretes

The replacement of OPC by SCMs remarkably increased the initial slump although low dosages of WRA were used compared with OPC concretes (Table 3.3, chapter 3). According to previous studies [3,4], the surface smoothness and denseness of FA and BFS enhance their dispersion in cement. Therefore, the initial slumps of FA and BFS concretes improved.

Regardless of concrete mixture proportion, the slumps of concretes decreased with increasing elapsed time; however, there was no significant difference in slump loss at 60 min between NSS and DSS concretes. This indicates that the chloride ion in NSS did not influence the slump variance of concretes with time. It is inconsistent with the conclusion of Younis et al. [5] who concluded that the chloride ion in seawater remarkably affected the properties of fresh concrete. The initial slump flow and setting time of concrete using seawater was 20% and 30% lower than those of the reference concrete (concrete using freshwater) [5]. Also, the slump flow of seawater concrete decreased much more quickly than that of reference concrete. It is due to the much higher presence of chloride ion in seawater presented by Younis et al. [5] (approximately 1.8235% by mass) than that in NSS (0.1968% by mass). Additionally, slight bleeding occurred during the casting of OPC–DSS, but mixtures containing FA and BFS or using NSS showed no bleeding. This is attributed to the effect of the fine particles. Although the mass of cementitious materials was the same in all the concretes (i.e., 350 kg/m^3), the volumes of cementitious materials of the FA and BFS concretes were 6.5% and 4.2% higher than that of OPC concrete, respectively. The greater the proportion of fine particles, the higher the water demand. Therefore, FA or BFS could increase the cohesiveness and water retention of concretes after mixing.

4.1.2. Air content

The variations of air contents of all the concretes are given in Fig. 4.2. The difference in the initial air contents between the DSS and NSS concretes was only 0.1%. This indicates that NSS had no significant influence on the initial air content of concretes, regardless of SCMs replacement. However, the air content of concretes containing FA was remarkably reduced compared with the others from 30 min after mixing. This is attributed to the absorption of AE on unburned carbon particles in FA [6]. The air content of NSS concretes was similar to that of

DSS concretes at 60 min after mixing, which implies that the chloride ion in NSS did not affect the air content of concrete for this aging time.

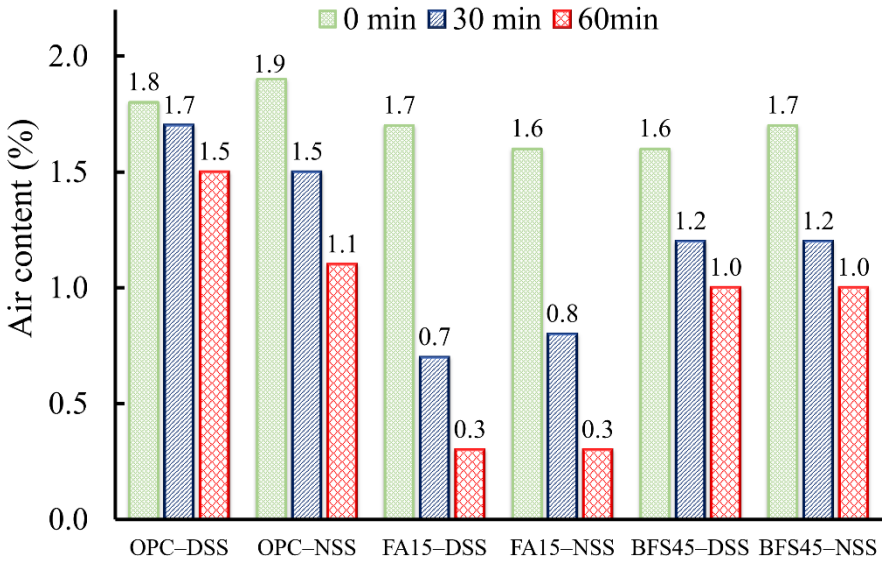

Fig. 4.2. Air content variances of concretes

4.2. Properties of hardened concrete

4.2.1. Compressive strength

The morphology and surface texture of fine aggregate can affect the compressive strength of concrete. Basically, NSS and DSS had the same morphology and surface texture because they came from the same source. The desalination process does not influence the changes of morphology and surface texture of DSS. Therefore, the effect of the difference in the morphology and surface texture between NSS and DSS on the compressive strength was negligible

To assess the effect of chloride ion in NSS and SCMs replacement on the compressive strength of concrete, their compressive strength increments for the concrete specimens were calculated using Eqs. (4-1) and (4-2), respectively:

$$Compressive\ strength\ increment\ (chloride\ ion)\ (\%) = \frac{f'_{c,NSS} - f'_{c,DSS}}{f'_{c,DSS}} \times 100, \quad (4\text{-}1)$$

$$Compressive\ strength\ increment\ (SCMs)\ (\%) = \frac{f'_{c,SCMs} - f'_{c,OPC}}{f'_{c,OPC}} \times 100, \quad (4\text{-}2)$$

where $f'_{c,NSS}$, $f'_{c,DSS}$, $f'_{c,SCMs}$, and $f'_{c,OPC}$ are the compressive strengths of concretes containing NSS, DSS, FA or BFS, and OPC alone, respectively.

The effect of chloride ion in NSS on the compressive strength of concretes is presented in Fig. 4.3. The compressive strength of concrete using NSS was 8.9% to 15.1% higher at 3 days than that of concrete using DSS. It is assumed that NSS improved the compressive strength of concrete at an early age due to the presence of chloride ion [7]. Chloride is known to accelerate cement hydration by reacting with tricalcium aluminate (C_3A) to generate $3CaO{\cdot}Al_2O_3{\cdot}CaCl_2{\cdot}10H_2O$ (Friedel's salt) via Eq. (4-3) [8]. Friedel's salt can fill the pore space of concrete and make the concrete more compact, leading to an increase in compressive strength [7].

$$3CaO \cdot Al_2O_3 + Ca(OH)_2 + 2NaCl + 10H_2O \rightarrow 3CaO \cdot Al_2O_3 \cdot CaCl_2 \cdot 10H_2O + 2NaOH, \quad (4\text{-}3)$$

In addition, the presence of chloride ion in concrete accelerated the hydration of tricalcium silicate (C_3S), resulting in the formation of more calcium silicate hydrate (C–S–H) [9]. Consequently, the total pore volume of NSS concretes could be decreased compared with that of DSS concretes. It could be supported by the result in Section 4.5 in terms of pore structure. However, the difference in compressive strength between DSS and NSS concretes gradually decreased with elapsed time up to 28 days and was constant at approximately 5% from 28 to 91 days. The results indicate that the effect of chloride ion in NSS on the compressive strength of concrete was great only at an early age, but decreased with the progress of cement hydration because the chloride ion was bound with hydration products during hydration, resulting in the

elimination of acceleration of hydration [10,11]. In contrast, the effect of chloride ion in NSS on the compressive strength increment of SCMs concretes was higher than that of OPC concretes at 3 days, especially for BFS concretes. This implies that the chloride ion accelerated not only the hydration of cement, but also SCMs reactivity. The acceleration of the hydration of C_3S due to the presence of chloride ion also led to the formation of more CH [9] which could promote the SCMs reactivity. The formation of CH is discussed more in Section 4.4 in terms of CH content. Because the particle size of the SCMs was smaller than that of OPC, the chloride ion could easily accelerate their activity, especially the hydraulicity of BFS.

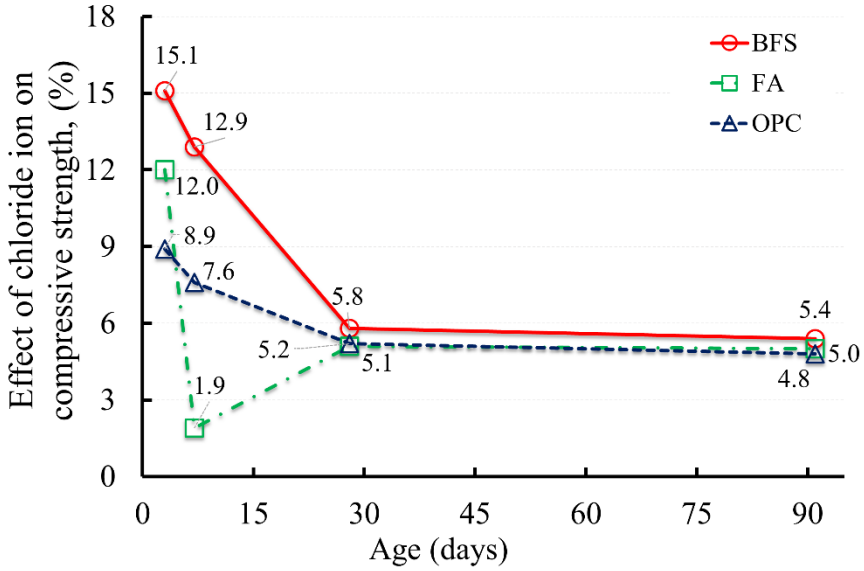

Fig. 4.3. Effects of chloride ion in non-desalted sea sand (NSS) on compressive strength of concretes

Fly ash and BFS replacements also reduced the compressive strength of concrete at early ages due to the dilution effect, even when NSS was used as fine aggregate, as seen in Fig. 4.4. The compressive strength of BFS concretes increased slightly by 2.0%, while that of FA concretes decreased by 2.7% in comparison with OPC concretes at 28 days. This is attributed to the slow reactivity of FA [3]. At 91 days, the compressive strength of FA concretes was

almost the same as that of OPC concretes and there was no difference between FA concretes using NSS and DSS. Owing to hydraulicity [12–14], the compressive strength of BFS45-DSS concrete increased by 8.8% and that of BFS45-NSS concrete increased by 9.5% at 91 days.

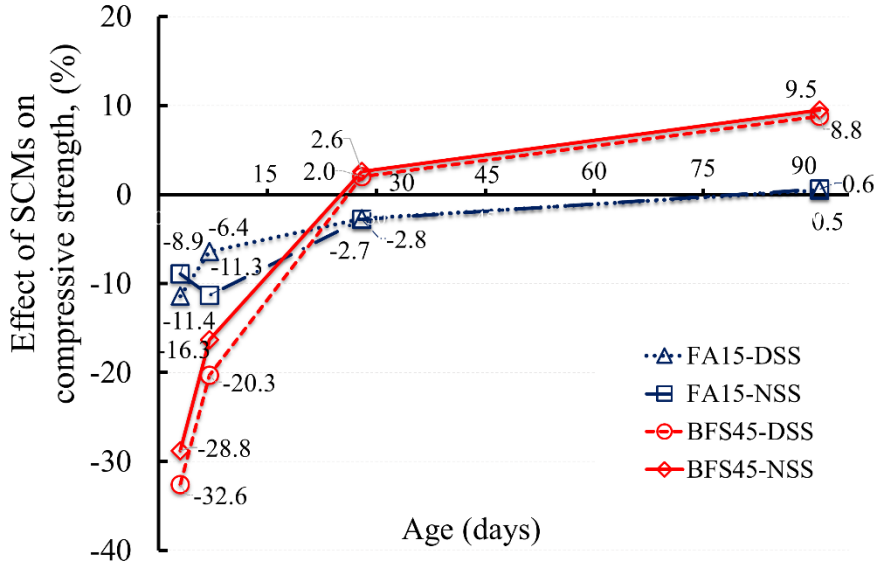

Fig. 4.4. Effects of supplementary cementitious materials (SCMs) on compressive strength of concretes

Figure 4.5 demonstrates the change in compressive strength of all the concrete specimens relative to that of OPC-DSS. It is obvious that the compressive strength of OPC-NSS concrete was higher than that of reference concrete until 91 days. This is in contrast with the results of some previous studies [15–17] which reported that the NSS concrete had nearly the same or even lower compressive strength compared to RS or pit sand concrete after 28 days. The difference could be due to the various characteristics and composition of NSS from different regions. The combination of chloride ion in NSS and SCMs replacement showed better effects on the strength development than SCMs replacement alone. In particular, FA replacement decreased the compressive strength by 2.7% at the age of 28 days, but when FA concrete

contained additional NSS, its compressive strength was 2.2% higher than that of the reference. Although the compressive strength increment of BFS45-DSS concrete was only 8.8% higher than the reference, that of BFS45-NSS increased by 14.7% at 91 days. This trend was also observed for FA15-NSS concrete. This result extensively demonstrated that chloride ion in NSS improved the strength development of not only NSS concrete using 100% OPC as reported in the previous study [18] but also NSS concrete containing SCMs.

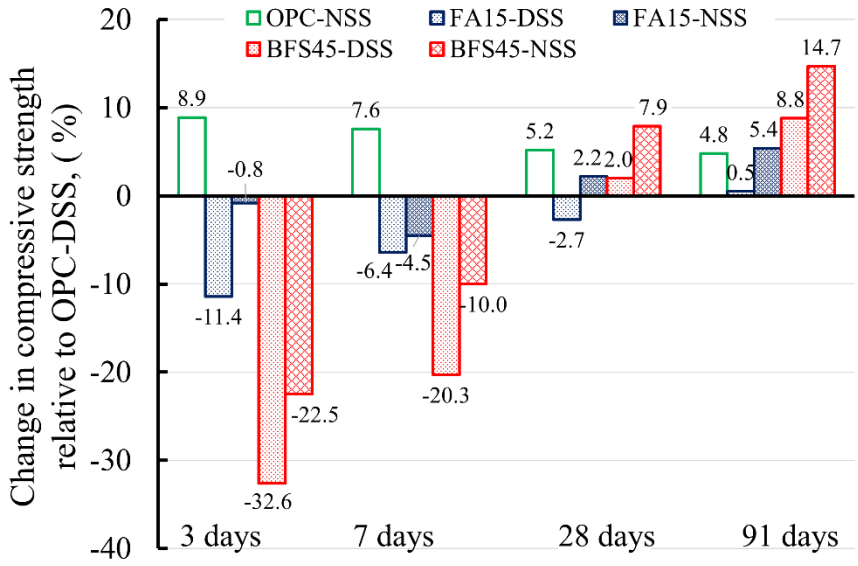

Fig. 4.5. Change in compressive strength relative to OPC-DSS

4.2.2. Modulus of elasticity

The effects of chloride ion and SCMs replacement on the modulus of elasticity were evaluated using Eqs. (4-4) and (4-5), respectively:

$$Modulus\ of\ elasticity\ increment\ (chloride\ ion)\ (\%) = \frac{E_{NSS} - E_{DSS}}{E_{DSS}} \times 100, \quad (4\text{-}4)$$

$$Modulus\ of\ elasticity\ increment\ (SCMs)\ (\%) = \frac{E_{SCMs} - E_{OPC}}{E_{OPC}} \times 100, \quad (4\text{-}5)$$

where E_{NSS}, E_{DSS}, E_{SCMs}, and E_{OPC} are the moduli of elasticity of concretes containing NSS, DSS, FA or BFS, and OPC alone, respectively.

Figure 4.6 shows the effect of chloride ion in NSS on the moduli of elasticity of the concretes. Chloride ion in NSS noticeably affected the modulus of elasticity at 3 days: the increment at 3 days ranged from 9.6% to 21.9%. Thereafter, the modulus of elasticity increment of BFS concrete gradually decreased up to 91 days, while that of OPC and FA concretes significantly decreased at 28 days. The effect of chloride ion on the modulus of elasticity of OPC and FA concretes was not observed at 91 days. The reason was explained in Section 4.2.1 in terms of the compressive strength. The effects of SCMs on the moduli of elasticity of the concretes are shown in Fig. 4.7. Although chloride ion can contribute to the modulus of elasticity, the modulus of elasticity of BFS concrete was still decreased by 13.7% at 3 days due to dilution effect; however, owing to the hydraulicity, the modulus of elasticity of BFS concrete using NSS remarkably increased and was 4.7% higher than that of the corresponding OPC concrete at 91 days. FA replacement gave slightly lower modulus of elasticity for both DSS and NSS concretes from 7 to 91 days. Previous studies reported that a high FA replacement ratio led to a decrease in the modulus of elasticity because of a reduction in the stiffness of concrete [19,20]. Wang et al. [20] also proposed that a higher FA replacement ratio (i.e., above 15%) could reduce the modulus of elasticity. The reduction of modulus of elasticity due to FA replacement was also observed by a previous study [21]. The reason was explained that the high silicate content in FA and its very slow reactivity leads to an increase in elasticity or reduction in stiffness of the concrete [21].

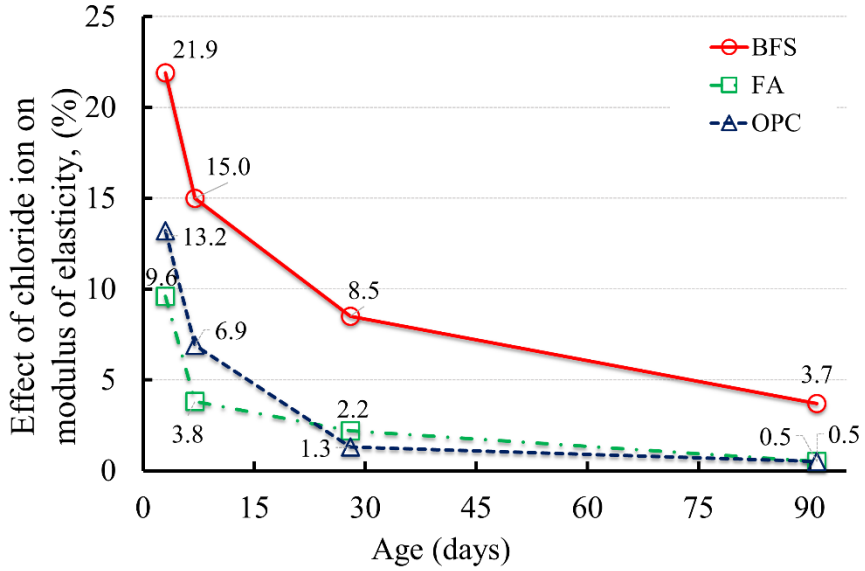

Fig. 4.6. Effects of chloride ion in non-desalted sea sand (NSS) on moduli of elasticity of concretes

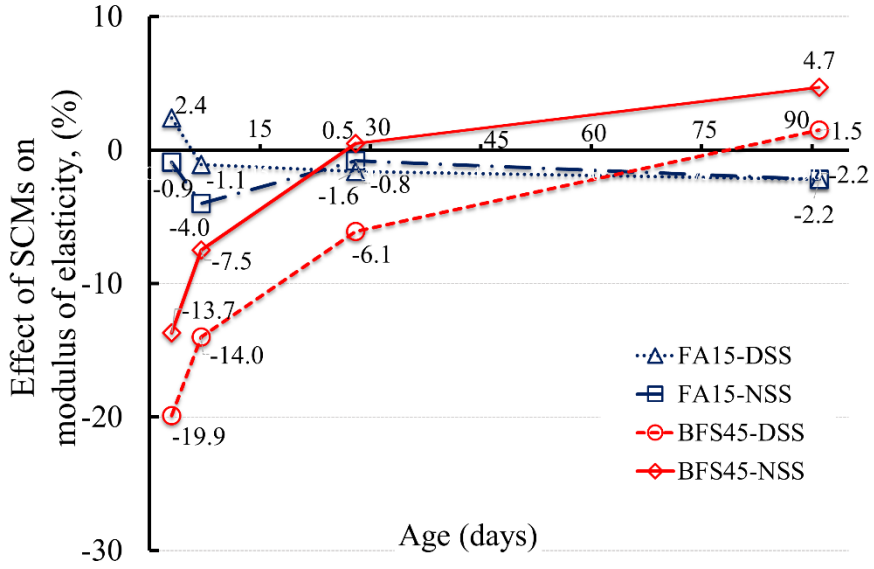

Fig. 4.7. Effects of supplementary cementitious materials (SCMs) on moduli of elasticity of concretes

The change in moduli of elasticity of all the concrete specimens relative to that of OPC-DSS are shown in Fig. 4.8. The effect of BFS replacement on the modulus of elasticity increased with time, whereas that of FA replacement decreased, regardless of the presence of chloride ion. According to these results, BFS replacement increased the modulus of elasticity of concrete by

1.5% in comparison with the reference concrete at 91 days; the increment in modulus of elasticity was 5.2% when NSS was used. However, the combined effect of chloride ion and FA replacement still showed a reduction in relative modulus by 1.7%.

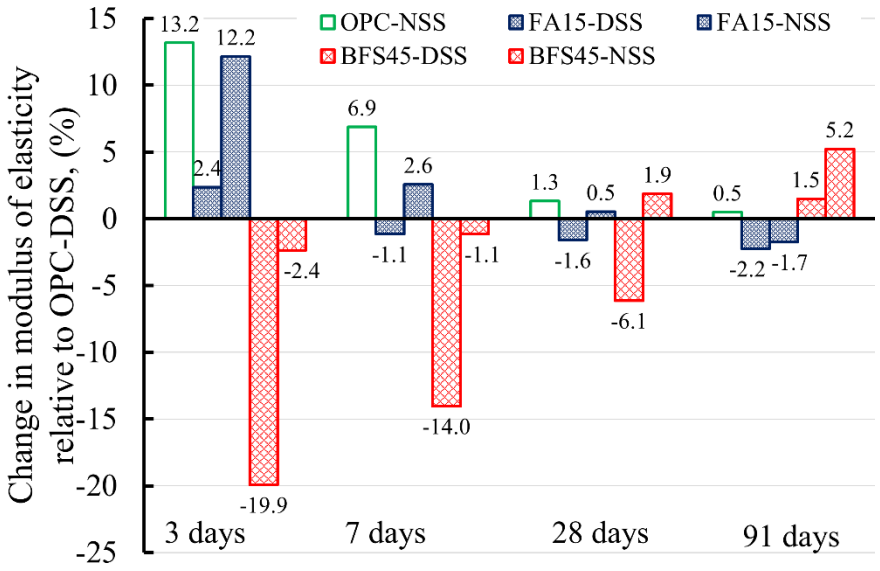

Fig. 4.8. Change in modulus of elasticity relative to OPC-DSS

4.3. Durability of concrete

4.3.1. Permeability

The permeability of concrete was measured according to a method proposed in previous studies [22,23] using the apparent porosity and connectivity of pores under saturated conditions, which are related to the transportation of water and other aggressive chemicals containing harmful ions into concrete. The results of the water absorption of all the concrete specimens at 28 and 91 days are shown in Table 4.1. It is clear that the water absorption continuously decreased with an increase in curing time. The water absorption of NSS concretes was slightly lower than that of DSS concretes regardless of ages and SCMs replacement. This indicates that NSS had a beneficial effect on the reduction of water absorption of concrete. This is probably

due to the contribution of chloride ion in NSS. As mentioned in Section 4.2.1, the formation of Friedel's salt can fill spaces between the granular skeleton and convert connected pores in concrete to relatively independent unconnected pores, leading to a decrease in its water absorption [7]. Replacements by FA and BFS also decreased the water absorption. For instance, compared with OPC concrete, FA and BFS replacements decreased the water absorption at 91 days by approximately 5% and 10%, respectively. Moreover, water absorption was noticeably reduced by up to 7.8% by the combined effect of chloride ion and FA replacement, whereas the reduction in water absorption by the combination of chloride ion and BFS replacement was 13.7% in comparison with OPC-DSS.

Table 4.1. Water absorption, apparent porosity, and sorptivity of concrete

Mixtures	Water absorption (%)		Apparent porosity (%)		Sorptivity × 10^{-3} ($mm/sec^{0.5}$)	
	28 days	91 days	28 days	91 days	28 days	91 days
OPC-DSS	6.19	6.04	13.8	13.6	3.75	3.55
OPC-NSS	5.95	5.84	13.3	13.1	3.28	3.06
FA15-DSS	6.02	5.69	13.4	12.7	3.63	3.04
FA15-NSS	5.89	5.57	13.2	12.5	3.03	2.75
BFS45-DSS	5.74	5.44	12.8	12.2	2.74	1.57
BFS45-NSS	5.33	5.21	11.9	11.7	2.30	1.56

Transport properties of concrete are generally strongly dependent on its porosity. The lower water absorption reflected lower porosity and permeability. As shown in Table 4.1, the apparent porosity of concrete continuously decreased with the increase in curing time because of continuous formation of products from cement hydration, the pozzolanic reaction of FA, and

the hydraulicity of BFS, which refined the pore structure and voids of the cement matrix [13,24,25]. Chloride ion in NSS contributed to the slight decrease in the apparent porosity of all concretes at 91 days. The FA and BFS concretes also showed lower apparent porosity than OPC concretes. According to previous studies [26,27], the strength and durability of concrete with high water absorption and porosity are easily reduced by physical and chemical phenomena. The reduction in the apparent porosity of all the concrete specimens relative to OPC-DSS is shown in Fig. 4.9. Reduction in the apparent porosity of concrete significantly increased when FA or BFS were combined with chloride ion in NSS, from 6.6% to 8.1% for FA concrete and from 10.3% to 14.0% for BFS concrete at 91 days.

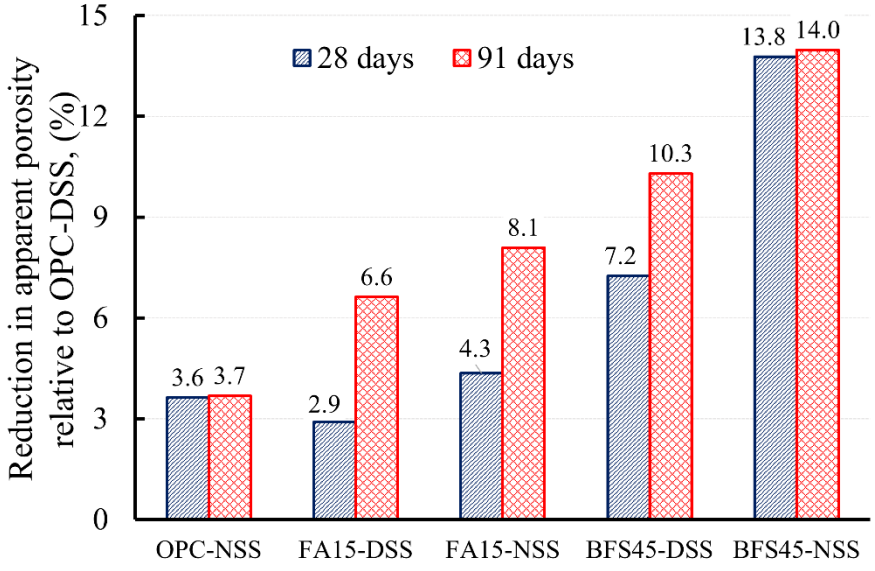

Fig. 4.9. Reduction in apparent porosity of all concrete specimens relative to OPC-DSS at 28 and 91 days

4.3.2. Sorptivity

The durability of concrete is strongly related to the properties of its surface layer, which can control the transport of water into the concrete. The sorptivity test measures the

penetration rate of water into the concrete pores by capillary suction, and can therefore be considered an effective method to evaluate the durability of concrete [18,23]. Table 4.1 shows the sorptivity of all concrete specimens at 28 and 91 days. The reduction in sorptivity of all concrete specimens relative to OPC-DSS is presented in Fig. 4.10. It is evident that the sorptivity of NSS concretes was lower than that of DSS concretes, irrespective of age and SCMs replacement. When the curing time was extended from 28 to 91 days, the sorptivity continuously decreased, especially for concretes containing SCMs. The sorptivity of concretes containing FA and BFS decreased by approximately 3% and 27%, respectively, when compared with concrete made with OPC at 28 days; however, the reduction in the sorptivity of concretes containing FA and BFS significantly increased by around 14% and 56% at 91 days, respectively. These results are in accordance with previous studies that reported that the addition of SCMs contributed to the refinement of capillary pores and reduced the sorptivity of concrete [14,23]. The combination of chloride ion in NSS and SCMs enhanced the quality of concrete in term of sorptivity. In particular, reduction in the sorptivity of NSS concrete containing FA and BFS significantly increased at 91 days, by 22.5% and 56.1%, respectively (see Fig. 4.10). Reduction in the sorptivity can reduce the ingress of water containing aggressive substances that can cause serious damage to concrete, especially concretes exposed to marine environments.

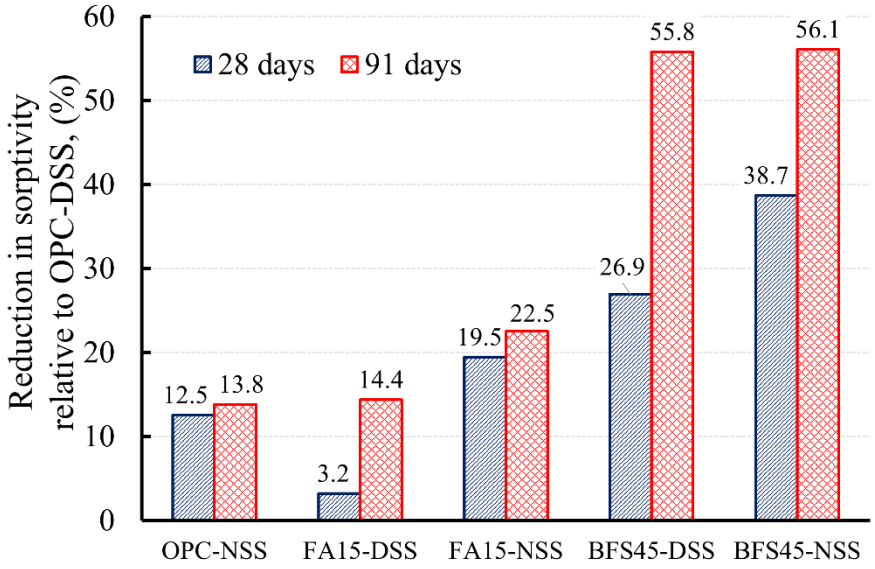

Fig. 4.10. Reduction in sorptivity of all concrete specimens relative to OPC-DSS at 28 and 91 days

4.4. Effect of chloride ion on portlandite content in concrete

Differential thermal analysis and thermogravimetry (DTA-TG) was employed to measure the portlandite content in concrete. Figure 4.11 shows the CH content in the pastes of concrete specimens at 3, 7, 28, and 91 days. As mentioned in Section 4.2.1 in terms of compressive strength, the acceleration of cement hydration by the presence of chloride ion should lead to the greater generation of CH in NSS concretes. However, FA and BFS concretes combined with chloride ion in NSS showed slightly lower CH content than those without chloride ion. It implied that an amount of CH could be consumed by the pozzolanic reaction of FA and hydraulicity of BFS. In other words, the SCMs reactivity could be enhanced by the presence of chloride ion in NSS.

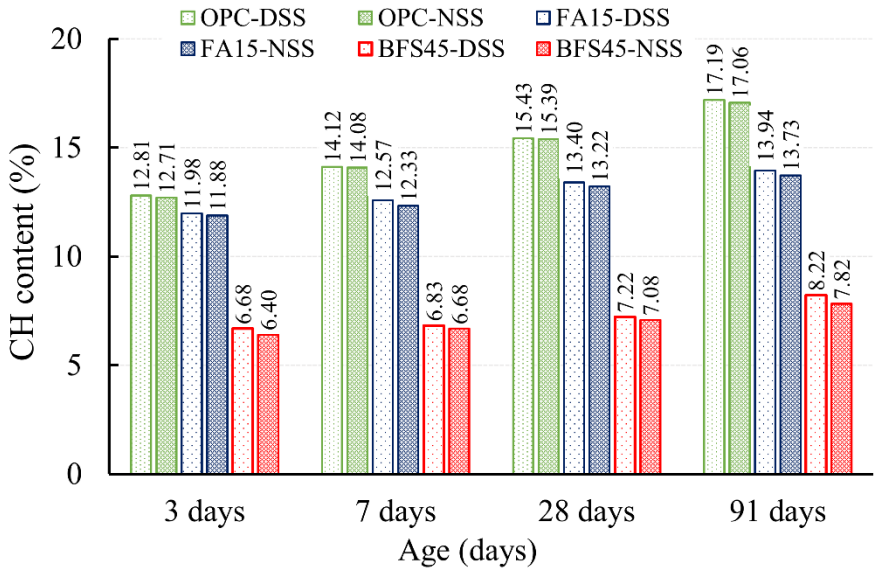

Fig. 4.11. Calcium hydroxide (CH) content in paste of concrete specimens at 3, 7, 28, and 91 days

The CH consumptions of the concrete specimens were calculated using Eq. (4-6) to evaluate the pozzolanic reaction of FA and hydraulicity of BFS:

$$CH\ consumption\ (\%) = \frac{r \times CH_{OPC} - CH_{SCMs}}{r \times CH_{OPC}} \times 100, \quad (4\text{-}6)$$

where, CH_{SCMs} is the CH content of concretes containing FA or BFS, CH_{OPC} is the CH content of OPC concretes, and r is the mass ratio of cement in the cementitious materials (r = 1 for OPC concretes; r = 0.85 for FA concretes and r = 0.55 for BFS concretes).

The effect of SCMs on the CH consumption of concrete is shown in Fig. 4.12. In general, the CH consumption of the FA and BFS concretes increased with time due to the pozzolanic reaction of FA and hydraulicity of BFS, leading to additional C–S–H formation [13,14]. Moreover, the CH consumption of BFS concretes was higher than that of FA concretes. Sakai et al. [28] concluded that the early hydration of cement (before 28 days) was accelerated in the presence of FA due to the fine powder effect. In addition, the reactivity of FA is slower than

that of BFS, depending on its glass content and mineralogical composition [12,28]. Therefore, the CH consumption of FA concretes was negative before 28 days, but the converse happened for BFS concretes. CH is considered to be the main factor leading to the weakness of the interfacial transition zone, which influences the strength, pore structure, and durability of concrete. Therefore, the decrease in CH content and increase in C–S–H content resulted in an improvement of the mechanical properties, permeability, and sorptivity of concrete which were demonstrated in Sections 4.2.1, 4.2.2, 4.3.1, and 4.3.2.

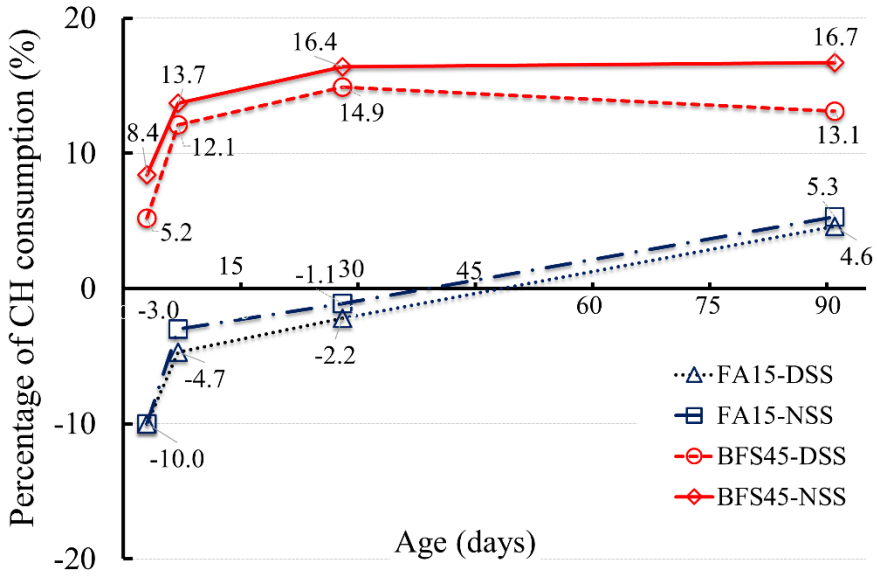

Fig. 4.12. Effect of supplementary cementitious materials (SCMs) on CH consumption

4.5. Effect of chloride ion on pore structure of concrete

The mercury intrusion porosimetry (MIP) was carried out to evaluate the effects of chloride ion as well as SCMs on pore structure of concrete. The MIP test was conducted only at early ages (i.e., at 3 and 7 days) because the effect of chloride ion on strength development was remarkably observed. According to a previous study [29], the pore structure of concrete can be classified into harmless pores (< 20 nm), less harmful pores (20–200 nm), and harmful pores

(> 200 nm), which exhibit impermeability, less permeability, and high permeability, respectively. The results are shown in Table 4.2 and Fig. 4.13. As shown in Table 4.2, the total pore volume of NSS concretes at 3 and 7 days was lower than that of DSS concretes regardless of the addition of FA or BFS. The presence of chloride ion reduced not only the total pore volume of concrete, but also the volume of pores less than 200 nm in diameter regardless of FA or BFS replacement (see Table 4.2). It confirmed again that the chloride ion promoted the cement hydration and SCMs reactivity. The total pore volumes of FA and BFS concretes were higher than that of OPC concretes. These MIP results were consistent with the compressive strength results: the denser the pore structure, the higher the compressive strength. It can be clearly seen from Fig. 4.14 which shows the relationship between compressive strength and total pore volume of concretes at the ages of 3 and 7 days.

Table 4.2. Pore size distribution of all concrete specimens at 3 and 7 days

Mixtures	3 days				7 days			
	Pore size distribution (mm^3/g)			Total pore volume (mm^3/g)	Pore size distribution (mm^3/g)			Total pore volume (mm^3/g)
	>200 nm	20–200 nm	<20 nm		>200 nm	20–200 nm	<20 nm	
OPC-DSS	0.2	4.7	85.7	90.6	0.1	3.0	70.7	73.8
OPC-NSS	0.1	4.6	84.4	89.1	0.1	2.8	61.8	64.7
FA15-DSS	0.2	4.7	92.7	97.6	0.2	4.4	80.7	85.3
FA15-NSS	0.1	3.9	86.5	90.5	0.1	3.8	80.9	84.8
BFS45-DSS	0.1	4.8	100.6	105.5	0.0	4.8	91.5	96.3
BFS45-NSS	0.1	4.5	95.7	100.3	0.1	3.7	79.8	83.6

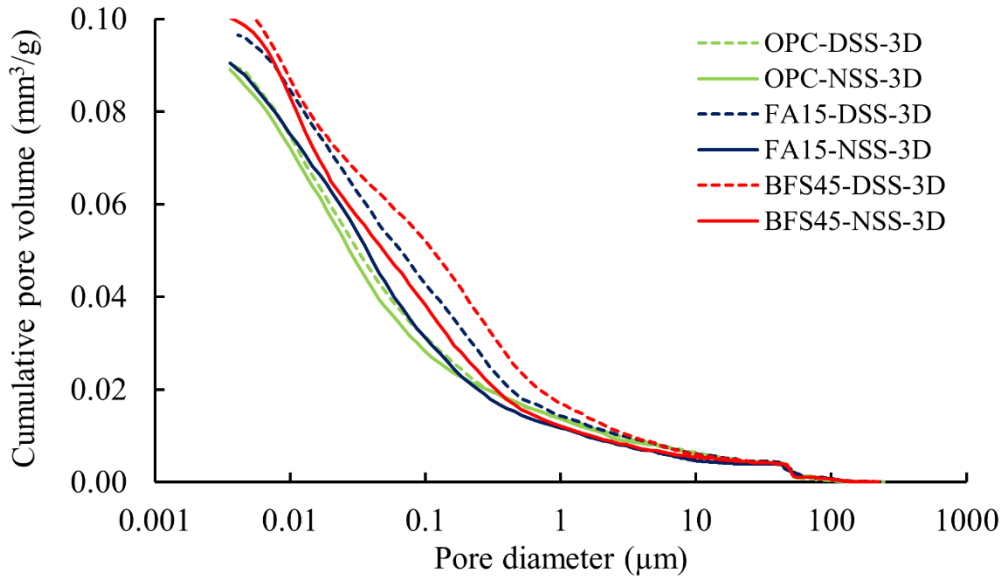

(a) Cumulative pore volume of concrete at 3 days

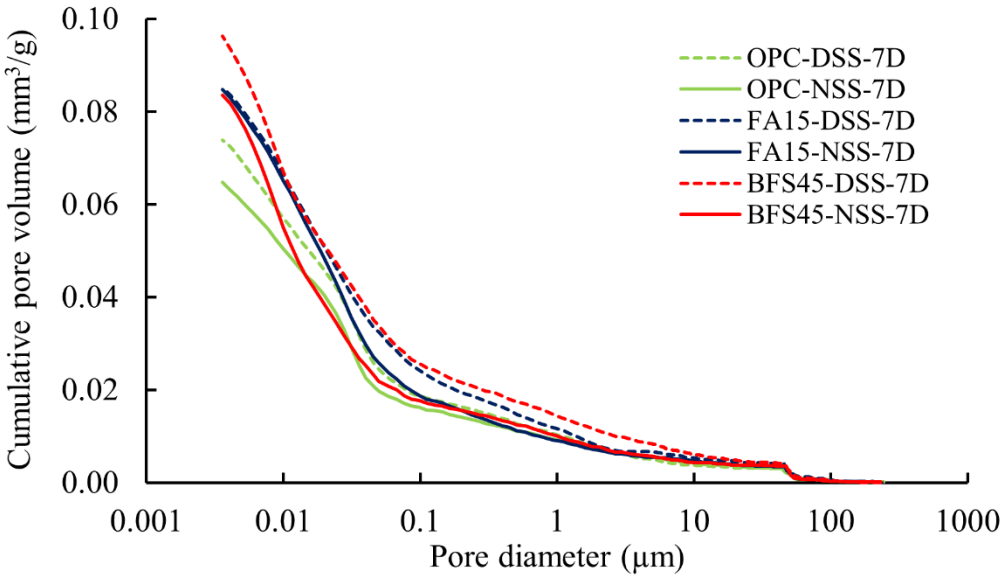

(b) Cumulative pore volume of concrete at 7 days

Fig. 4.13. Cumulative pore volume of concrete at 3 and 7 days

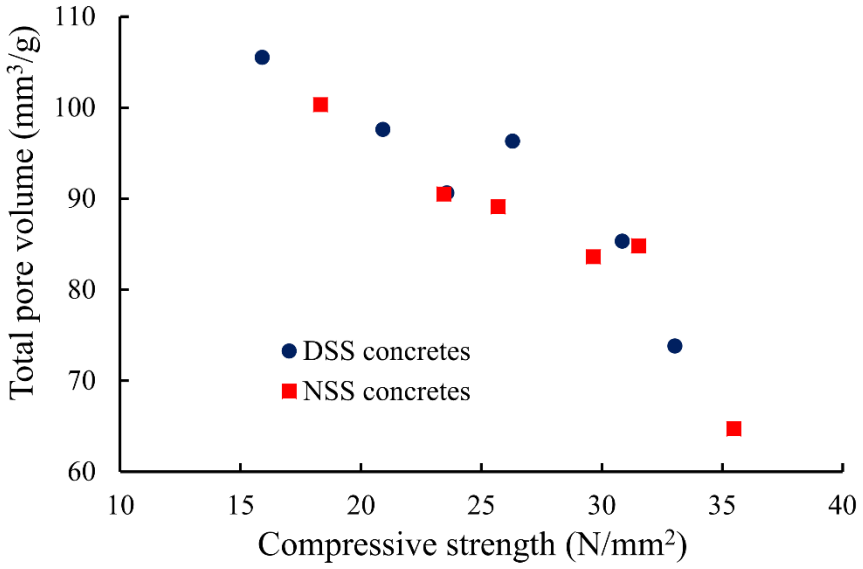

Fig. 4.14. Relationship between compressive strength and total pore volume of concretes at the ages of 3 and 7 days

4.6. Summary

The effects of chloride ion in NSS on the properties of fresh and hardened concretes using SCMs (i.e., FA or BFS) were investigated to intensively verify the applicability of NSS for concrete production. According to the experimental results, the following conclusions in this chapter can be drawn:

1. Non-desalted sea sand reduced the initial slump of fresh concretes, whereas it had almost no effect on the initial air content of all the concretes. Replacement of OPC by FA and BFS increased the initial slump of fresh concrete, even when NSS was used.
2. No effect of chloride ion in NSS on the slump loss and air content reduction of concrete for 60 min after mixing was observed regardless of FA and BFS replacement.
3. The FA and BFS concretes combined with chloride ion in NSS showed slightly lower CH content than those without chloride ion. It implied that an amount of CH could be consumed by the pozzolanic reaction of FA and hydraulicity of BFS. Therefore, the chloride ion in NSS not only accelerated cement hydration but also enhanced the

pozzolanic reactivity of FA and hydraulicity of BFS at early ages (i.e., 3 and 7 days). As a result, the compressive strength and elastic modulus of FA and BFS concretes combined with NSS were significantly increased at the early ages compared with concrete without chloride ion. This was verified through the pore structure of these concretes.

4. Compared to reference concrete using OPC and DSS, even in the presence of chloride ion, the replacement of OPC by FA and BFS reduced the compressive strength of concrete at early age (3 days) due to the dilution effect. However, the result showed that the total porosity was remarkably enhanced when concretes contained FA or BFS together with the presence of chloride ion in NSS in comparison with the reference concrete at the age of 91 days. As a result, the mechanical properties (compressive strength and modulus of elasticity) and durability (water absorption and sorptivity) of FA and BFS concretes combined with NSS were improved at later age.

Based on the outcomes of this study, NSS concretes did not perform inferior in mechanical properties and permeability as well as sorptivity compared to DSS concretes. As a result, NSS could be considered as the alternative fine aggregate for plain concrete production at coastal areas. The sulfate ion in NSS might also affect the mechanical properties and durability of concrete even though its effect was not observed. Further consideration for the effect of sulfate ion in NSS on mechanical properties and investigation on additional durability measurements, i.e., steel corrosion and alkali-silica reaction, should be done. Moreover, the microstructure analysis by scanning electron microscopy with energy dispersive X-ray spectrometry should be conducted to strengthen the explanation of the mechanism effect of chloride ion on mechanical properties as well as durability of concrete. The replacement of OPC by 15% FA or 45% BFS together with the presence of chloride ion in NSS can not only maintain the mechanical performance of concretes but also improve their impermeability and sorptivity at 91 days. The

obtained results may contribute to the useful knowledge and discussion for verifying the applicability of NSS for concrete production.

References of chapter 4:

[1] W. Liu, Y. J. Xie, B. Q. Dong, F. Xing, Study on characteristics of dredged marine sand and the mechanical properties of concrete made with dredged marine sand, Bulletin of the Chinese Ceramic Society. 33 (2014) 15–22.

[2] P. Ozer-Erdogan, H. M. Basar, I. Erden, L. Tolun, Beneficial use of marine dredged materials as a fine aggregate in ready-mixed concrete: Turkey example, Construction and Building Materials. 124 (2016) 690–704.

[3] M. A. Megat Johari, J. J. Brooks, S. Kabir, P. Rivard, Influence of supplementary cementitious materials on engineering properties of high strength concrete, Construction and Building Materials. 25 (2011) 2639–2648.

[4] A.C.I. Committee 226, Ground Granulated Blast-Furnace Slag as a Cementitious Constituent in Concrete, MJ. 84 (1987) 327–342.

[5] A. Younis, U. Ebead, P. Suraneni, A. Nanni, Fresh and hardened properties of seawater-mixed concrete, Construction and Building Materials. 190 (2018) 276–286.

[6] L. Du, K. J. Folliard, Mechanisms of air entrainment in concrete, Cement and Concrete Research. 35 (2005) 1463–1471.

[7] C. Chen, T. Ji, Y. Zhuang, X. Lin, Workability, mechanical properties and affinity of artificial reef concrete, Construction and Building Materials. 98 (2015) 227–236.

[8] N. Saikia, S. Kato, T. Kojima, Thermogravimetric investigation on the chloride binding behaviour of MK–lime paste, Thermochimica Acta. 444 (2006) 16–25.

[9] A. Traetteberg, V. S. Ramachandran, P. E. Grattan-Bellew, A study of the microstructure and hydration characteristics of tricalcium silicate in the presence of calcium chloride, Cement and Concrete Research. 4 (1974) 203–221.

[10] M. D. A. Thomas, R. D. Hooton, A. Scott, H. Zibara, The effect of supplementary cementitious materials on chloride binding in hardened cement paste, Cement and Concrete Research. 42 (2012) 1–7.

[11] J. Liu, G. Ou, Q. Qiu, X. Chen, J. Hong, F. Xing, Chloride transport and microstructure of concrete with/without fly ash under atmospheric chloride condition, Construction and Building Materials. 146 (2017) 493–501.

[12] S. C. Pal, A. Mukherjee, S. R. Pathak, Investigation of hydraulic activity of ground granulated blast furnace slag in concrete, Cement and Concrete Research. 33 (2003) 1481–1486.

[13] G. Hannesson, K. Kuder, R. Shogren, D. Lehman, The influence of high volume of fly ash and slag on the compressive strength of self-consolidating concrete, Construction and Building Materials. 30 (2012) 161–168.

[14] A. Hadjsadok, S. Kenai, L. Courard, F. Michel, J. Khatib, Durability of mortar and concretes containing slag with low hydraulic activity, Cement and Concrete Composites. 34 (2012) 671–677.

[15] W. S. Deepak, Effect on compressive strength of concrete using sea sand as a partial replacement for fine aggregate, International Journal of Research in Engineering and Technology. 04 (2016) 180–183.

[16] R. Mahendran, K. Godwin, T. G. Selvan, M. Murugan, Experimental study on concrete using sea sand as fine aggregate, 7 (2016) 4.

[17] S. K. Tulashie, F. Kotoka, D. Mensah, A. K. Kwablah, Investigation of the compressive strength of pit sand, and sea sand mortar prisms produced with rice husk ash as additive, Construction and Building Materials. 151 (2017) 383–387.

[18] J. Limeira, M. Etxeberria, L. Agulló, D. Molina, Mechanical and durability properties of concrete made with dredged marine sand, Construction and Building Materials. 25 (2011) 4165–4174.

[19] J. Xie, J. Wang, R. Rao, C. Wang, C. Fang, Effects of combined usage of GGBS and fly ash on workability and mechanical properties of alkali activated geopolymer concrete with recycled aggregate, Composites Part B: Engineering. 164 (2019) 179–190.

[20] W. Wang, C. Lu, G. Yuan, Y. Zhang, Effects of pore water saturation on the mechanical properties of fly ash concrete, Construction and Building Materials. 130 (2017) 54–63.

[21] M. Olivia, H. Nikraz, Properties of fly ash geopolymer concrete designed by Taguchi method, Materials & Design (1980-2015). 36 (2012) 191–198.

[22] J. J. Chen, A. K. H. Kwan, Y. Jiang, Adding limestone fines as cement paste replacement to reduce water permeability and sorptivity of concrete, Construction and Building Materials. 56 (2014) 87–93.

[23] E. Güneyisi, M. Gesoğlu, E. Booya, K. Mermerdaş, Strength and permeability properties of self-compacting concrete with cold bonded fly ash lightweight aggregate, Construction and Building Materials. 74 (2015) 17–24.

[24] B. Lothenbach, K. Scrivener, R.D. Hooton, Supplementary cementitious materials, Cement and Concrete Research. 41 (2011) 1244–1256.

[25] P. Duan, Z. Shui, W. Chen, C. Shen, Effects of metakaolin, silica fume and slag on pore structure, interfacial transition zone and compressive strength of concrete, Construction and Building Materials. 44 (2013) 1–6.

[26] J. F. Young, Review of the Pore Structure of Cement Paste and Concrete and its Influence on Permeability, SP. 108 (1988) 1–18.

[27] L. Basheer, J. Kropp, D. J. Cleland, Assessment of the durability of concrete from its permeation properties: a review, Construction and Building Materials. 15 (2001) 93–103.

[28] E. Sakai, S. Miyahara, S. Ohsawa, S. H. Lee, M. Daimon, Hydration of fly ash cement, Cement and Concrete Research. 35 (2005) 1135–1140.

[29] S. Cheng, Z. Shui, T. Sun, R. Yu, G. Zhang, Durability and microstructure of coral sand concrete incorporating supplementary cementitious materials, Construction and Building Materials. 171 (2018) 44–53.

CHAPTER 5. MECHANICAL PROPERTIES OF NSS CONCRETE CONTAINING SCMs EXPOSED TO ACCELERATED CARBONATION

This chapter discusses the effect of chloride ion in NSS on the mechanical properties of concrete containing SCMs exposed to accelerated carbonation. Mechanical properties in terms of compressive strength and modulus of elasticity of concrete under carbonation condition were investigated. Estimation of portlandite (CH), calcite (CC) contents, and apparent porosity, scanning electron microscopy, and crack evaluation were also carried out to explain the effect of chloride ion on mechanical properties of concrete.

5.1. Effect of chloride ion and carbonation on CH and C–S–H contents

The effects of chloride ion and carbonation on CH and C–S–H contents were evaluated through TG-DTA. It is assumed that cement hydration after 28 days would be negligible and could not be affected by carbonation. In addition, it was supposed that the carbonation did not affect the pozzolanic reaction of FA or the hydraulicity of BFS. It means that there were no differences in the cementitious materials reactions between sealed and carbonation conditions up to the age of 182 days. Cement hydration produced CH that was most likely consumed by carbonation and pozzolanic reactions. The carbonation of cement hydrate products (CH and C–S–H) mostly generated CC. Therefore, the amount of CC formed from CH was calculated based on the difference between the amount of CH presence in the sealed and carbonation samples. Meanwhile, the amount of CC produced from C–S–H was determined by the difference in the amount of CC between the sample measurement and the conversion from the amount of carbonated CH. Thus, the CH and CC contents of paste in sealed and carbonation conditions were calculated using Eqs. (5-1) – (5-3) and shown in Table 5.1.

$$Carbonated\ CH\ (\%) = CH_{Sealed} - CH_{Carb} \quad (5\text{-}1)$$

$$CC_{C-S-H}\ (\%) = CC_{Carb} - \frac{100}{74} \times Carbonated\ CH \quad (5\text{-}2)$$

$$CH_{Consumption}\ (\%) = \frac{CH_{OPC} - CH_{SCMs}}{CH_{OPC}} \times 100, \quad (5\text{-}3)$$

where $Carbonated\ CH$ is the CH content of paste in the sample which was carbonated, CH_{Sealed} and CH_{Carb} are the CH contents of sealed and carbonated pastes in the samples after aging for 182 days, CC_{Carb} is the CC content of carbonated paste in the sample after aging for 182 days, CC_{C-S-H} is the CC content of the sample paste produced from C–S–H carbonation, $CH_{Consumption}$ is the CH consumption of the paste due to pozzolanic reactions, CH_{SCMs} is the CH content of the paste containing FA or BFS, and CH_{OPC} is the CH content of OPC paste.

Table 5.1. CH and CC contents in sealed and carbonation conditions at the age of 182 days

Mixtures	Sealed condition		Carbonation condition			
	CH_{Sealed} (%)	$CH_{Consumption}$ (%)	CH_{Carb} (%)	CC_{Carb} (%)	Carbonated CH (%)	CC_{C-S-H} (%)
OPC-DSS	18.07	–	4.02	64.24	14.05	45.25
OPC-NSS	17.89	–	4.32	59.77	13.58	41.43
FA15-DSS	16.41	9.20	2.42	70.48	13.99	51.57
FA15-NSS	15.84	11.50	2.98	65.51	12.87	48.13
BFS45-DSS	14.60	19.20	0.00	85.26	14.60	65.52
BFS45-NSS	13.90	22.30	0.00	75.77	13.90	56.99

* It is noted that the values of CH and CC in Table 5.1 were calculated as a percentage of cement content (mass%).

According to the result, NSS concretes showed slightly lower CH content than the DSS concretes regardless of FA and BFS replacements under sealed condition. The lower CH content in NSS concretes is attributed to the presence of chloride ion which can react with tricalcium aluminate (C_3A), CH, and aluminum oxide (Al_2O_3), thereby leading to the formation

of Friedel's salt ($3CaO{\cdot}A_2O_3{\cdot}CaCl_2{\cdot}10H_2O$) [1–3]. The formation of Friedel's salt can be described by the Eqs. (5-4) – (5-6).

$$Ca(OH)_2 + 2NaCl \rightarrow CaCl_2 + 2NaOH \quad (5\text{-}4)$$

$$3CaO \cdot Al_2O_3 + CaCl_2 + 10H_2O \rightarrow 3CaO \cdot Al_2O_3 \cdot CaCl_2 \cdot 10H_2O \quad (5\text{-}5)$$

$$3Ca(OH)_2 + CaCl_2 + Al_2O_3 + 7H_2O \rightarrow 3CaO \cdot Al_2O_3 \cdot CaCl_2 \cdot 10H_2O \quad (5\text{-}6)$$

From Table 5.1, the pozzolanic reactions of FA and the hydraulicity of BFS concretes reduced the CH content by approximately 10% and 20%, respectively. This resulted in the additional formation of C–S–H gels and calcium aluminosilicate hydrate [4–6]. Furthermore, both CH and C–S–H were carbonated. The results in Table 5.1 also show that the amount of carbonated C–S–H in FA and BFS concretes under carbonation condition was higher than that in the OPC concretes, irrespective of the presence of chloride ion. From Table 3.1 of Section 3.1.1, it can be seen that FA and BFS have lower CaO content and higher SiO_2 content than OPC. Therefore, it is believed that the Ca/Si ratio in hydration products (C–S–H) of FA and BFS concretes is lower than that of OPC concretes [7–9]. As a result, FA and BFS concretes are thought to be more vulnerable to carbonation shrinkage than OPC concretes [10], leading to the decalcification of C–S–H. It was also found that NSS concretes have less carbonated C–S–H content than DSS concretes.

5.2. Effect of carbonation on crack formation

The crack evaluation by fluorescent resin was performed on concrete samples under both sealed and accelerated carbonation conditions in order to confirm the formation of cracks due to carbonation. The images taken under the ultraviolet light are shown in Fig. 5.1. It can be seen that the fluorescent resin only penetrated into the entrained air bubbles in the samples under

sealed condition (white voids). For the samples under carbonation condition, cracks were clearly observed at interfacial transition zone between aggregates and cement paste matrix, especially in concretes containing SCMs. According to previous studies, the formation of cracks was due to shrinkages [7,11–18]. The carbonation shrinkage was caused by the decalcification of C–S–H while the drying shrinkage was caused by the drying process during carbonation [11,13–18]. Previous studies [7,11,12,14,16] state that carbonation shrinkage is the primary cause for crack formation under accelerated carbonation. The decalcification of C–S–H in carbonated concretes can be clearly observed through the results in Table 5.1. The amount of CC formation in OPC concretes from the carbonated C–S–H was approximately 40%, whereas that in FA and BFS concretes was over 50% at the age of 182 days. However, carbonation can also release the free water originally combined in CH [14,17]. At the initial period after concrete casting, most of the pores in concrete are filled with liquid water. Thus, the relative humidity in concrete should be equal or close to 100% due to the high amount of liquid water in the pores, which makes the water–vapor pressure in the pore is equal or very close to the vapor pressure when the water vapor is saturated. The water content in concrete decreased gradually with the continuous cement hydration. When the vapor pressure becomes lower than the saturated value and the relative humidity starts to decrease from 100%. Therefore, it is believed that when changed concrete specimens from sealed condition (i.e. the internal relative humidity of specimen was higher than 60%) to accelerated carbonation chamber (60% relative humidity), there was a reduction in free water in concrete specimens due to the moisture gradient until the moisture of the concrete surface is in equilibrium with that of the outer environment (chamber) [13,14,17]. This leads to the drying process and therefore, it can be theorized that the drying shrinkage is prominent cause in the formation of cracks [15,18]. To illustrate this, Auroy et al. [14] placed samples in a carbonation chamber (3% CO_2, 25 ^oC, and 55% RH) for one year. The results showed a 12% loss in the water content of the sample. However, it must be noted that

the change in moisture of the concrete specimen after exposure to carbonation was not measured in this study. The replacement of FA or BFS resulted in the formation of distinguished cracks during carbonation. Meanwhile, when comparing carbonated concretes using DSS and NSS, the effect of chloride ion on the formation of cracks was not clearly observed. Carbonation caused C–S–H decalcification, but the results in Section 5.1 confirmed that chloride ion in NSS restricted C–S–H decalcification, irrespective of SCMs replacement. It is consistent with a previous study [19]. Therefore, it is believed that chloride ion may also contribute to the restriction in the formation of cracks in NSS concretes compared with DSS concretes under carbonation condition.

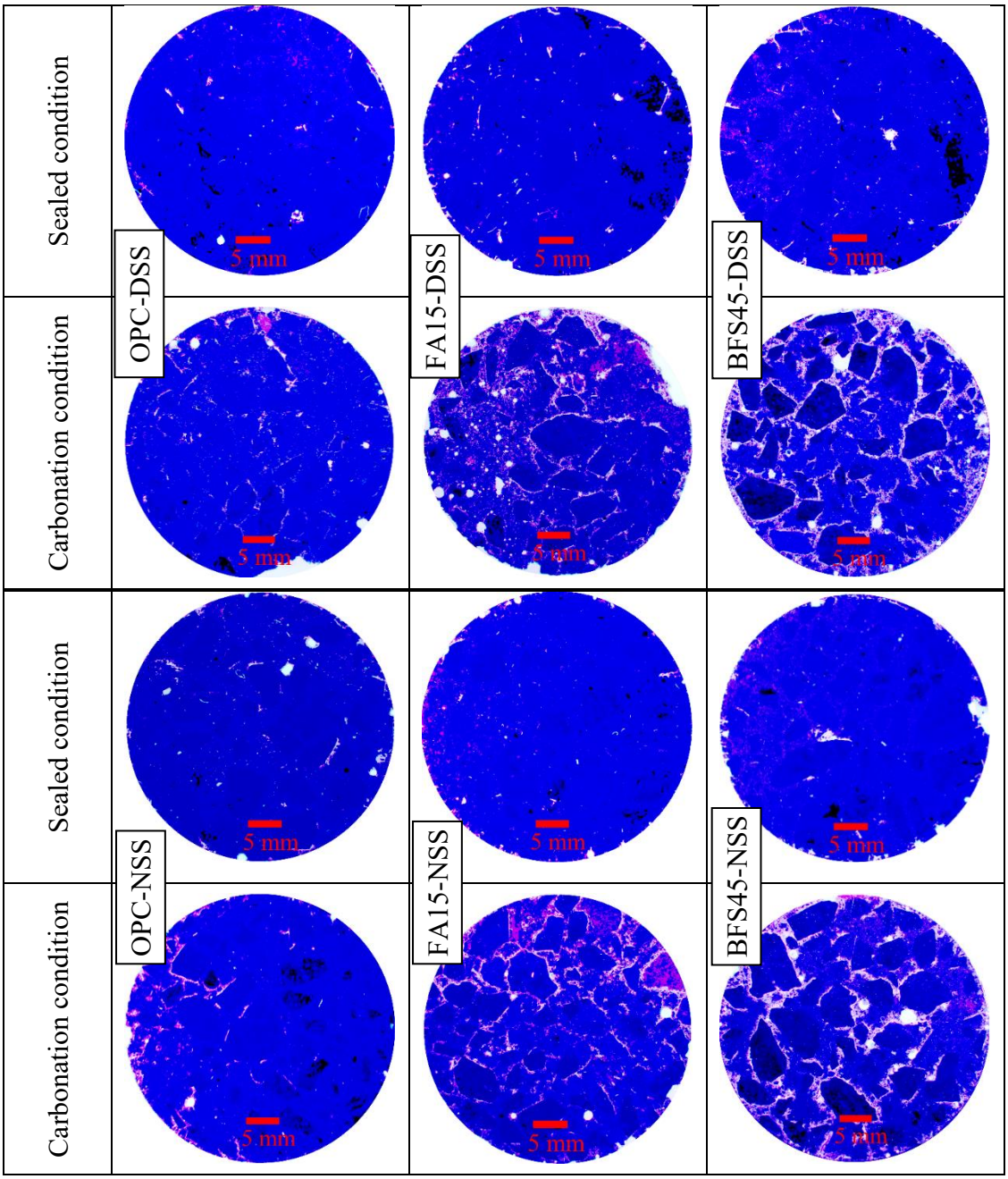

Fig. 5.1. Crack evaluation by fluorescent resin on concrete samples under both sealed and accelerated carbonation conditions (light white: cracks and voids; dark to blue: aggregates and cement matrix)

The samples were also cut to evaluate the development of cracks from the exposed surface to the sample core. These results are shown in Fig. 5.2. The cracks not only developed on the surface of the sample but also propagated toward the core. The average crack length was

approximately 10 mm. It should be noted that it is consistent with the results of carbonation depth which is mentioned in Section 6.1.

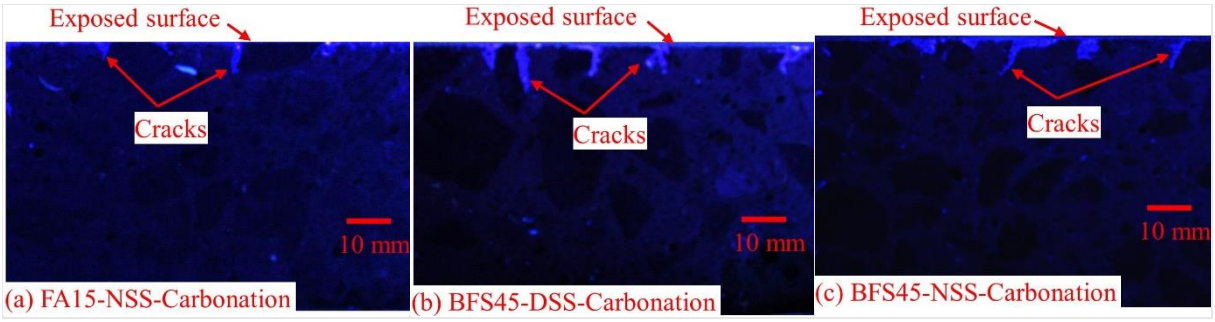

Fig. 5.2. Crack development from exposed surface toward the core of concrete sample

5.3. Effect of carbonation on microstructure of concrete

The microstructure of concretes at the age of 182 days was qualitatively evaluated through a SEM analysis which was also used to evaluate the microstructure of samples in previous studies [3,20]. The SEM images with a magnification of 500 of sealed and carbonated specimens at 182 days are shown in Fig. 5.3. Costa et al. [21] suggested that the roughness of specimen morphology could be interpreted as empty spaces between hydrated cement products. The sealed microstructure of OPC-DSS (Fig. 5.3a) seemed to be more porous than that of OPC-NSS (Fig. 5.3c). This might be attributed to the formation of Friedel's salt that filled the empty spaces, resulting in a more compact cement matrix [22]. Besides, with the addition of FA or BFS, no voids were observed on the sealed microstructure of concrete specimens (Figs. 5.3e and 5.3g) compared to OPC-DSS concrete (Fig. 5a). This was due to the additional formation of C–S–H gels and reduction of CH that bridged the voids between the cement matrix and aggregates, leading to dense microstructures in FA or BFS concretes compared with the reference concrete [4–6]. It is noted that these explanations were obtained from the literature. Hence, other better methods such as the backscattered electron (BSE) imaging technique should be carried out in future works to reinforce findings.

When concrete is carbonated, calcium carbonate ($CaCO_3$) is formed by the reactions between CO_2 and CH or C–S–H as shown in Eqs. (5-7) and (5-8). The formation of $CaCO_3$ not only fills the empty spaces but also covers the surface of the aggregate particles. Therefore, boundary between cement matrix and aggregates of specimens under carbonation condition could not be easily distinguished as seen in Figs. 5.3 (b), (d), (f) and (h). Additionally, it should be noticed that the microcracks also occurred around aggregates (Figs. 5.3 (b) and (d)), especially FA and BFS carbonated specimens (Figs. 5.3 (f) and (h)). The generation of microcracks was attributed to carbonation shrinkage. This is in agreement with the results in Section 5.2 and the observations of previous studies [11,13,14].

$$Ca(OH)_2 + CO_2 \rightarrow CaCO_3 + H_2O \quad (5\text{-}7)$$

$$(CaO)_x(SiO_2)(H_2O) + xCO_2 \rightarrow xCaCO_3 + (SiO_2)(H_2O)_t + (z-t)H_2O \quad (5\text{-}8)$$

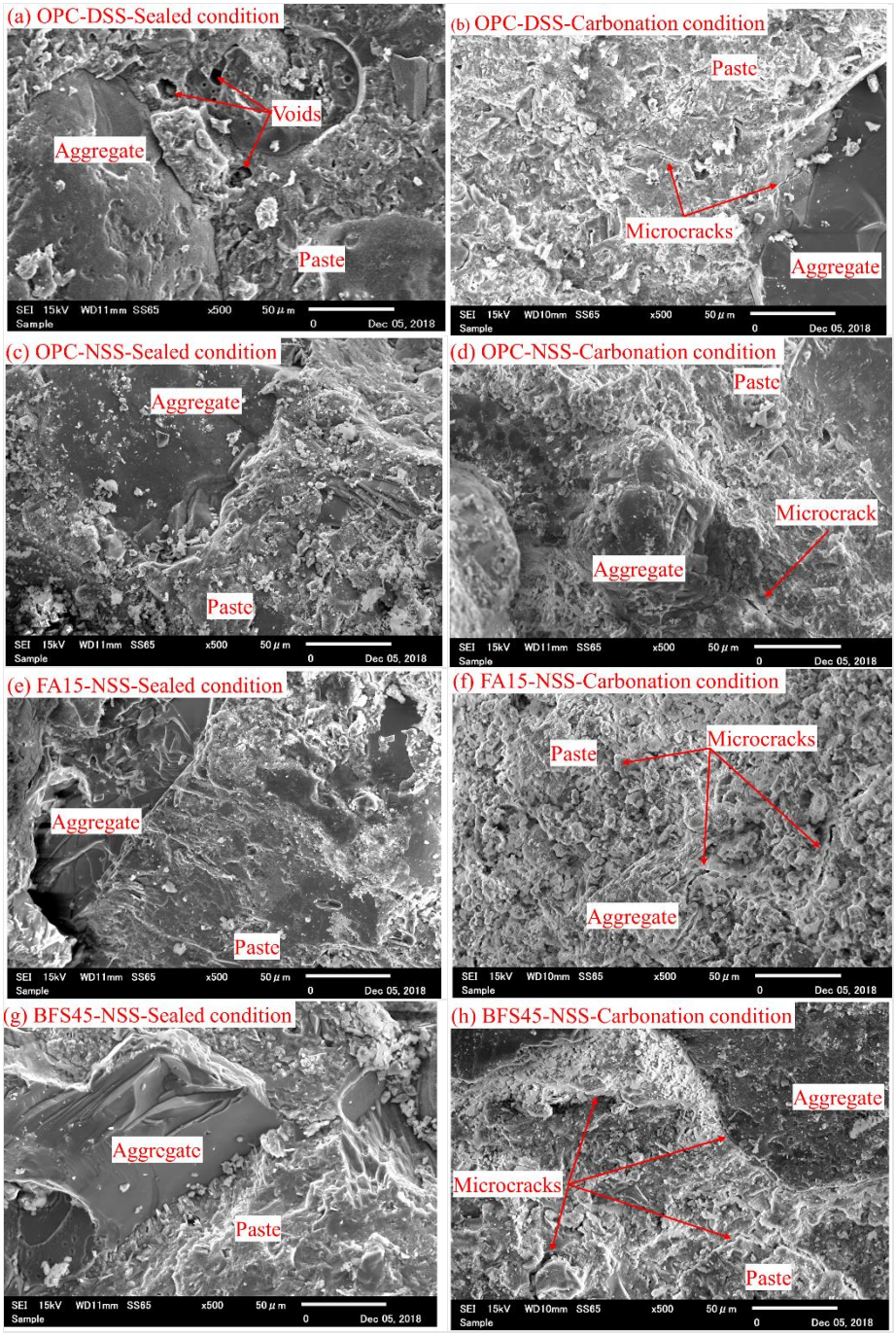

Fig. 5.3. SEM images of non-carbonated and carbonated specimens at 182 days.

5.4. Effect of chloride ion and carbonation on porosity

The apparent porosity of all the concretes under sealed and carbonation conditions is shown in Fig. 5.4. The apparent porosity of NSS concretes at 182 days was lower than that of DSS concretes irrespective of SCMs replacement and exposure conditions. This is attributed to the formation of Friedel's salt. The formation of Friedel's salt acts as a filler in the pores of the

concrete which reduces the connected pores and increases the compactness of the concrete [22–24]. The addition of FA or BFS noticeably reduced the apparent porosity of concrete under the sealed condition regardless of curing age. The apparent porosity as compared to OPC-NSS concrete under sealed condition at the age of 182 days was approximately 10.8% lower for BFS45-NSS and 6.2% lower for FA15-NSS. On the other hand, the apparent porosity of concretes under carbonation condition was significantly reduced. It is due to the significant formation of CC which clogs the pore microstructures of concrete, as shown in Table 5.1. This is consistent with many studies [11,13,15,25–27].

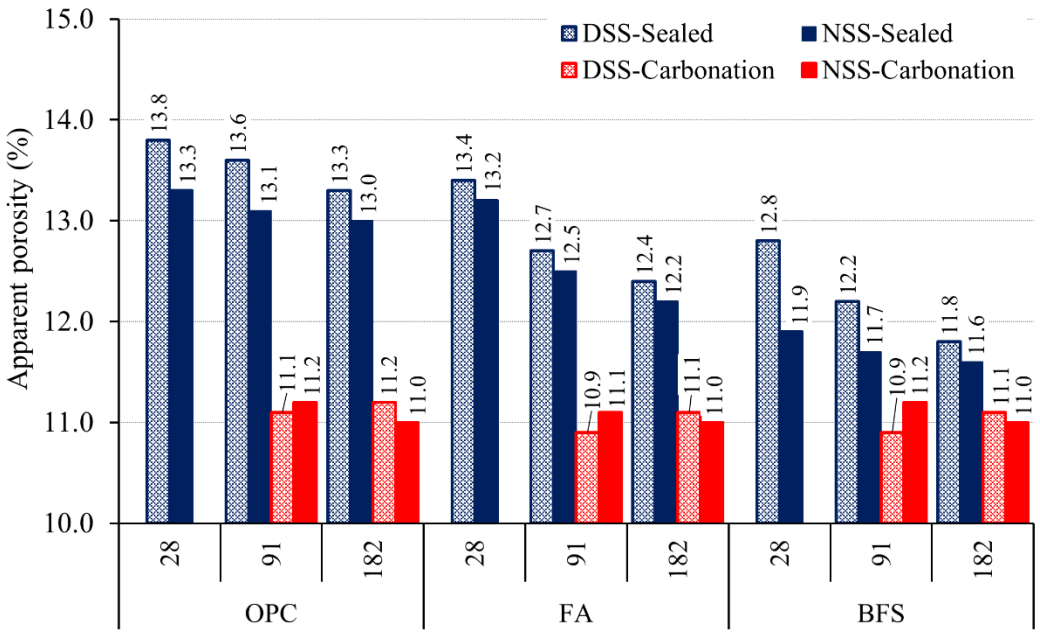

Fig. 5.4. Apparent porosity of all concretes under sealed and carbonation conditions

Figure 5.5 shows the change in apparent porosity of all the concrete specimens relative to that of OPC-DSS concrete under sealed and carbonation conditions at 91 and 182 days, which was calculated by Eq. (5-9). It is clearly seen that the contribution of FA and BFS to the reduction of apparent porosity of concrete under carbonation condition was small at 182 days, whereas that under sealed condition was significant, especially when NSS was used.

$$\text{Change in apparent porosity} = \frac{P_c - P_{c,OPC\text{-}DSS}}{P_{c,OPC\text{-}DSS}} \times 100\% \quad (5\text{-}9)$$

where, $P_{c,OPC\text{-}DSS}$ is the apparent porosity of OPC-DSS concrete at the ages of 91 and 182 days under sealed and carbonation conditions; P_c is the apparent porosity of all concretes, excepted for OPC-DSS concrete at the ages of 91 and 182 days under the corresponding curing condition.

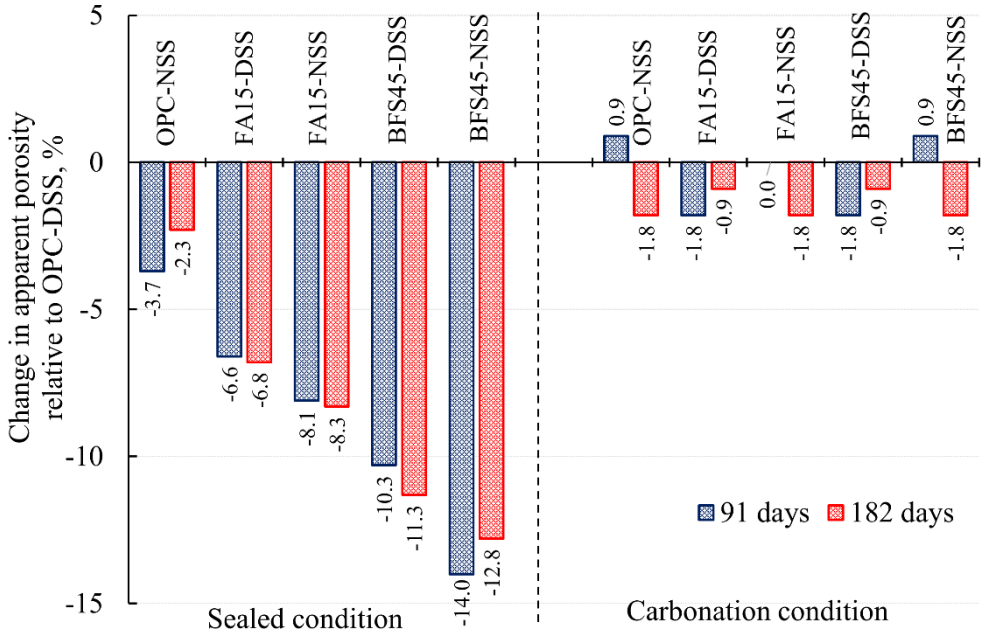

Fig. 5.5. Change in apparent porosity of all concretes relative to OPC-DSS under sealed and carbonation conditions

5.5. Mechanical properties of concrete

5.5.1. Compressive strength

Figure 5.6 shows the compressive strengths of all the concrete specimens under sealed and carbonation conditions. It should be noted that the concrete samples were partially carbonated. The compressive strengths of NSS concretes were always slightly higher than those of DSS concretes of the same age, irrespective of exposure conditions and replacement of SCMs. This shows that the compressive strength of concrete slightly improved using NSS. The

apparent porosity of NSS concretes under both sealed and carbonation conditions was lower than that of DSS concretes at 182 days (see Section 5.4). Therefore, chloride ion is also believed to contribute to increasing the compressive strength of NSS concretes compared to DSS concretes. Under sealed condition, the compressive strength of OPC concretes increased by 17.7%-22.7% from 28 to 182 days. Meanwhile, the increase rate of compressive strength of FA and BFS concretes was 23.3%-27.6% and 24.3%-25.3%, respectively. Eventually, the compressive strength of FA and BFS concretes was slightly higher than that of OPC concrete under sealed condition at 182 days.

The compressive strength of concretes under carbonation condition was higher than that of concretes under sealed condition irrespective of ages and SCMs replacement. For instance, the compressive strength of OPC-NSS concrete under the carbonation condition was 18.0% higher than that under the sealed condition aged 182 days. Meanwhile, the compressive strength as compared to the sealed conditions was 11.0% higher for FA15-NSS and 6.7% higher for BFS45-NSS under carbonation condition. It can be concluded that the carbonation significantly increased the compressive strength of concretes. This fact can be explained by the formation of $CaCO_3$ (see Eqs. (5-7) and (5-8)). Calcium carbonate has a very low solubility, and its precipitation contributes to the clogging of the pore system, leading to a decrease in the porosity of concrete. The lower porosity, the higher compressive strength. The results from Section 5.4 showed that the porosity of OPC-NSS under carbonation was 15.4% lower than that under sealed condition at the age of 182 days. The porosity of FA15-NSS and BFS45-NSS concretes under carbonation condition in compared to that under sealed condition was decreased by 9.8% and 5.2%, respectively.

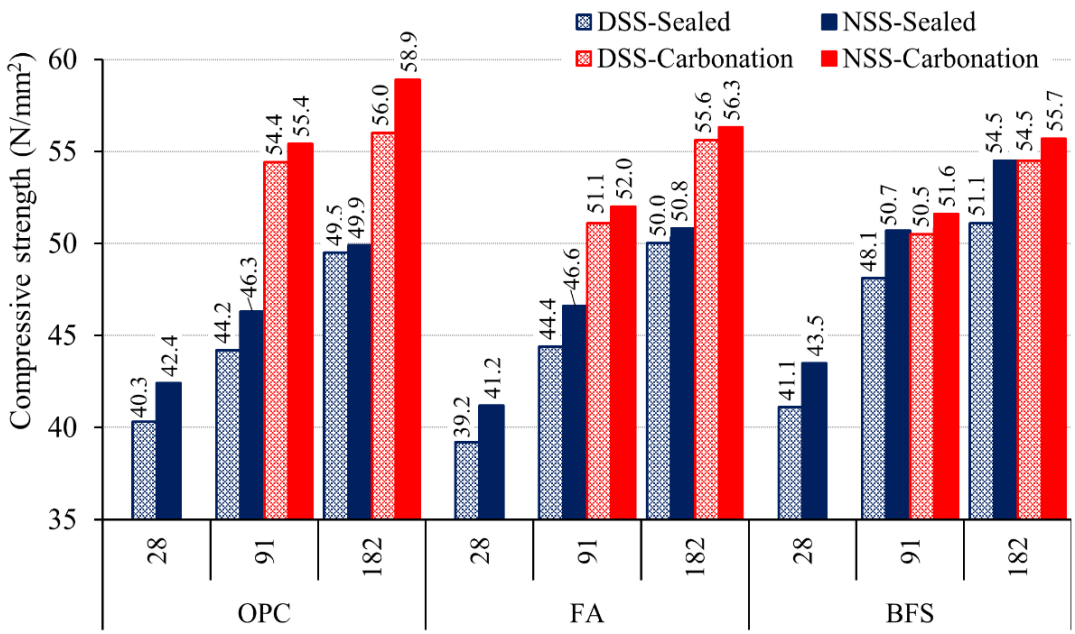

Fig. 5.6. Compressive strength of all concretes under sealed and carbonation conditions

The change in compressive strength of all the concrete specimens with respect to that of OPC-DSS concrete under sealed and carbonation conditions at 91 and 182 days was calculated by Eq. (5-10) and shown in Fig. 5.7. It can be seen that the compressive strength of OPC-NSS concrete was higher by 0.8% and 5.2% than that of OPC-DSS concrete at 182 days under sealed and carbonated conditions, respectively. Additionally, FA and BFS concretes using DSS had higher compressive strength than OPC-DSS concrete under sealed condition at 182 days by 1.0 and 3.2%, respectively. This compressive strength could increase by 2.6% and 10.1% for the FA and BFS concretes using NSS. On the contrary, under carbonation condition, the compressive strength of FA and BFS concretes using DSS was slightly reduced by 0.7% and 2.7% when compared with the OPC-DSS concrete. However, when FA and BFS concretes incorporated NSS, the compressive strength was nearly the same as that of OPC-DSS at 182 days. It indicated that the FA and BFS replacement could maintain the compressive strength of the concrete incorporating with NSS under carbonation condition.

$$\text{Change in compressive strength} = \frac{f_c' - f_{c,OPC\text{-}DSS}'}{f_{c,OPC\text{-}DSS}'} \times 100\% \quad (5\text{-}10)$$

where, $f_{c,OPC\text{-}DSS}'$ is the compressive strength of OPC-DSS concrete at the ages of 91 and 182 days under sealed or carbonation condition; f_c' is the compressive strength of all concretes, excepted for OPC-DSS concrete at the ages of 91 and 182 days under the corresponding curing condition.

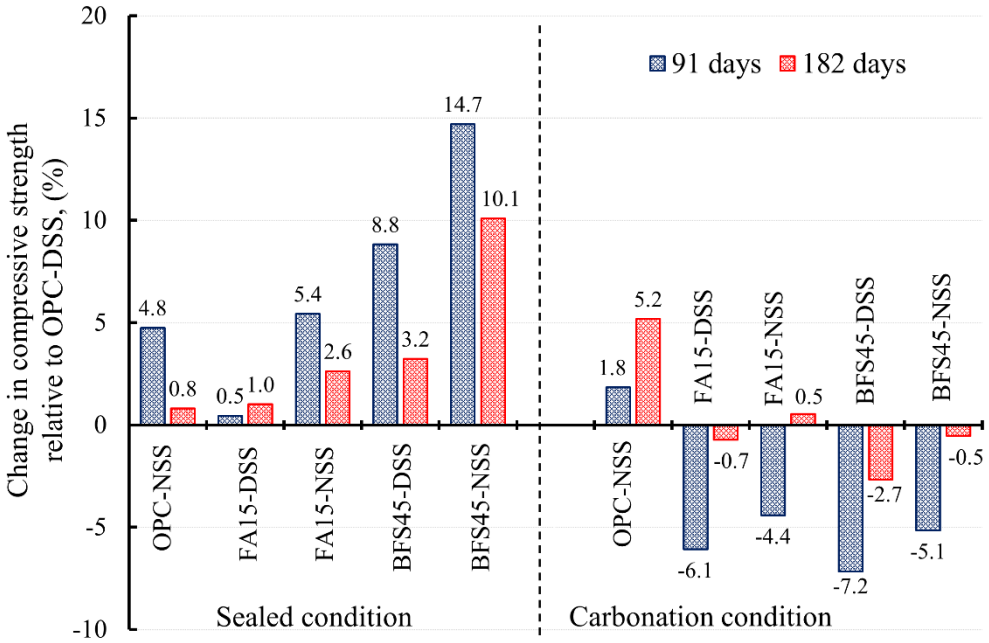

Fig. 5.7. Change in compressive strength of concrete relative to OPC-DSS under sealed and carbonation conditions

5.5.2. Modulus of elasticity

The modulus of elasticity of all the concretes under both sealed and carbonation conditions is presented in Fig. 5.8. Similar to compressive strength, NSS concretes also showed a higher modulus of elasticity than DSS concretes, regardless of age, replacement of SCMs, and exposure conditions. This finding indicates that the chloride ion in NSS slightly improved not only the compressive strength of concrete but also the modulus of elasticity. It has been reported

that the deformation of concrete depends on the stiffness of phases, such as aggregates, cement paste, and interfacial transition zone (ITZ) [28]. The formation of Friedel's salt due to the presence of chloride ion can further lead to the compaction of ITZ [22–24]. Therefore, the presence of chloride ion in NSS may be responsible for improving the modulus of elasticity of NSS concretes when compared to DSS concretes.

Under the sealed condition, the modulus of elasticity of SCMs-incorporated concretes showed a trend similar to compressive strength after 182 days, higher than that of concretes without SCMs. The increase rate in the modulus of elasticity for the OPC concretes from 28 to 182 days was around 5%, with the SCMs concrete showing almost twice this amount. With a longer sealed condition, the ITZ could be improved through additional C–S–H formation from the pozzolanic reaction of FA and hydraulicity of BFS [5,29,30]. However, the modulus of elasticity results of SCMs concretes were completely reversed under the carbonation condition. The carbonation process reduced the modulus of elasticity of FA and BFS concretes from 2.4% to 2.7% and 2.8% to 8.4% after 28 and 182 days, respectively. In contrast to the results of compressive strength, the modulus of elasticity results of all the concretes under the carbonation condition were lower than those under the sealed condition after 182 days. This result is consistent with the conclusion of previous study which showed a decrease in modulus of elasticity of SCMs concrete due to carbonation [15].

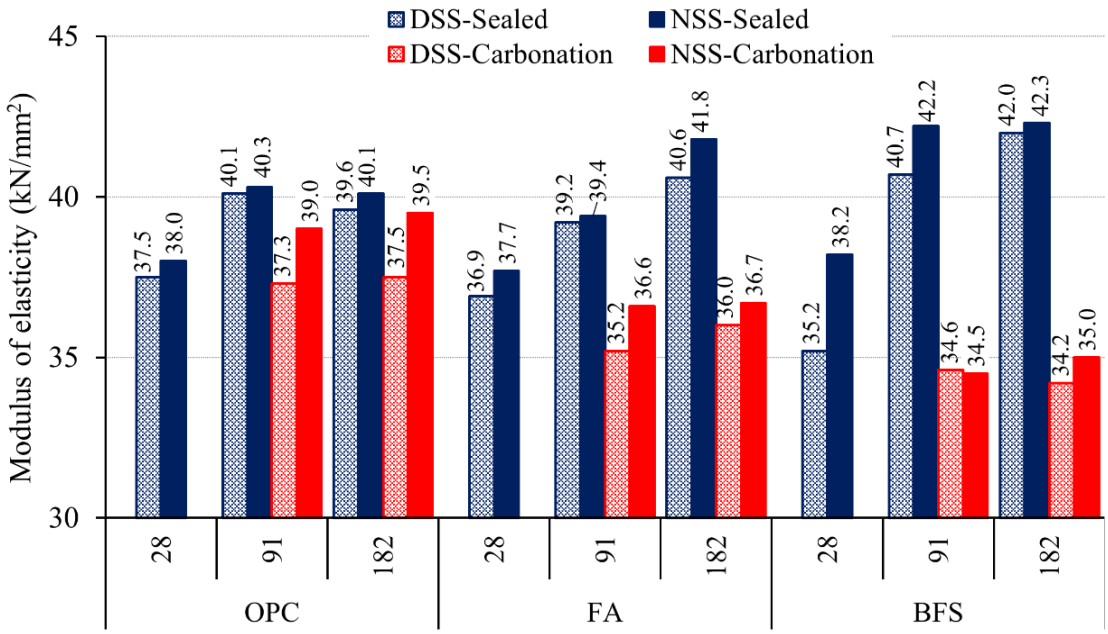

Fig. 5.8. Modulus of elasticity of all concretes under sealed and carbonation conditions

The change in modulus of elasticity of all the concrete specimens relative to that of OPC-DSS concrete under sealed and carbonation conditions at 91 and 182 days was calculated as Eq. (5-11) and shown in Fig. 5.9. It can be observed that the modulus of elasticity of OPC-NSS concrete was slightly higher than that of OPC-DSS under both sealed and carbonation conditions irrespective of ages. Meanwhile, the modulus of elasticity of FA and BFS concretes was only higher under sealed condition, but it was lower under carbonation regardless of the use of NSS as fine aggregate than that of OPC-DSS concrete at 182 days.

$$\text{Change in modulus of elasticity} = \frac{E_c - E_{c,OPC\text{-}DSS}}{E_{c,OPC\text{-}DSS}} \times 100\% \quad (5\text{-}11)$$

where, $E_{c,OPC\text{-}DSS}$ is the modulus of elasticity of OPC-DSS concrete at the ages of 91 and 182 days under sealed and carbonation conditions; E_c is the modulus of elasticity of all concretes, excepted for OPC-DSS concrete at the ages of 91 and 182 days under the corresponding curing condition.

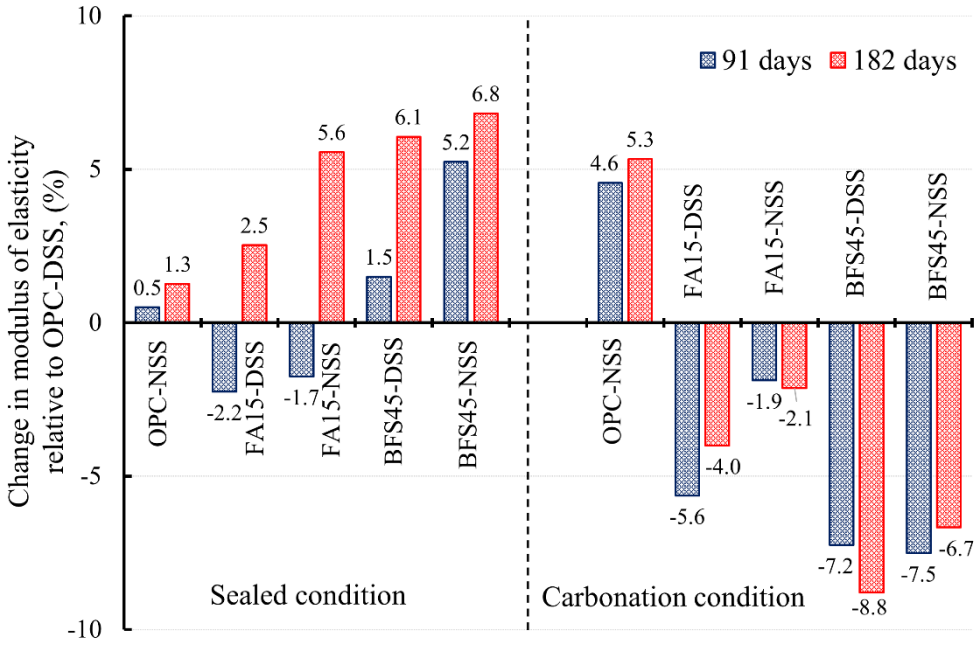

Fig. 5.9. Change in modulus of elasticity of concrete relative to OPC-DSS under sealed and carbonation conditions

Under carbonation condition, there is a competition between two simultaneous phenomena: the precipitation of $CaCO_3$ and formation of cracks. The precipitation of $CaCO_3$ contributed to the decrease in porosity as shown in Section 5.4, resulting in the increase in compressive strength of concrete. Meanwhile, the formation of cracks decreased modulus of elasticity. As demonstrated in Sections 5.2 and 5.3, the cracks were clearly observed for concretes under carbonation due to the carbonation shrinkage, especially concretes containing FA and BFS. Maruyama et al. [31] reported that the increase in the number of voids due to the formation of internal cracks mainly caused the decrease in modulus of elasticity of concrete. It is assumed that pore clogging in OPC concretes can equilibrate or control the formation of cracks. Therefore, the modulus of elasticity of OPC concrete did not change under the carbonation condition. Meanwhile, the decrease in porosity was not able to satisfactorily compensate for the marked increase in deformation (crack formation prevailed over pore clogging) due to the

widespread cracking in FA and BFS concretes (see Figs. 5.2, 5.3 and 5.4). Therefore, the modulus of elasticity of FA and BFS concretes decreased after 182 days.

5.6. Summary

The present study investigated the effect of chloride ion on the change in compressive strength, modulus of elasticity and apparent porosity of sea sand concrete containing FA and BFS under accelerated carbonation. Based on the results, following conclusions can be drawn:

1. Non-desalted sea sand concretes always showed higher compressive strength than DSS concretes regardless of curing ages, FA or BFS replacement even under carbonation condition. It could be proved by the results of apparent porosity. The chloride ion contributed to the reduction of apparent porosity of NSS concretes compared with DSS concretes at the age of 182 days regardless of exposure conditions, and FA or BFS replacement.
2. Carbonation significantly reduced the porosity, resulting in the increase in compressive strength of concrete under carbonation at the age of 182 days as compared to sealed condition. The compressive strength of FA15-DSS and BFS45-DSS concretes under carbonation condition was slightly lower than that of the reference concrete (OPC-DSS) at 182 days. However, when concretes contained FA and BFS together with the presence of chloride ion, the compressive strength under carbonation condition was almost the same as the reference concrete.
3. Carbonation significantly caused the formation of cracks, especially in the concretes containing FA and BFS. This could be confirmed by the SEM and crack observation tests. As a result, the modulus of elasticity of FA and BFS concretes was reduced by carbonation. However, the result of TG-DTA showed that the amount of carbonated C–S–H in concretes combined with chloride ion in NSS was lower than that in concretes

without chloride ion. Therefore, it is believed that cracks formation in FA and BFS concretes combined with chloride ion in NSS was less than that in concretes without chloride ion. As a consequence, the reduction of elastic modulus of FA and BFS concretes could be restricted by the presence of chloride ion in NSS.

It should be emphasized that the NSS concretes showed better mechanical properties than DSS concretes under both sealed and carbonation conditions regardless of SCMs replacement. The carbonation process might lead to the remarkable formation of cracks for FA or BFS concrete in comparison with OPC concrete, leading to the decrease in their modulus of elasticity. However, that could be restricted by the presence of chloride ion in NSS. Based on these results, it concludes that the use of NSS as fine aggregate can be potential materials for concrete production even when concerning the influence of carbonation.

References of chapter 5:

[1] N. Saikia, S. Kato, T. Kojima, Thermogravimetric investigation on the chloride binding behaviour of MK–lime paste, Thermochimica Acta. 444 (2006) 16–25.

[2] M. Saillio, V. Baroghel-Bouny, F. Barberon, Chloride binding in sound and carbonated cementitious materials with various types of binder, Construction and Building Materials. 68 (2014) 82–91.

[3] M. Jin, S. Gao, L. Jiang, H. Chu, M. Lu, F. F. Zhi, Degradation of concrete with addition of mineral admixture due to free chloride ion penetration under the effect of carbonation, Corrosion Science. 138 (2018) 42–53.

[4] B. Lothenbach, K. Scrivener, R.D. Hooton, Supplementary cementitious materials, Cement and Concrete Research. 41 (2011) 1244–1256.

[5] P. Duan, Z. Shui, W. Chen, C. Shen, Effects of metakaolin, silica fume and slag on pore structure, interfacial transition zone and compressive strength of concrete, Construction and Building Materials. 44 (2013) 1–6.

[6] E. Güneyisi, M. Gesoğlu, E. Booya, K. Mermerdaş, Strength and permeability properties of self-compacting concrete with cold bonded fly ash lightweight aggregate, Construction and Building Materials. 74 (2015) 17–24.

[7] E. Gruyaert, P. Van den Heede, N. De Belie, Carbonation of slag concrete: Effect of the cement replacement level and curing on the carbonation coefficient – Effect of carbonation on the pore structure, Cement and Concrete Composites. 35 (2013) 39–48.

[8] K. De Weerdt, M. B. Haha, G. Le Saout, K. O. Kjellsen, H. Justnes, B. Lothenbach, Hydration mechanisms of ternary Portland cements containing limestone powder and fly ash, Cement and Concrete Research. 41 (2011) 279–291.

[9] J. I. Escalante-Garcia, J. H. Sharp, The chemical composition and microstructure of hydration products in blended cements, Cement and Concrete Composites. 26 (2004) 967–976.

[10] B. Šavija, M. Luković, Carbonation of cement paste: Understanding, challenges, and opportunities, Construction and Building Materials. 117 (2016) 285–301.

[11] P. H. R. Borges, J. O. Costa, N. B. Milestone, C. J. Lynsdale, R. E. Streatfield, Carbonation of CH and C–S–H in composite cement pastes containing high amounts of BFS, Cement and Concrete Research. 40 (2010) 284–292.

[12] M. Auroy, S. Poyet, P. Le Bescop, J. M. Torrenti, T. Charpentier, M. Moskura, X. Bourbon, Comparison between natural and accelerated carbonation (3% CO2): Impact on mineralogy, microstructure, water retention and cracking, Cement and Concrete Research. 109 (2018) 64–80.

[13] A. Morandeau, M. Thiéry, P. Dangla, Impact of accelerated carbonation on OPC cement paste blended with fly ash, Cement and Concrete Research. 67 (2015) 226–236.

[14] M. Auroy, S. Poyet, P. Le Bescop, J. M. Torrenti, T. Charpentier, M. Moskura, X. Bourbon, Impact of carbonation on unsaturated water transport properties of cement-based materials, Cement and Concrete Research. 74 (2015) 44–58.

[15] M. Nedeljković, B. Šavija, Y. Zuo, M. Luković, G. Ye, Effect of natural carbonation on the pore structure and elastic modulus of the alkali-activated fly ash and slag pastes, Construction and Building Materials. 161 (2018) 687–704.

[16] J. J. Chen, J. J. Thomas, H. M. Jennings, Decalcification shrinkage of cement paste, Cement and Concrete Research. 36 (2006) 801–809.

[17] A. Morandeau, M. Thiéry, P. Dangla, Investigation of the carbonation mechanism of CH and C-S-H in terms of kinetics, microstructure changes and moisture properties, Cement and Concrete Research. 56 (2014) 153–170.

[18] I. Maruyama, H. Sasano, Strain and crack distribution in concrete during drying, Mater Struct. 47 (2014) 517–532.

[19] H. Chang, Chloride binding capacity of pastes influenced by carbonation under three conditions, Cement and Concrete Composites. 84 (2017) 1–9.

[20] A. Bouikni, R. N. Swamy, A. Bali, Durability properties of concrete containing 50% and 65% slag, Construction and Building Materials. 23 (2009) 2836–2845.

[21] Bruno L. de S. Costa, Julio C. de O. Freitas, Dulce M. de A. Melo, Romero G. da S. Araujo, Yvis H. de. Oliveira, Cristina A. Simão, Evaluation of density influence on resistance to carbonation process in oil well cement slurries, Construction and Building Materials. 197 (2019) 331–338.

[22] C. Chen, T. Ji, Y. Zhuang, X. Lin, Workability, mechanical properties and affinity of artificial reef concrete, Construction and Building Materials. 98 (2015) 227–236.

[23] Q. Xu, T. Ji, Z. Yang, Y. Ye, Preliminary investigation of artificial reef concrete with sulphoaluminate cement, marine sand and sea water, Construction and Building Materials. 211 (2019) 837–846.

[24] X. Li, X. Lin, K. Lin, T. Ji, Study on the degradation mechanism of sulphoaluminate cement sea sand concrete eroded by biological sulfuric acid, Construction and Building Materials. 157 (2017) 331–336.

[25] Q.T. Phung, N. Maes, D. Jacques, E. Bruneel, I. Van Driessche, G. Ye, G. De Schutter, Effect of limestone fillers on microstructure and permeability due to carbonation of cement pastes under controlled CO2 pressure conditions, Construction and Building Materials. 82 (2015) 376–390.

[26] V. T. Ngala, C. L. Page, Effects of carbonation on pore structure and diffusional properties of hydrated cement pastes, Cement and Concrete Research. 27 (1997) 995–1007.

[27] B. Wu, G. Ye, Development of porosity of cement paste blended with supplementary cementitious materials after carbonation, Construction and Building Materials. 145 (2017) 52–61.

[28] C. C. Yang, Effect of the Transition Zone on the Elastic Moduli of Mortar, Cement and Concrete Research. 28 (1998) 727–736.

[29] G. Hannesson, K. Kuder, R. Shogren, D. Lehman, The influence of high volume of fly ash and slag on the compressive strength of self-consolidating concrete, Construction and Building Materials. 30 (2012) 161–168.

[30] M. A. Megat Johari, J. J. Brooks, S. Kabir, P. Rivard, Influence of supplementary cementitious materials on engineering properties of high strength concrete, Construction and Building Materials. 25 (2011) 2639–2648.

[31] I. Maruyama, H. Sasano, Y. Nishioka, G. Igarashi, Strength and Young's modulus change in concrete due to long-term drying and heating up to 90°C, Cement and Concrete Research. 66 (2014) 48–63.

CHAPTER 6. DURABILITY OF NSS CONCRETE CONTAINING SCMs EXPOSED TO ACCELERATED CARBONATION

This chapter discusses the effect of chloride ion in NSS on the durability of concrete containing SCMs exposed to accelerated carbonation. Durability in terms of carbonation resistance, water permeability, and sorptivity of concrete under carbonation condition was investigated. In addition, the chloride ion content in concrete samples was also investigated to evaluate the effect of SCMs as well as carbonation on chloride binding capacity. Scanning electron microscopy examination was conducted to confirm the result.

6.1. Carbonation resistance

Based on the recommendation from the previous studies [1–3], the carbonation coefficient of concrete can be calculated from the slope of the straight line representing the relationship between carbonation depth and square root of exposure time obtained by regression. The relationship between carbonation depth of all the concrete specimens under accelerated carbonation and square root of exposure time is shown in Fig. 6.1. It can be seen from Fig. 6.1 that NSS concretes showed a slightly lower carbonation coefficient than DSS concretes irrespective of SCMs replacement. For instance, the carbonation coefficient of OPC-NSS concrete was 1.50 mm/week$^{0.5}$ while that of the reference concrete (OPC-DSS) was 1.40 mm/week$^{0.5}$. Meanwhile, carbonation coefficient of FA and BFS concretes using NSS was reduced by approximately 10% when compared with the corresponding concretes using DSS. The reason was due to the presence of chloride ion in NSS which could chemically or physically bound by cement hydration products to form the Friedel's salt (mentioned in Section 5.1), leading to the refinement of microstructure of NSS concretes compared with DSS concretes.

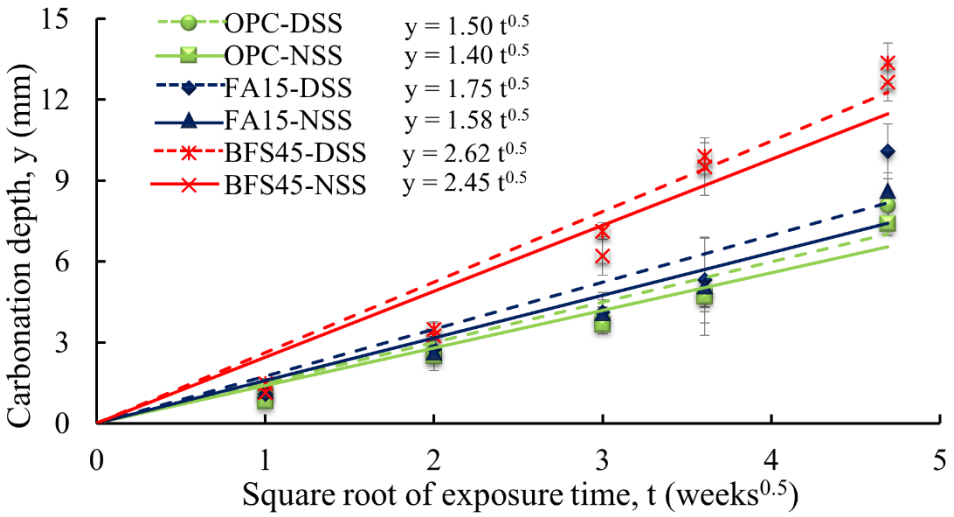

Fig. 6.1. Relationship between carbonation depth (y) of all concrete specimens under accelerated carbonation and square root of exposure time (t)

On the other hand, the FA and BFS replacements led to significant increase in carbonation coefficient of concrete in comparison with the reference concrete, irrespective of the presence of chloride ion, as shown in Fig. 6.2. The phenomenon was consistent with previous studies when concrete contained SCMs [1,2,4]. For example, in comparison to the reference concrete, the carbonation coefficient of FA15-NSS concrete increased slightly (5.3%) while the carbonation coefficient of BFS45-NSS concrete increased dramatically (63.3%). This can be explained by the lower CH content in the FA or BFS concretes compared to the OPC concretes, discussed in Section 5.1. The lower CH in FA or BFS concrete is due to the lower clinker content and the pozzolanic reaction as well as latent hydraulicity which consumed the CH content.

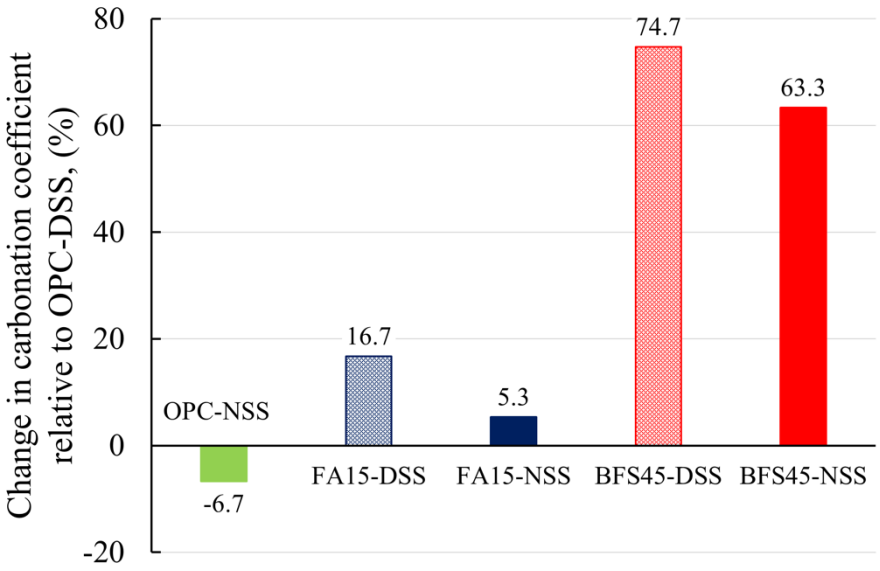

Fig. 6.2. Change in carbonation coefficient of all concretes relative to OPC-DSS

6.2. Sorptivity

The ingress of external chemical contaminants (e.g. sulfate) is usually related to the deterioration of concrete. Therefore, the durability of concrete is strongly governed by the quality of surface material which is related to the penetration of fluid or aggressive agents [5]. Sorptivity characterizes the tendency of material to absorb and transmit fluids into the body of the material by capillary suction. Sorptivity is also considered as chemical durability index because it directly relates to the resistance of materials against the penetration of external aggressive agents [5–7]. Figure 6.3 shows the sorptivity coefficient of all the concretes under sealed and carbonation conditions. Meanwhile, Fig. 6.4 shows the change in sorptivity coefficient of all the concretes relative to the reference concrete under sealed and carbonation conditions at the ages of 91 and 182 days, which was calculated by using Eq. (6-1)

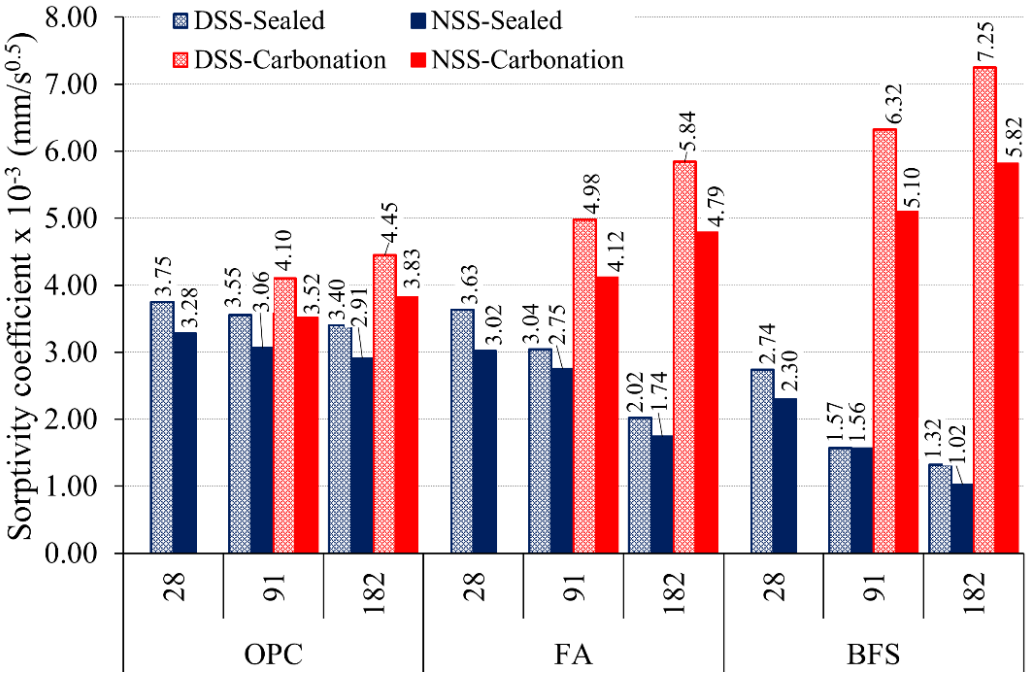

Fig. 6.3. Sorptivity coefficient of all concretes under sealed and carbonation conditions

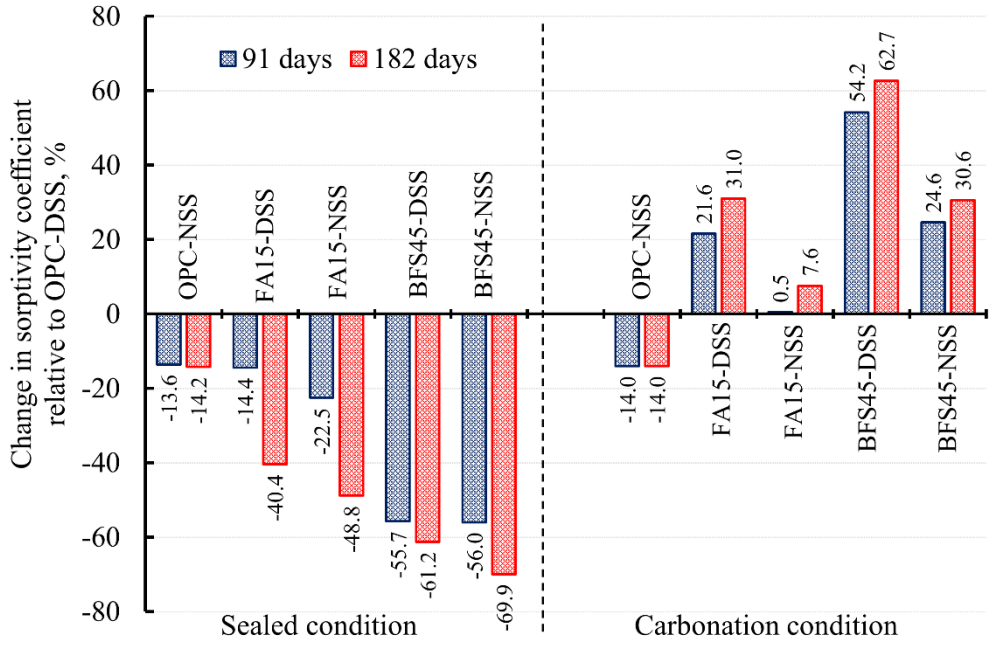

Fig. 6.4. Change in sorptivity coefficient of all concretes relative to OPC-DSS under sealed and carbonation conditions

$$\text{Change in sorptivity coefficient} = \frac{S_c - S_{c,OPC\text{-}DSS}}{S_{c,OPC\text{-}DSS}} \times 100\% \quad (6\text{-}1)$$

Where, $S_{c,OPC\text{-}DSS}$ is the sorptivity coefficient of OPC-DSS concrete at the ages of 91 and 182 days under sealed and carbonation conditions; S_c is the sorptivity coefficient of all concretes, excepted for OPC-DSS concrete at the ages of 91 and 182 days under the same condition;

It is evident from Fig. 6.3 that NSS concretes showed lower sorptivity coefficients than DSS concretes regardless of curing age, exposure conditions, and SCMs replacement. Additionally, the sorptivity coefficient of concretes under sealed condition decreased constantly over time, especially in concretes containing SCMs. It can be seen from Fig. 6.4 that the addition of FA and BFS reduced the sorptivity coefficient of concrete by 40.4% and 61.2%, respectively, after aging for 182 days under sealed condition compared with the reference concrete. Meanwhile, when mixed with NSS, the reduction of the sorptivity coefficient of FA and BFS concretes was 48.8% and 69.9%, respectively. This phenomenon implies that NSS concretes could better restrict the accessibility of fluids or aggressive agents than DSS concretes.

On the contrary, as shown in Fig. 6.3, the carbonation process slightly increased the sorptivity coefficient of OPC concretes, but the sorptivity coefficients of FA and BFS concretes were more remarkable. For instance, the increase in sorptivity coefficient of FA15-NSS concrete was approximately 58%, whereas that of BFS45-NSS concrete was 153% after exposing to carbonation. The formation of cracks due to carbonation shrinkage was presumed to be the major cause to increase the sorptivity of concrete under carbonation condition despite a decrease in apparent porosity. The apparent porosity of FA15-NSS and BFS45-NSS concretes was reduced by approximately 16.7% and 7.5%, respectively, when exposing to carbonation from the age of 28 to 182 days, as shown in Section 5.4. Moreover, the formation of cracks in carbonated concretes was clearly observed, especially concretes containing FA and BFS, as

confirmed in Sections 5.2 and 5.3. Therefore, the formation of cracks results in the promotion of the water ingress into the concrete by capillary suction, leading to the increase in the sorptivity coefficient of carbonated concrete. This is consistent with the observations of Borges et al. [1] and Auroy et al [8]. Borges et al. [1] illustrated that the oxygen permeability of cement pastes blended with BFS was increased after carbonation, while Auroy et al. [8] found that the carbonation caused the increase in water permeability of blended cement pastes under unsaturated condition even if the total porosity of specimens was decreased. However, this result is not consistent with the findings of Dias [9] or Song and Kwon [10]. Dias [9] showed that the sorptivity of OPC concrete exposed to natural carbonation for 3.5 years decreased, but Song and Kwon [10] showed that the water permeability coefficient of carbonated mortars was three times less than that of non-carbonated mortars. The differences between the previous studies and the present work may be due to the differences in mixture proportions (water-to-cement ratio), OPC mineral composition, and carbonation conditions (CO_2 concentration, R.H., temperature, etc.). Mixture proportions and carbonation conditions can affect the carbonation rate of concrete, while the mineral composition of OPC can affect the amount of carbonation products (such as CC) or hydration rates in different ways.

As seen in Fig. 6.4, although the sorptivity coefficient of FA and BFS concretes under carbonation condition in comparison with OPC-DSS was remarkably increased, it was significantly decreased when concretes mixed with NSS. Particularly, while the presence of chloride ion reduced the sorptivity coefficient of OPC concrete by 14.0%, it contributed to the reduction of sorptivity coefficients of FA and BFS concretes from 31.0% to 7.6% and from 62.7% to 30.6% at 182 days, respectively. It can be attributed to the presence of chloride ion which increased the carbonation resistance of concrete as mentioned in Section 6.1 of carbonation depth, resulting in the reduction in the influence of carbonation on sorptivity.

6.3. Chloride ion content

Figure 6.5 shows the free chloride ion content and chloride binding ratio in carbonated and uncarbonated zones of NSS concretes at the age of 182 days. Normally, chloride ion is present in concrete in two states: free and binding states. The corrosion risk of steel bar in reinforced concrete is only attributed to the free chloride [11,12]. Therefore, the decrease in free chloride ion and increase in chloride binding ratio can reduce the corrosion of steel bar in reinforced concrete. With regards to chloride binding, the Friedel's salt formation can be described by two mechanisms: adsorption and anion exchange [13,14]. According to the adsorption mechanism, the bulk Cl^- ions in the pore solution absorb into the interlayers of principle layers, $[Ca_2Al(OH^-)_6 \cdot 2H_2O]^+$ of AFm (aluminate ferrite monosulfate) structure to balance the charge, resulting in Friedel's salt formations. In the case of the anion exchange mechanism, a fraction of the free chloride ion is exchanged with the OH^- ions which are released from the AFm hydrates (or other AFm hydrates derivation), keeping the fundamental structure the same. As shown in Fig. 6.5, it can be clearly seen that the concretes containing FA or BFS can effectively improve the chloride binding ratio, leading to the decrease in the free chloride ion content in concrete under sealed condition (uncarbonated zone) [7,15,16]. For instance, the chloride binding ratio was increased by approximately 10% when OPC was partially replaced by BFS. This finding is in agreement with the studies of W. Liu et al. [17] and J. Liu et al. [18]. The results from Table 5.1 showed that the CH content in FA and BFS concretes under sealed condition was consumed approximately 10% and 20% after the age of 182 days, respectively. The CH consumption due to pozzolanic reaction of FA and hydraulicity of BFS additionally generates C–S–H. Consequently, the replacement of OPC by FA and BFS increased the chloride binding capacity, resulting in the reduction in free chloride ion in pore solution.

It can be also seen that the chloride binding ratio of FA and BFS concretes under carbonation condition (carbonated zone) was remarkably lower than that under sealed condition

(uncarbonated zone). For example, the chloride binding ratio of BFS concrete under sealed condition at the age of 182 days was 89.1%. Meanwhile, that under carbonation condition was 4.9%. Table 5.1 showed that when concrete was exposed to carbonation, a large amount of C–S–H in concrete was carbonated, especially concrete containing FA and BFS. Therefore, the decalcification of C–S–H reduced the physical chloride binding of concretes [19,20]. Additionally, carbonation process also decreased the chemical chloride binding due to the dissolution of Friedel's salt in carbonated zone as shown in Eq. (6-2). As a consequence, the chloride binding ratio of FA and BFS concretes under carbonation condition (carbonated zone) was significantly decreased, resulting in the increase in the free chloride ion content in concrete.

$$3CaO.Al_2O_3.CaCl_2.10H_2O \rightarrow 4Ca^{2+} + 2Cl^- + 6OH^- + 2Al(OH)_3 + 4H_2O \quad (6\text{-}2)$$

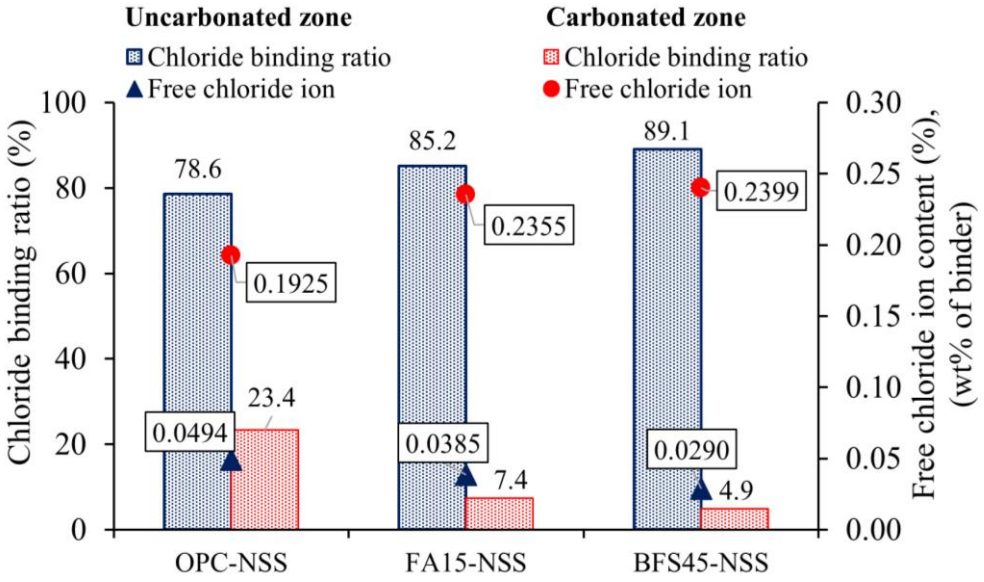

Fig. 6.5. Free chloride ion and chloride binding ratio in uncarbonated and carbonated zone at the age of 182 days.

6.4. Relationship among characteristics

The correlation between compressive strength and modulus of elasticity of concretes at the ages of 182 days under sealed condition as well as carbonation condition is shown in Fig. 6.6. All the moduli of elasticity obtained from experiment were approximately 10% higher than the recommendation of Japan Society of Civil Engineering JSCE 2017 [21]. It is obvious that concretes under carbonation had higher compressive strength, but lower modulus of elasticity compared with concretes under sealed condition. It implies that the carbonation could improve the compressive strength of concrete due to the CC formation; however, the carbonation could adversely affect the modulus of elasticity of concrete because of the formation of cracks.

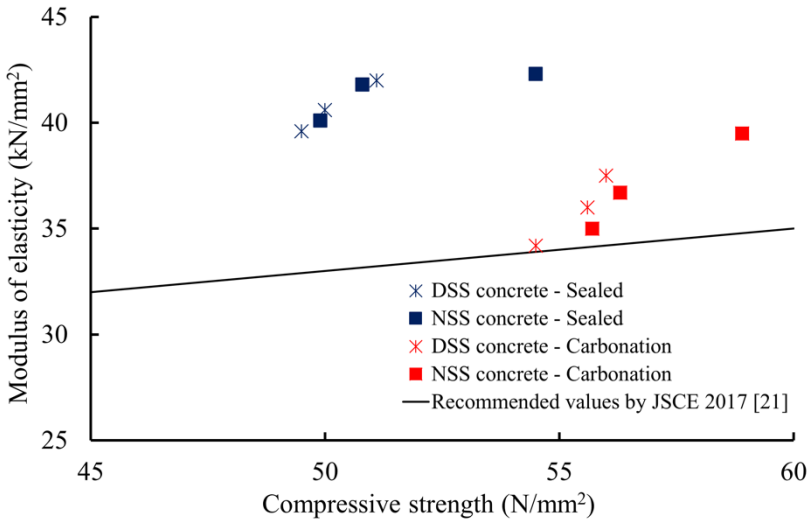

Fig. 6.6. Relationship between compressive strength and modulus of elasticity under sealed and carbonation conditions at the age of 182 days

Figure 6.7 shows the correlation between the sorptivity coefficient and apparent porosity under sealed and carbonation conditions at the age of 182 days. Under sealed condition, NSS concrete has lower apparent porosity and sorptivity coefficient than DSS concrete. However, NSS concrete under carbonation condition has almost the same apparent porosity as DSS

concrete, but it has lower sorptivity. It indicates that NSS as fine aggregate could be better for limiting the water penetration into the pores of unsaturated concrete by capillary suction than DSS. Besides, it can be seen that, although the apparent porosity of concretes under carbonation condition was lower, the sorptivity coefficient of concretes under carbonation condition was higher than that under sealed condition. On the other hand, the correlation between the sorptivity coefficient and apparent porosity was clearly different for two conditions. The correlation is a regression line under sealed condition, while it is an approximately vertical line (parallel to the vertical axis) under carbonation condition. It means that the carbonation did not cause any noticeable differences in apparent porosity among concretes; however, it led to a change in sorptivity coefficient between them. It implies that the sorptivity coefficient of concrete under carbonation condition depends not only the total porosity of concrete, but also the other factors, e.g., the amount of crack formation or the change in pore size distribution.

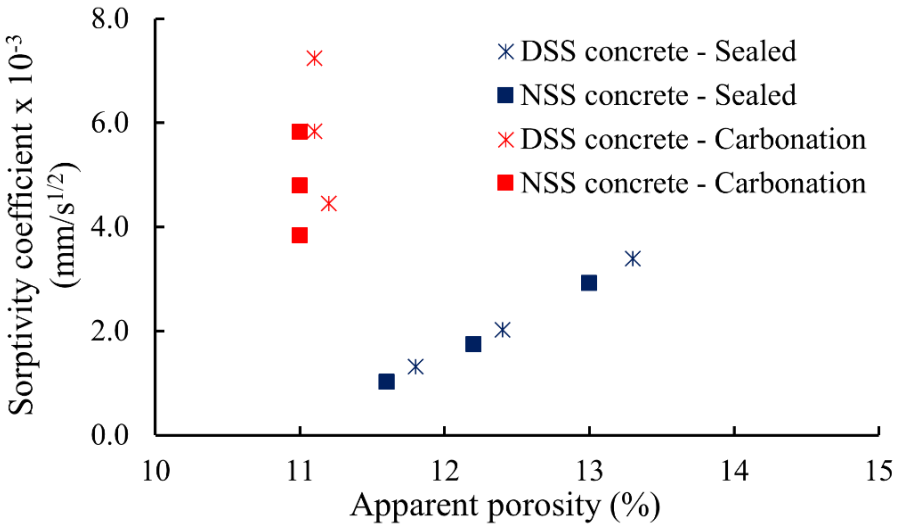

Fig. 6.7. Correlation between sorptivity coefficient and apparent porosity under sealed and carbonation conditions at the age of 182 days

Figure 6.8 shows the correlation between the sorptivity coefficient and modulus of elasticity at the age of 182 days. It can be deduced that the sorptivity coefficient had negative

correlation with the modulus of elasticity of concrete. The lower sorptivity coefficient corresponded to the higher modulus of elasticity of concrete. It is obvious that the formation of cracks due to carbonation had the adverse influence on sorptivity and modulus of elasticity of concrete. The increase in the sorptivity and the decrease in the modulus of elasticity of concrete could be resisted by the presence of chloride ion in NSS.

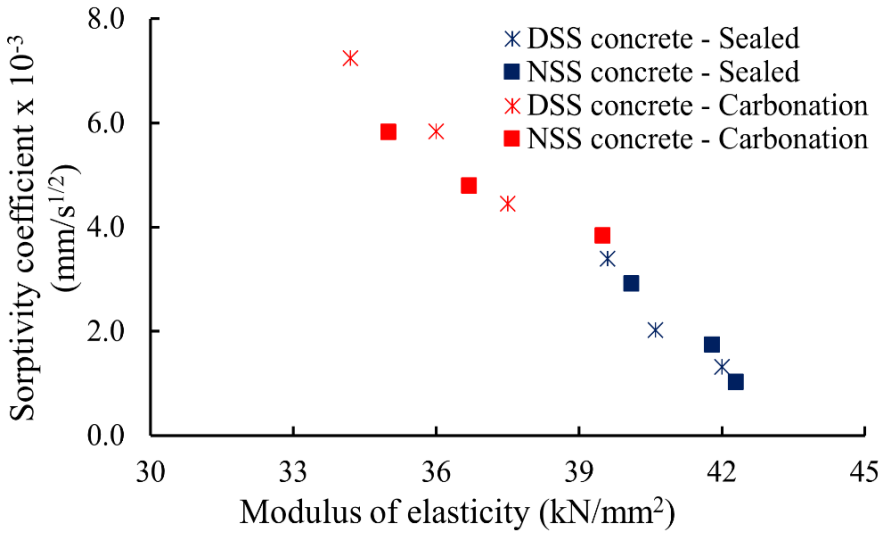

Fig. 6.8. Correlation between sorptivity coefficient and modulus of elasticity under sealed and carbonation conditions at the age of 182 days

On the other hand, the correlation between the apparent porosity and compressive strength at the age of 182 days is presented in Fig. 6.9. The compressive strength increased with the decrease in apparent porosity. In contrast with sorptivity coefficient and modulus of elasticity, it is assumed that the effect of cracks due to carbonation on apparent porosity and compressive strength was insignificant. Consequently, the microstructure of concrete was also improved, leading to the increase in the compressive strength of concrete under carbonation condition.

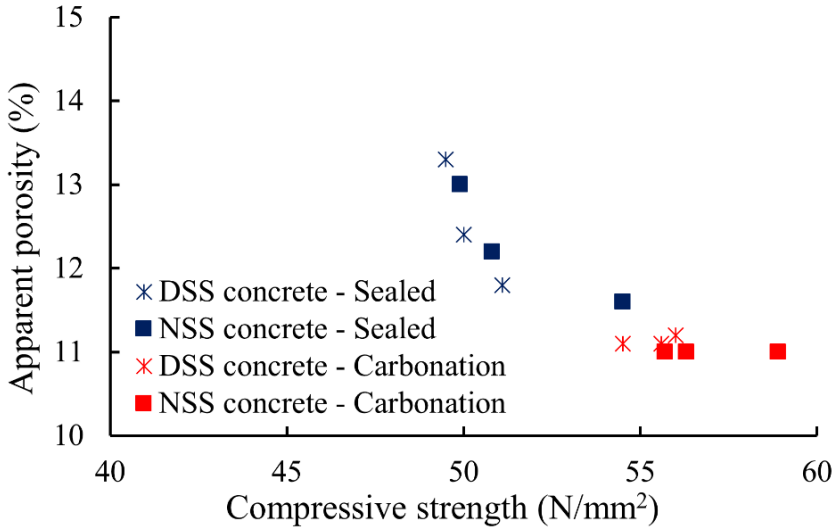

Fig. 6.9. Correlation between apparent porosity and compressive strength under sealed and carbonation conditions at the age of 182 days

6.5. Effect of chloride ion on mechanical properties and durability of concrete containing FA and BFS considering carbonation

It is well known that the total bound chloride content in concrete includes the chemical and physical bound chloride content. While chemical bound chloride content depends on the content of Friedel's salt ($3CaO{\cdot}Al_2O_3{\cdot}CaCl_2{\cdot}10H_2O$), physical bound chloride content is decided by the content of C–S–H [22]. Since the chloride ion is introduced by NSS during casting, the chemical reaction between chloride ion and tricalcium aluminate ($3CaO.Al_2O_3$) is occurred to form Friedel's salt, as shown in Eqs. (6-3) and (6-4). Besides, the formation of Friedel's salt is resulted from chloride ion and aluminum oxide (Al_2O_3) in FA and BFS, as shown in Eq. (6-5). As mentioned in Section 5.1, the CH content in concretes was consumed by approximately 10% and 20% due to the pozzolanic reaction of FA and hydraulicity of BFS after 182 days, respectively. Hence, concretes containing FA and BFS is believed to produce a higher amount of C–S–H compared to OPC concrete. As a result, the chloride binding capacity of concretes incorporating FA or BFS was increased. It could be found from Fig. 6.5 that the bound chloride content of concretes added with FA or BFS is higher than that of OPC concrete.

Therefore, it is believed that the more Friedel's salt was formed in FA and BFS concretes. The formation of Friedel's salt, as well as C–S–H gel from pozzolanic reaction of FA and hydraulicity of BFS, could make the microstructure of concrete denser. This was confirmed by SEM and apparent porosity examinations described in Sections 5.3 and 5.4. Consequently, the mechanical properties and durability of NSS concretes under sealed condition was improved compared to DSS concretes, as shown in Figs. 6.7 and 6.9.

$$Ca(OH)_2 + 2NaCl \rightarrow CaCl_2 + 2NaOH \quad (6\text{-}3)$$

$$3CaO \cdot Al_2O_3 + CaCl_2 + 10H_2O \rightarrow 3CaO \cdot Al_2O_3 \cdot CaCl_2 \cdot 10H_2O \quad (6\text{-}4)$$

$$3Ca(OH)_2 + CaCl_2 + Al_2O_3 + 7H_2O \rightarrow 3CaO \cdot Al_2O_3 \cdot CaCl_2 \cdot 10H_2O \quad (6\text{-}5)$$

When concrete was carbonated, not only CH but also C–S–H reacts with carbon dioxide (CO_2), as shown in Eqs. (5-7) and (5-8). Carbonation caused C–S–H decalcification, resulting in the formation of cracks. The more C–S–H was decomposed, the more cracks were formed. Cracks were clearly observed for concretes under carbonation, especially concrete containing FA or BFS. It was confirmed by results demonstrated in Sections 5.2 and 5.3. As a result, the formation of cracks could increase the deformation, leading to the decrease in modulus of elasticity. Additionally, the formation of cracks also promoted the penetration of water into the concrete by capillary suction, increasing the sorptivity coefficient of carbonated concrete, as shown in Fig. 6.8. However, the results from Section 5.1 showed that the amount of C–S–H in NSS concretes which was carbonated was lower than that of DSS concretes. It implies that when CO_2 penetrates concrete, CO_2 will be captured by Friedel's salt. As a result, Friedel's salt is primarily dissolved before the decalcification of C–S–H, leading to fewer crack formation in NSS concretes than that in DSS concretes. Chang [22] and Villain et al. [23] concluded that the specimen containing more Friedel's salt showed higher C–S–H content after carbonation when

compared with the specimen containing less Friedel's salt. Consequently, the increase in sorptivity coefficient and the decrease in modulus of elasticity of concretes could be restricted by the presence of chloride ion in NSS. This is illustrated through the results in Figs. 5.9 and 6.3.

6.6. Summary

Based on experimental results in this chapter, the following conclusions can be drawn:

1. The presence of chloride ion in NSS contributed to the improvement of carbonation resistance of concrete. The FA and BFS replacements caused the increase in carbonation coefficient of concrete. However, the carbonation coefficient of FA and BFS concretes could be reduced approximately 10 % when using NSS.
2. Under sealed condition, FA and BFS seemed to have a beneficial effect on the reduction of sorptivity coefficient of concrete due to the pozzolanic reaction of FA and hydraulicity of BFS. However, the formation of cracks due to carbonation shrinkage led to the significant increase in sorptivity coefficient of FA and BFS concretes in comparison with that of OPC-DSS concrete. This increase could be restricted when FA or BFS concretes were produced using NSS.
3. Supplementary cementitious materials replacement could improve the chloride binding of concrete under sealed condition. However, the chloride binding of concrete was remarkably decreased under carbonation condition, especially concrete containing SCMs.

In this study, all the experimental results indicate that NSS concretes had the better durability than DSS concretes under both sealed and carbonation conditions regardless of SCMs replacement. The cracks were significantly generated in SCMs concretes due to carbonation,

leading to the increase in their sorptivity. The increase in sorptivity results in the easier ingress of aggressive ions (e.g. sulfate ions) which will affect the durability of concrete. However, the presence of chloride ion in NSS could restrict the formation of cracks due to carbonation. Based on these results, it concludes that the use of NSS as fine aggregate can be potential for concrete production even when concerning the influence of carbonation.

References of chapter 6:

[1] P. H. R. Borges, J. O. Costa, N. B. Milestone, C. J. Lynsdale, R. E. Streatfield, Carbonation of CH and C–S–H in composite cement pastes containing high amounts of BFS, Cement and Concrete Research. 40 (2010) 284–292.

[2] E. Gruyaert, P. Van den Heede, N. De Belie, Carbonation of slag concrete: Effect of the cement replacement level and curing on the carbonation coefficient – Effect of carbonation on the pore structure, Cement and Concrete Composites. 35 (2013) 39–48.

[3] L. S. Ho, K. Nakarai, Y. Ogawa, T. Sasaki, M. Morioka, Effect of internal water content on carbonation progress in cement-treated sand and effect of carbonation on compressive strength, Cement and Concrete Composites. 85 (2018) 9–21.

[4] B. Šavija, M. Luković, Carbonation of cement paste: Understanding, challenges, and opportunities, Construction and Building Materials. 117 (2016) 285–301.

[5] J. Limeira, M. Etxeberria, L. Agulló, D. Molina, Mechanical and durability properties of concrete made with dredged marine sand, Construction and Building Materials. 25 (2011) 4165–4174.

[6] E. Güneyisi, M. Gesoğlu, E. Booya, K. Mermerdaş, Strength and permeability properties of self-compacting concrete with cold bonded fly ash lightweight aggregate, Construction and Building Materials. 74 (2015) 17–24.

[7] A. Hadjsadok, S. Kenai, L. Courard, F. Michel, J. Khatib, Durability of mortar and concretes containing slag with low hydraulic activity, Cement and Concrete Composites. 34 (2012) 671–677.

[8] M. Auroy, S. Poyet, P. Le Bescop, J. M. Torrenti, T. Charpentier, M. Moskura, X. Bourbon, Impact of carbonation on unsaturated water transport properties of cement-based materials, Cement and Concrete Research. 74 (2015) 44–58.

[9] W. P. S. Dias, Reduction of concrete sorptivity with age through carbonation, Cement and Concrete Research. 30 (2000) 1255–1261.

[10] H. W. Song, S. J. Kwon, Permeability characteristics of carbonated concrete considering capillary pore structure, Cement and Concrete Research. 37 (2007) 909–915.

[11] U. Angst, B. Elsener, C. K. Larsen, Ø. Vennesland, Critical chloride content in reinforced concrete — A review, Cement and Concrete Research. 39 (2009) 1122–1138.

[12] Y. Cao, C. Gehlen, U. Angst, L. Wang, Z. Wang, Y. Yao, Critical chloride content in reinforced concrete — An updated review considering Chinese experience, Cement and Concrete Research. 117 (2019) 58–68.

[13] N. Saikia, S. Kato, T. Kojima, Thermogravimetric investigation on the chloride binding behaviour of MK–lime paste, Thermochimica Acta. 444 (2006) 16–25.

[14] M. R. Jones, D. E. Macphee, J. A. Chudek, G. Hunter, R. Lannegrand, R. Talero, S. N. Scrimgeour, Studies using 27Al MAS NMR of AFm and AFt phases and the formation of Friedel's salt, Cement and Concrete Research. 33 (2003) 177–182.

[15] B. Lothenbach, K. Scrivener, R.D. Hooton, Supplementary cementitious materials, Cement and Concrete Research. 41 (2011) 1244–1256.

[16] G. Hannesson, K. Kuder, R. Shogren, D. Lehman, The influence of high volume of fly ash and slag on the compressive strength of self-consolidating concrete, Construction and Building Materials. 30 (2012) 161–168.

[17] W. Liu, H. Cui, Z. Dong, F. Xing, H. Zhang, T.Y. Lo, Carbonation of concrete made with dredged marine sand and its effect on chloride binding, Construction and Building Materials. 120 (2016) 1–9.

[18] J. Liu, M. Ba, Y. Du, Z. He, J. Chen, Effects of chloride ions on carbonation rate of hardened cement paste by X-ray CT techniques, Construction and Building Materials. 122 (2016) 619–627.

[19] M. Saillio, V. Baroghel-Bouny, F. Barberon, Chloride binding in sound and carbonated cementitious materials with various types of binder, Construction and Building Materials. 68 (2014) 82–91.

[20] M. Jin, S. Gao, L. Jiang, H. Chu, M. Lu, F. F. Zhi, Degradation of concrete with addition of mineral admixture due to free chloride ion penetration under the effect of carbonation, Corrosion Science. 138 (2018) 42–53.

[21] Standard specifications for concrete structures - 2017, Japan Society of Civil Engineers, (2018).

[22] H. Chang, Chloride binding capacity of pastes influenced by carbonation under three conditions, Cement and Concrete Composites. 84 (2017) 1–9.

[23] G. Villain, M. Thiery, G. Platret, Measurement methods of carbonation profiles in concrete: Thermogravimetry, chemical analysis and gammadensimetry, Cement and Concrete Research. 37 (2007) 1182–1192.

CHAPTER 7. CONCLUSIONS AND RECOMMENDATIONS FOR FUTURE WORKS

7.1. Conclusions

The present study investigated the effect of chloride ion in NSS on the performance of concrete containing FA and BFS under considering the accelerated carbonation to intensively verify the applicability of NSS for concrete production. The mixture proportions of concrete was designed with a constant water to cementitious materials ratio of 0.50, supposing common concrete used for plain concrete structures in the marine environments such as breakwater or artificial reef. The non-desalted sea sand used as fine aggregate in this study was exploited from the karatsu harbor in Saga prefecture, Japan. According to the mixture proportions, the chloride ion content in DSS and NSS concretes was approximately calculated and corresponded to 0.02% and 0.48 – 0.49% per mass of binder, respectively. Based on the results, the following conclusions can be drawn:

❖ **Properties of fresh concrete**

1. Non-desalted sea sand reduced the initial slump of fresh concretes, whereas it had almost no effect on the initial air content of all concretes.
2. Replacement of OPC by FA and BFS increased the initial slump of fresh concrete, even when NSS was used.
3. No effect of chloride ion in NSS on the slump loss and air content reduction of concrete for 60 min after mixing was observed regardless of FA and BFS replacement.

❖ **Mechanical properties of hardened concrete**

1. Chloride ion in NSS not only accelerated cement hydration but also enhanced the pozzolanic reactivity of FA and hydraulicity of BFS at early ages (i.e., 3 and 7 days). As a consequence, the compressive strength and elastic modulus of concretes containing NSS ion were noticeably higher than those of concretes without chloride ion at the early ages.
2. Compared to reference concrete, even in the presence of chloride ion, the replacement of OPC by FA and BFS reduced the compressive strength of concrete at early age (3 days.
3. At later age (182 days), the compressive strength and modulus of elasticity of NSS concretes were higher than those of DSS concretes regardless of FA or BFS replacement and curing conditions.
4. The compressive strength of FA and BFS concretes without chloride ion under carbonation condition was slightly lower than that of the reference concrete (OPC-DSS) at 182 days. When concretes contained FA and BFS together with chloride ion, the compressive strength under carbonation condition was almost similar to the reference concrete.
5. The modulus of elasticity of FA and BFS concretes under carbonation condition was decreased due to the carbonation shrinkage. The use of NSS could restrict the reduction of modulus of elasticity of FA and BFS concretes under carbonation condition.
6. The chloride ion reduced apparent porosity of concretes at 182 days regardless of exposure conditions, and FA or BFS replacement. Fly ash and BFS replacements significantly decreased apparent porosity of concrete under sealed condition. Conversely, these replacements did not substantially affect the apparent porosity compared to the reference concrete at 182 days under carbonation carbonation.

❖ **Durability of hardened concrete**

1. The presence of chloride ion in NSS contributed to the improvement of carbonation resistance of concrete. The FA and BFS replacements caused the increase in carbonation coefficient of concrete. However, the carbonation coefficient of FA and BFS concretes could be reduced by approximately 10 % when concrete mixed with NSS.
2. The chloride ion was ascribed to the reduction in water absorption of concretes regardless of FA and BFS replacements. Additionally, FA and BFS replacements significantly decreased water absorption of concrete under sealed condition.
3. Under sealed condition, FA and BFS seemed to have a beneficial effect on the reduction of sorptivity of concrete due to the formation of secondary C–S–H gel. This reduction could be increased when FA or BFS concretes were produced using NSS. However, the formation of cracks due to carbonation shrinkage led to the significant increase in sorptivity of FA and BFS concretes in comparison with that of OPC-DSS concrete.
4. Supplementary cementitious materials replacement could improve the chloride binding of concrete under sealed condition. However, the chloride binding of concrete was remarkably decreased under carbonation, especially concrete containing SCMs due to susceptible carbonation shrinkage.

In this study, it should be emphasized that the NSS concretes did not perform worse in mechanical properties, permeability, sorptivity, and carbonation resistance than DSS concretes under both sealed and carbonation conditions regardless of SCMs replacement. The carbonation can change the chloride ion behavior, leading to increase the free chloride in concrete and the possibility of steel bar corrosion. This can be dealt with the use of fiber reinforced polymer bar instead of steel bar. Additionally, the carbonation process might lead to the remarkable formation of cracks for FA or BFS concrete in comparison with OPC concrete. This could

facilitate the penetration of water containing some aggressive ions (e.g. sulfate ions) which will affect the durability of FA or BFS concrete than OPC concrete. However, the presence of chloride ion in NSS could restrict the formation of cracks, resulting in the extensive durability of concrete.

The compressive strength after 182 days under both sealed and carbonation conditions was over 40 N/mm^2 regardless of 15% FA or 45% BFS replacement by mass. This compressive strength level normally represents the plain concrete structures used in the marine environments such as breakwater or artificial reef. Based on results mentioned above, it concludes that NSS as fine aggregate can be a potential material for concrete production even when concerning the influence of carbonation. The obtained results may contribute to the useful knowledge and discussion for verifying the applicability of NSS for concrete production.

7.2. Recommendations for future works

Based on the results from this study and previous studies, some recommendations for the future works can be drawn as follows:

1. Non-desalted sea sand in this study was exploited from the Karatsu habor in Saga prefecture, Japan. The physical properties (e.g., particle size distribution) and chemical composition (e.g., chloride ion content or sulfate ion content) of NSS from different regions of the world can be various. Therefore, NSS from the other regions should be carried out to extensively verify its applicability for concrete production.
2. In this study, the effect of chloride ion in NSS on mechanical properties and durability of concrete was observed for 182 days under considering accelerated carbonation. In order to evaluate more accurately, it has been recommended to investigate their variation in mechanical properties and durability for long term (10 or 20 years or more). Especially, other conditions such as exposure to to natural carbonation (≈ 0.3 % CO_2), immersion in

solution containing aggressive ions (sodium chloride, sulfate ion), and investigation under wet-dry cycles, should be applied to reflect the influence of real environment on concrete structure. On the other hand, the effect of the curing period on mechanical properties and durability performance of concrete before being subjected to carbonation should be investigated. It is a fact that the use of SCMs is being encouraged for concrete production in order mitigate the huge CO_2 emission into the atmosphere. However, this study was only considered the effect of FA and BFS with the replacement ratio of 15% and 45 % by mass, respectively. Therefore, the other SCMs such as metakaolin or rice husk as well as other replacement ratios are recommended to be investigated for concrete using NSS.

3. This study was still limited due to the investigation of only NSS on mechanical properties and durability of concrete. The experiment should be expanded not only for NSS but also for seawater to utilize the local materials at coastal region. The higher chloride ion concentration and other ions such as SO_4^{2-} in seawater may significantly affect the performance of concrete.
4. The effect of chloride ion in NSS on the corrosion of steel bar of reinforced concrete should be carefully investigated to establish the limitation of chloride ion concentration in concrete under considering each specific condition, such as sealed condition, carbonation, with or without SCMs, etc.
5. Stainless steel or FRP composites are not expected to corrode in the presence of chloride ion. Hence, they are proposed to be used use in concrete structures using NSS. The bonding behavior between FRP and NSS concrete should be carried out for long term under considering of the influences of carbonation, immersion in solution containing aggressive ions (sodium chloride, sulfate ion) and SCMs.